

Investigation of Polychloride Anions Stabilized by Quaternary Ammonium and Other N-based Cations

Inaugural-Dissertation

to obtain the academic degree

Doctor rerum naturalium (Dr. rer. nat.)

submitted to the Department of Biology, Chemistry and Pharmacy
of Freie Universität Berlin

by

Dipl.-Chem. Robin Kieran Brückner

from Villingen-Schwenningen

2016

Die vorliegende Arbeit wurde von November 2011 bis Juli 2016 am Institut für Anorganische und Analytische Chemie der Albert-Ludwigs-Universität Freiburg und am Institut für Chemie und Biochemie der Freien Universität Berlin unter der Anleitung von Prof. Dr. Sebastian Hasenstab-Riedel angefertigt.

1. Gutachter: Prof. Dr. Sebastian Hasenstab-Riedel

2. Gutachter: Prof. Dr. Dieter Lentz

Disputation am 23.09.2016

Danksagung

Mein erster Dank gilt meinem Doktorvater Prof. Dr. Sebastian Riedel für das spannende Doktorarbeitsthema, die sehr gute Betreuung, seine Fairness und sein offenes Ohr bei allen auftretenden Problemen.

Des Weiteren danke ich Prof. Dr. Dieter Lentz für die Übernahme der Zweitkorrektur.

Meinen Bachelorstudenten und Forschungspraktikanten Ines Lindner, Stephan Burger und Patrick Pröhm für Ihren Beitrag zu einem wahrhaft komplizierten Thema.

Thomas Drews, Jan-Hendrick Nissen, Anja Wiesner und Mathias Ellwanger für die tolle Stimmung im Labor.

Heike Haller, Lisa Mann und Anja Wiesner für die Hilfe beim Messen der Kristallstrukturen.

Ihnen sowie Maximilian Stahnke, Karsten Sonnenberg, Maxim Gawrilow, Felix Brosi, Tony Stüker, Sebastian Hämmerling, Helmut Beckers, Simon Steinhauer, Tobias Schlöder, Inge Kanakaris-Wirtl, Ulf Sachs, Lisa Mann und allen ehemaligen Bachelorstudenten und Forschungspraktikanten danke ich für die nette Stimmung und die unterhaltsamen Kaffeepausen in der AG Riedel.

Tobias Schlöder für die Hilfe bei den quantenchemischen Rechnungen.

Simon Steinhauer für die viele Hilfe bei allen sachlichen Fragen und dem Ausformulieren der Arbeiten.

Anja Wiesner, Mathias Ellwanger und Simon Steinhauer fürs Korrekturlesen und die hilfreichen Anregungen.

Janine Ackermann und Sarah Breslau für die stimmungsvolle Auflockerung der Kaffeepausen.

Carsten Lüdtkke, Marija Habicht, Clemens Scholtysik, Steven Giese und Janine Ackermann für die gute Stimmung bei der Praktikumsbetreuung.

Dem ganzen AK Krossing für die viele Hilfe und die gute Zeit in Freiburg.

Der AG Lentz für die nette Aufnahme und Hilfe in Berlin.

Meinen Freunden in Freiburg, Bremen, Berlin und anderswo; Patrick Lauer, Anna Bauß, Christine Grumbt, Michael Nedelcu und Marco DiFeo für die ungezählten DoKo-Runden; ihnen sowie Ansgar Sage, Carolin Meyer, Sven Denking, Michael Jehle, Michael Schwarz, Martin Fabritius, Joachim Heck, Bianca Herrmann und Oliver Hoffmann für die tolle Zeit und die vielen Feiern während des Studiums; Daniel und Katharina Fonte, Elke Tänzel, Klaus Tänzel, Melanie Traulin und Klaus Riemann für die Erkenntnis, dass es auch noch eine Welt außerhalb der Uni gibt; allen oben genannten für die langen Freundschaften.

Meinen Geschwistern und Eltern für die moralische und finanzielle Unterstützung in den letzten Jahren.

Und last but not least meiner Frau Maria für ihre grenzenlose Geduld, Liebe und Unterstützung in all den Jahren.

List of Abbreviations

a.u.	Atomic Units
BMP	N-butyl-N-methyl-pyrrolidinium
BP86	Becke-Perdew 86
Bu	Butyl
B3-LYP	Becke-Three-Parameter-Lee-Yang-Parr
CCDC	Cambridge Crystallographic Data Centre
C ₁₀ MP	N-decyl-N-methyl-pyrrolidinium
CCSD(T)	Coupled Cluster with Single, Double and perturbative Triple excitations
COSMO	Conductor Like Screening Model
DFT	Density Functional Theory
DCM	Dichloro-methane
DSSC	Dye Sensitized Solar Cells
D3	Dispersion Correction 3
EMIm	1-Ethyl-3-methylimidazolium
Et	Ethyl
Et ₂ O	Diethyl-Ether
Exp.	Experimental
HF	Hartree-Fock
HMIm	1-Hexyl-3-methylimidazolium
HOMO	Highest Occupied Molecular Orbital
IL	Ionic Liquid
IR	Infrared
I ₂ b15c5	Diiodo-Benzo-15-Crown-5
LUMO	Lowest Unoccupied Molecular Orbital
Me	Methyl
MeCN	Acetonitrile
MO	Molecular Orbital
MPWB1K	Modified Perdew-Wang Becke 95
MP2	Second-Order Møller-Plesset Perturbation Theory
Naph ₂	2,2'-Biquinoline

NMR	Nuclear Magnetic Resonance
NPA	Natural Population Analysis
NTf ₂	Bis-(Trifluoromethylsulfonyl)-Imide
OTf	Triflate
Ph	Phenyl
PPN	Bis-(Triphenylphosphine)-Iminium
Pr	Propyl
RHF	Restricted Hartree-Fock
RI-MP2	Resolution Of The Identity-MP2
RTIL	Room Temperature Ionic Liquid
r.t.	Room Temperature
SCS	Spin-Component Scaled
SI	Supporting Information
SVP	Split-Valence Basis Set
TMA	Trimesic Acid
UV/Vis	Ultraviolet-Visible
X,Y,Z	Halogen Atom

Abstract in English

This thesis deals with the synthesis and characterization of novel polychloride salts. The synthetic approach of conducting the reactions involving neat halogens, was adapted to fit the requirements of using chlorine as a gaseous reactant. Several previously unknown polychlorides were synthesized and characterized by means of vibrational spectroscopy and X-ray single crystal structure determination. This includes $[\text{Cl}_8]^{2-}$ the first polychloride dianion to be reported in literature as well as the first higher polychloride network $[\text{Et}_4\text{N}]_2[(\text{Cl}_3)_2\cdot\text{Cl}_2]$. Additionally two new structures of trichloride salts were found. One of which (N,N'-dimethyl-2-chloro-imidazolinium trichloride) containing the most regular trichloride anions to be reported so far. Under the use of different ionic liquids a convenient way to synthesize and crystallize higher polychloride salts was developed. Furthermore a broad variety of substances were tested towards their ability to chemically withstand treatment with elemental chlorine.

The polychloride monoanions $[\text{Cl}_5]^-$ and $[\text{Cl}_9]^-$ were successfully synthesized and characterized by Raman spectroscopy. All preparative work was accompanied by quantum-chemical calculations confirming and helping to interpret the results allowing insights to the bonding situation.

Having prepared a couple of polychloride salts it was possible to compare polychloride chemistry to that of polybromides and polyiodides, showing similarities as well as differences. Although not as manifold as polybromides and especially polyiodides, polychlorides exhibit similar structural motives and similar thermodynamic stability could be predicted. Major differences arise from the weaker bond energies enabling even higher polychlorides to form structures involving discrete anions that do not show any tendency to form networks as well as compounds that – very similar to known heavier polyhalides – form networks which are held together by halogen bonding as the driving force and main factor of their stability.

Finding a way to prove the existence of higher polychlorides in substances certainly cleared the way to attain a deeper understanding of polyhalide chemistry now being able to compare structures of all polyhalides except polyfluorides.

Zusammenfassung auf Deutsch

Die vorliegende Arbeit behandelt die Synthese und Charakterisierung neuartiger Polychloridsalze. Der Ansatz die Synthese mittels elementarer Halogene durchzuführen, wurde erfolgreich an die Anforderungen angepasst, die die Arbeit mit gasförmigem Chlor mit sich bringt. Mehrere unbekannte Polychloride konnten dargestellt und spektroskopisch, sowie strukturell charakterisiert werden. Dies beinhaltete $[\text{Cl}_8]^{2-}$, das bisher erste und einzige Polychloriddianion, sowie das erste Polychloridnetzwerk $[\text{Et}_4\text{N}]_2[(\text{Cl}_3)_2\cdot\text{Cl}_2]$. Des Weiteren konnten zwei neue Trichloridsalze strukturell aufgeklärt werden, darunter N,N'-dimethyl-2-chloroimidazoliniumtrichlorid, welches das regelmäßigste bislang bekannte Trichloridanion enthält. Durch den Einsatz verschiedener ionischer Flüssigkeiten konnte ein zur Synthese und Kristallisation höherer Polychloridsalze geeignetes Verfahren entwickelt werden. Ferner wurde ein breites Spektrum von Substanzen auf ihre chemische Stabilität in Bezug auf elementares Chlor untersucht.

Die Polychloridmonoanionen $[\text{Cl}_5]^-$ und $[\text{Cl}_9]^-$ konnten erfolgreich dargestellt und Raman-spektroskopisch charakterisiert werden. Alle präparativen Arbeiten wurden von quantenchemischen Berechnungen unterstützt, die wesentlich zu einem tieferen Verständnis der vorliegenden Bindungsverhältnisse beitrugen.

Nach der Darstellung mehrerer verschiedener Polychloridsalze eröffnete sich die Möglichkeit, durch den Vergleich mit Polybromiden und –iodiden Ähnlichkeiten, sowie Unterschiede aufzuzeigen. Trotz geringerer Vielfalt weisen die Strukturen von Polychloriden große Ähnlichkeit mit denen von Polyiodiden und –bromiden auf. Unterschiede kommen durch die geringeren Bindungsenergien zustande, welche dazu führen, dass Polychloridstrukturen sowohl diskrete Anionen ohne die Neigung zur Bildung von Netzwerken ausbilden, als auch Netzwerke, die durch Halogenbindungen stabilisiert werden.

Mit dem Nachweis der Existenz höherer Polychloride in Substanz eröffnet sich die Möglichkeit durch strukturellen Vergleich aller Polyhalogene, mit Ausnahme von Polyfluoriden, ein tieferes Verständnis der zugrunde liegenden chemischen Verhältnisse zu erreichen.

1 Table of Content

1 TABLE OF CONTENT	1
2 INTRODUCTION	4
2.1 HISTORIC OVERVIEW	4
2.2 HALOGEN BONDING.....	5
2.3 POLYIODIDES	9
2.4 POLYBROMIDES	9
2.4.1 <i>Structural Diversity</i>	9
2.4.2 <i>Applications</i>	13
2.5 POLYCHLORIDES	14
2.5.1 <i>Structures</i>	14
2.5.2 <i>Applications</i>	17
2.6 POLYFLUORIDES	18
2.7 INTERHALIDE ANIONS	19
2.8 SYNTHETIC AND ANALYTICAL APPROACHES.....	22
3 OBJECTIVE	24
4 RESULTS AND DISCUSSION	25
4.1 QUANTUM CHEMICAL AND RAMAN SPECTROSCOPIC INVESTIGATION OF POLYCHLORIDE MONOANIONS.....	25
4.2 STABILITY OF CATIONS AGAINST ELEMENTAL CHLORINE	33
4.2.1 <i>Ammonium Cations</i>	34
4.2.2 <i>Other N-based Cations</i>	38
4.2.3 <i>Other Cations</i>	40

4.3 INVESTIGATION OF SUITABLE CONDITIONS FOR THE CONVENIENT CRYSTALLIZATION OF POLYCHLORIDE SALTS	41
4.4 CRYSTAL STRUCTURES	47
4.4.1 <i>N,N'</i> -Dimethyl-2-Chloroimidazoliniumtrichloride	47
4.4.2 Tetramethyl-Chloro-Amidinium Trichloride $[\text{CCl}(\text{NMe}_2)_2][\text{Cl}_3]$	50
4.4.3 $[\text{Et}_4\text{N}]_2[(\text{Cl}_3)_2\cdot\text{Cl}_2]$: A 2D Polychloride Network Held Together by Halogen–Halogen Interactions	54
4.4.4 Tetramethyl-Chloro-Amidinium Octachloride $[\text{CCl}(\text{NMe}_2)_2]_2[\text{Cl}_8]$: Structural Proof for the First Dianion of a Polychloride	60
4.4.5 Summarized Crystallographic Data	67
4.5 CONDUCTIVITY MEASUREMENTS	71
5 SUMMARY AND CONCLUSION	73
6 EXPERIMENTAL SECTION	76
6.1 PREPARATION OF $[\text{Et}_3\text{MEN}]\text{Cl}$ AND $[\text{Et}_3\text{PRN}]\text{Cl}$	76
6.2 METHODS OF CRYSTALLIZATION	76
6.3 PREPARATION OF TETRAMETHYLCHLOROAMIDINIUMTRICHLORIDE	77
6.4 PREPARATION OF <i>N,N</i> -DIMETHYL-2-CHLOROIMIDAZOLINIUMTRICHLORIDE	78
6.5 OBTAINING VIBRATIONAL AND CRYSTAL DATA	78
6.6 QUANTUM CHEMICAL CALCULATIONS	79
7 REFERENCES	80

Publications used for cumulative thesis:

- [RB1] R. Brückner, H. Haller, M. Ellwanger, S. Riedel, Polychloride Monoanions from $[\text{Cl}_3]^-$ to $[\text{Cl}_9]^-$, *Chem. Eur. J.*, **2012**, *18*, 5741-5747.
- [RB2] R. Brückner, H. Haller, S. Steinhauer, C. Müller, S. Riedel, A 2D Polychloride Network Held Together by Halogen-Halogen Interactions, *Angew. Chem. Int. Ed.* **2015**, *54*, 15579–15583, *Angew. Chem.* **2015**, *127*, 15800–15804.
- [RB3] R. Brückner, P. Pröhm, A. Wiesner, S. Steinhauer, C. Müller, S. Riedel, Structural Proof for the First Dianion of a Polychloride: Investigation of $[\text{Cl}_8]^{2-}$, *Angew. Chem. Int. Ed.* **2016** (accepted).

2 Introduction

2.1 Historic Overview

Polyhalide anions are a class of chemical compounds well known to chemists for almost two hundred years. The most commonly known polyhalides are probably polyiodides which are the reason for the well-known blue coloring of starch in the presence of iodine known as the iodine test, for example. First scientific reference dates back to 1819 when Pelletier and Caventou discovered strychnine triiodide.^[1] The first systematic investigation of polyiodides however, was started by Jörgensen in 1870.^[2] Today, the family of polyiodides exhibits a vast chemistry including mono-, di-, tri- and tetra-anions up to $[I_{26}]^{4-}$. This chemistry has already been systematically investigated and summarized in a number of reviews.^[3–8] It took about a century until the trihalides of the lighter homologues bromine and chlorine were discovered by Chattaway and Hoyle by adding elemental halogens to several alkylammonium halides in 1923.^[9] The tribromide $[Br_3]^-$ has for a long time been the only polybromide known. Evans et al. gave the first hint for the existence of higher polybromide monoanions by the spectroscopically investigation of $[Br_5]^-$ in 1967.^[10] Structural proof for higher polybromide monoanions has only been given recently for $[Br_5]^-$, $[Br_7]^-$, $[Br_9]^-$ and $[Br_{11}]^-$.^[11–15] Structural proofs of polybromide dianions exist for $[Br_4]^{2-}$, $[Br_8]^{2-}$, $[Br_{10}]^{2-}$, $[Br_{20}]^{2-}$ and $[Br_{24}]^{2-}$.^[16–20] The highest polybromide dianions known are $[Br_{20}]^{2-}$ and $[Br_{24}]^{2-}$ that were reported in 2011 by Feldmann et al.^[19] and 2015 by Maschmeyer et al.^[20] Both anions exhibit a complex network structure showing that the tendency to form large networks is not only limited to polyiodides. The chemistry of polychlorides is much more limited. So far only four crystal structures of trichlorides were known. Starting in 1981 $[AsPh_4][Cl_3]$ was reported by Bogaard et al.^[21] two further structures were given in 1985 by Boéré et al.^[22] as well as Chivers et al.^[23] the most recent structure $[PPh_4]Cl$ being reported in 1995 by Jansen et al.^[24] The only polychloride besides the pure $[Cl_3]^-$ was $[PPh_2Cl_2]^+ [Cl_3 \cdots Cl_2]^-$ reported by Taraba and Zak in 2003.^[25] Polychlorides with a higher chlorine content than $[Cl_3]^-$ or dianions are unknown. Yet only spectroscopic evidence for the $[Cl_5]^-$ anion could be given by Evans and Lo in 1966.^[26] Regarding polyfluorides there are no structural proofs of any

polyfluoride yet. However the trifluoride anion $[\text{F}_3]^-$ could be observed spectroscopically as part of an ion pair $[\text{M}]^+[\text{F}_3]^-$ ($\text{M} = \text{K}, \text{Rb}, \text{Cs}$) in argon matrices by Ault and Andrews in 1976.^[27] The free $[\text{F}_3]^-$ anion could be observed in rare gas and N_2 matrices at 4 K and 10 K in 2010.^[28,29] And very recently, the pentafluoride anion $[\text{F}_5]^-$ was found to be a stable species in Ne matrices at 4 K.^[30]

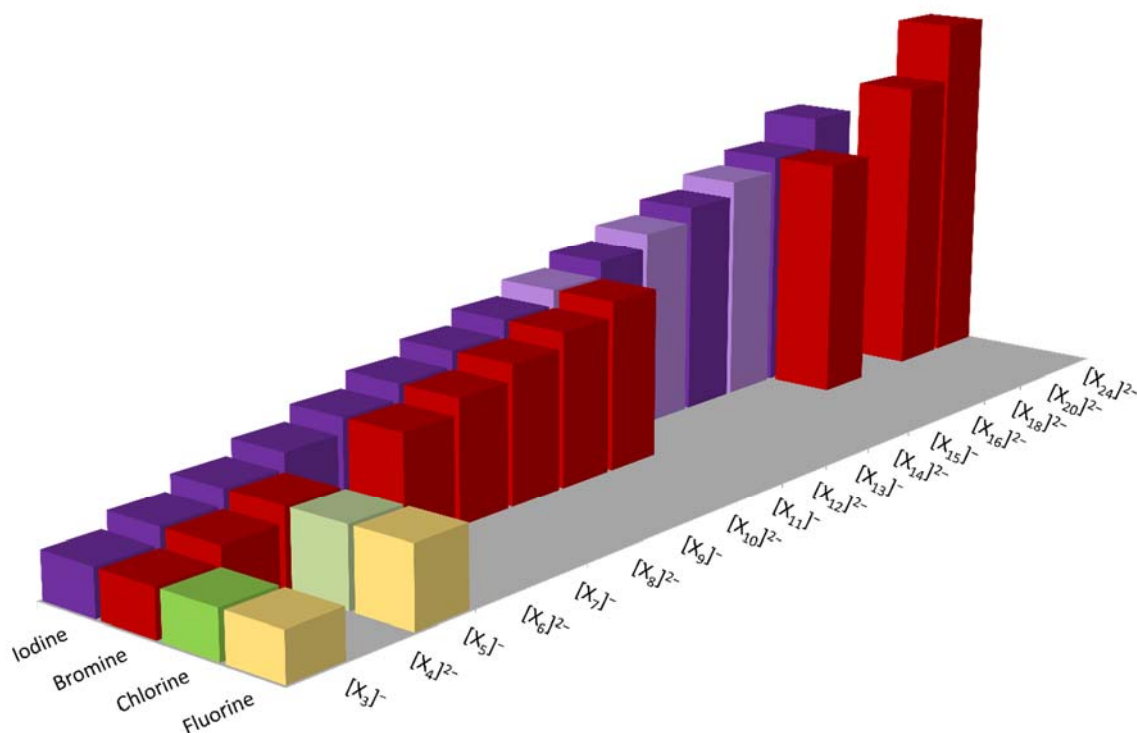
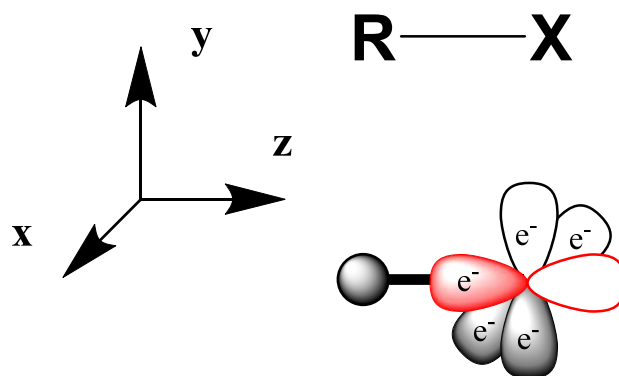


Figure 2.1 Display of known polyhalide mono- and dianions, pale colored items represent those only known by spectroscopic evidence (updated version of Figure 1 in ^[31], state 2012).

2.2 Halogen Bonding

Generally polyhalides can be described as donor-acceptor complexes with $[\text{X}]^-$ and $[\text{X}_3]^-$ as Lewis bases and the X_2 molecule as Lewis acid. All polyhalides are composed of these basic building blocks. The central halide ion donates electron density from its HOMO into the LUMO of the halogen molecule, thereby elongating the $\text{X}-\text{X}$ bond of the X_2 molecule. Depending on the specific halide this donation is not limited to only one halogen molecule but can lead to large anions up to $[\text{Br}_{11}]^-$, for example. This building concept allows access to a high number of different structures. Monoanions

usually being formed of an odd-numbered quantity of halogen atoms often form highly symmetrical structures such as tetrahedrons. With increasing halogen content the tendency to form complex 2- or 3-dimensional networks increases. This is even more relevant regarding di-, tri- or tetra-anions mostly existing as 3-dimensional networks which are difficult to describe due to problems in cutting the network into describable pieces. This type of behavior cannot solely be described through Lewis base/Lewis acid interactions anymore and is better described by the term of halogen bonding.^[32] A particular term often used along with the concept of halogen bonding are so-called σ -hole interactions.^[33] The so-called σ -hole derives from the unequal distribution of the electron density in halogen atoms. Halogen atoms possess a “belt” of negative electrostatic potential situated perpendicular to their bonding axis. In extension of this bonding axis the halogen atom is more positively charged leading to a “hole” of more positive electrostatic potential – the so-called σ -hole. This leads to electrostatic “belt-hole” interactions with a preferred bonding angle of around 90° . Although these σ -hole are not solely limited to halogens their appearance is most prominent in association with halogen bonding. Even though the discussion about the nature and the reason for the existence of σ -holes is not yet fully concluded, a possible explanation was very recently given by Kolar and Hobza.^[34] The valence shell of a bonded chlorine atom, for example, has an electron configuration of $3s^2 3p_x^2 3p_y^2 3p_z^1$, where the z-axis is similar to the Cl bond axis. The electron in the p_z orbital will mostly be localized in the bond region, leading to a lack of electron density in the opposite lobe of the p_z -orbital. Additionally the electron pairs in the p_x and p_y orbitals are mainly located perpendicularly to the bond axis, thus creating a region of negative electrostatic potential.^[34]



Scheme 2.1 Schematic display of p_x , p_y and p_z valence orbitals of a halogen atom, showing electron localization and electron deficiency in p_z , expressing itself as σ -hole.^[34]

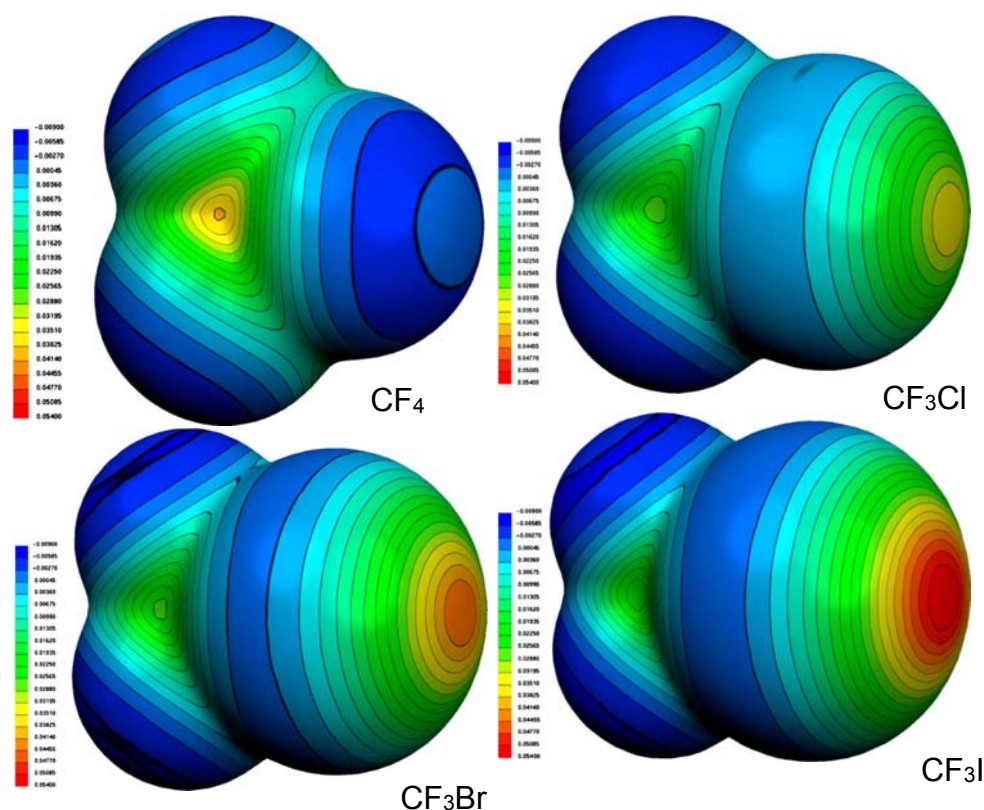
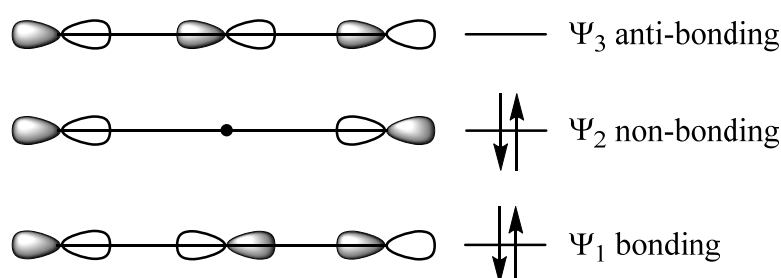


Figure 2.2 Mapping of the calculated molecular electrostatic potential, in Hartree, at the 0.001 e/bohr³ isodensity surface of CF₄, CF₃Cl, CF₃Br, and CF₃I. Copyright 2007 Springer.^[33]

Figure 2.2 shows mapped electrostatic potential of different halocarbons emphasizing the difference between the different halogens concerning their σ -hole.^[33] While the question whether fluorine possesses a σ -hole at all is not yet fully answered, the other halogens show σ -holes of different size and shape. Iodine exhibiting the most distinct σ -hole is therefore very often involved in halogen-bonded compounds but also bromine and chlorine are able to take part in this kind of interactions.^[35,36] These interactions provide a large contribution to the stability of halogen bonds in general, and particularly to halogen bonds between two or more halogen atoms, so-called halogen-halogen interactions. In the upcoming chapters we will often encounter bond angles of nearly 90° or at least the interacting polyhalide anions often form right-angled super-lattices. As already mentioned above σ -hole interactions are not limited to halogens only, but can also be found in chalcogens, pnictogens and even group 14 elements. In these elements however the σ -holes are composed differently therefore preferring different bond angles depending on the element observed.^[34] Recent publications investigating the electronic structure of halogen bonds have proved them to be closely related to

hydrogen bonds as both have indeed quite similar properties, especially regarding stabilization energies.^[32,34,35]

The bonding situation in the more simple trihalides can be described in a different way. If the trihalide is symmetric and linear and therefore iso(valence)electronic to XeF₂ the bond can be described as a 3-center/4-electron bond.



Scheme 2.2 Bonding situation in a simple trihalide anion.

For asymmetric trihalides and higher polyhalides the halogen bonded donor-acceptor complex is the more suitable description. Detailed discussion of the bonding situation in trihalides has been given by Hoffmann et al.^[37] and Aragoni et al.^[38] Scheme 2.2 indicates a concentration of the negative charge on the lateral atoms as these are the main contributors to the filled non-bonding MO. Quantum-chemical calculations support this assumption showing that the negative charge evenly concentrates on the lateral atoms, leaving the central atom with much less negative charge, see Table 2.1.

Table 2.1 NPA-charges and bond lengths of the halogen atoms in the different trihalides.^[37]

Element	Q(X _{term}) ^[a]	Q(X _{cent}) ^[a]	r(X ₂) ^[a]	r([X ₃]) ^[a]
F	-0.412	-0.177	142	177
Cl	-0.419	-0.162	204	237
Br	-0.415	-0.169	236	264
I	-0.419	-0.163	286	314

^[a]Charges and bond lengths optimized at BP86 level with triple- ζ basis set

2.3 Polyiodides

Polyiodides can be found as mono-, di-, tri- and tetra-anions of different size and composition, reaching from the small $[I_3]^-$ up to the large 3-dimensional network of $[I_{26}]^{4-}$. In general polyiodides show a high tendency to form polymeric networks driven by the strong halogen bonding ability of iodine. As already mentioned above, the chemistry of polyiodides is vast and exhibits a tremendous structural diversity that exceeds the length of this work. Therefore, polyiodides will not be discussed in detail in this work. Specific polyiodides will be discussed for comparison to bromide and chloride species later on. For detailed information consult the reviews of Kloo et al. from 2003 and 2013.^[7,8]

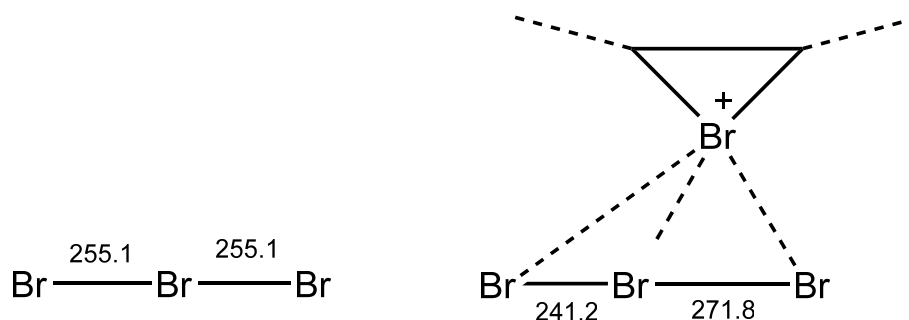
2.4 Polybromides

Even though polybromide anions were quite rare just a couple of years ago, intensive research in recent years have led to a great number of compounds and structures by now.^[31] Therefore a lot of different structural motives that give an insight into the composition of polyhalides in general and of polybromides particularly are known so far. Polybromides can be separated into odd-numbered monoanions and even-numbered dianions. Higher charged anions are unknown, so far.

2.4.1 Structural Diversity

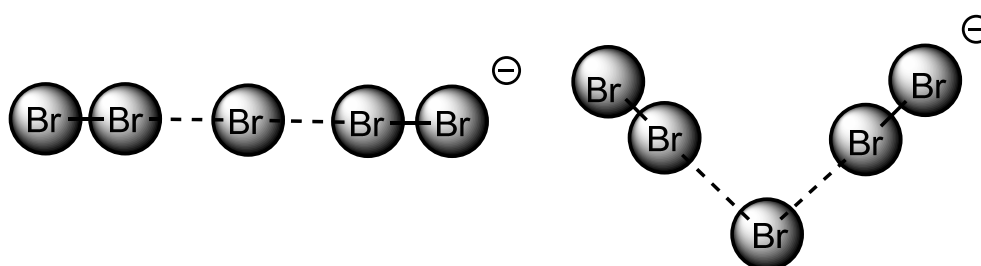
The smallest and simplest anion, the tribromide has been the only known polybromide for a long time. After the first description by Chattaway and Hoyle in 1923^[9] it took another 34 years until the first spectroscopic proof for the higher $[Br_5]^-$ was given by Evans et al. in 1967.^[10] Systematic spectroscopic investigation of the polybromide anions $[Br_3]^-$ to $[Br_9]^-$ was provided by Chen et al.^[39] Structural data for a lot of tribromides including many different counter ions is available.^[40,41] All known

tribromides are linear and symmetric geometry was found for about a fourth of the crystal structures. Asymmetry is due to anion-cation interactions within the crystal. Asymmetric tribromides mostly involve cations that possess a coordination site, such as bromonium-adamantylideneadamantane which exhibits a three-membered bromonium cation, see Scheme 2.3.^[42]



Scheme 2.3 Comparison of symmetric and asymmetric tribromides, the latter being distorted by anion-cation interactions.

The difference of the bond length of asymmetric tribromides may vary from a few pm up to 30 pm in case of the bromonium complex in Scheme 2.3.^[41] This phenomenon can also be observed for triiodides and trichlorides.^[7] First note of a crystal structure of $[\text{Br}_5]^-$, the next higher polybromide a pentabromide was given by Herbstein et al. in 1981.^[43] Unfortunately they failed to determine the structure of trimesic acid (TMA) pentabromide that was possibly isomorphous to a rare linear TMA pentaiodide reported in the same publication.



Scheme 2.4 Possible conformations of Br-atoms in $[\text{Br}_5]^-$.

Quantum-chemical calculations at different levels of theory (MPWB1K, B3LYP, HF and MP2) and different basis sets predict the V-shaped structure with C_{2v} symmetry to be about $16 \text{ kJ}\cdot\text{mol}^{-1}$ lower in energy than the linear structure.^[39,44] First structural proof

for a $[\text{Br}_5]^-$ anion was reported in 2012 by Himmel et al.^[14] The structure shows the predicted C_{2v} symmetry of the $[\text{Br}_5]^-$ anion as well as close contacts between different $[\text{Br}_5]^-$ anions which are below the sum of the van-der-Waals radii of bromine (370 pm).^[45] This indicates the tendency of polybromides to form networks in the solid state.

The next polybromide anion in line is the $[\text{Br}_7]^-$ anion. The spectroscopic results of Chen et al.^[39] were in agreement with quantum-chemical results by Pichierri,^[44] favoring a trigonal pyramidal structure (C_{3v}) over a trigonal planar one (D_{3h}). The first crystal structure of a $[\text{Br}_7]^-$ anion was provided by Feldmann et al. in 2011 by a reaction in an eutectic mixture of ionic liquids as reaction media, yielding $[(\text{Ph})_3\text{PBr}][\text{Br}_7]$.^[13] The structure contains C_{3v} -symmetrical trigonal pyramidal $[\text{Br}_7]^-$ anions which are again part of an extensive polybromide network. For this compound the cation also participates in a network as the Br – Br distance between the Br-atom of the cation and the nearest Br-atom of the $[\text{Br}_7]^-$ anion is only 349.9 pm and therefore, shorter than the sum of the van-der-Waals radii. Figure 2.3 shows the connectivity of the $[\text{Br}_7]^-$ units.

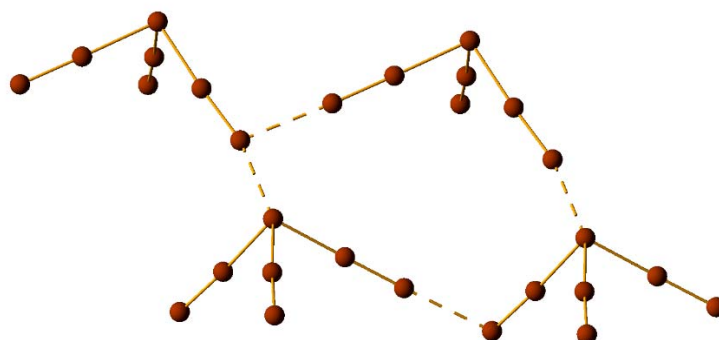


Figure 2.3 Detail of the anionic network in $[(\text{Ph})_3\text{PBr}][\text{Br}_7]$ showing connectivity of the $[\text{Br}_7]^-$ units.

Another compound containing $[\text{Br}_7]^-$ has been synthesized by Pritchard et al. in 2013,^[46] also exhibiting a C_{3v} -symmetrical trigonal pyramidal $[\text{Br}_7]^-$ anion which participates in a polybromide network.

$[\text{Br}_9]^-$ is the only higher polybromide which is known with a couple of different counter ions. This includes the symmetric quaternary ammonium cations $[\text{NMe}_4]^+$, $[\text{NEt}_4]^+$, $[\text{NPr}_4]^+$ and $[\text{NBu}_4]^+$ and imidazolium cations e.g. $[\text{HmIm}]^+$.^[11,12,47] The nonabromide anion generally exhibits a tetrahedral structure with four Br_2 -units coordinated to a

central bromide anion. The Br–Br bond lengths differ slightly according to the counter ion, but within the expected range taking into account those of $[\text{Br}_5]^-$ and $[\text{Br}_7]^-$. The exact geometry and connection of the nonabromide units strongly depends on the cation. While $[\text{NMe}_4][\text{Br}_9]$ and $[\text{NPr}_4][\text{Br}_9]$ show a quite regular tetrahedral structure, the structure of $[\text{NEt}_4][\text{Br}_9]$ and $[\text{HMIm}][\text{Br}_9]$ is more distorted, resulting in a six fold coordination of the central bromide anion, although two bond lengths are significantly longer than the other ones.^[12,47] Examples are given in Figure 2.4.

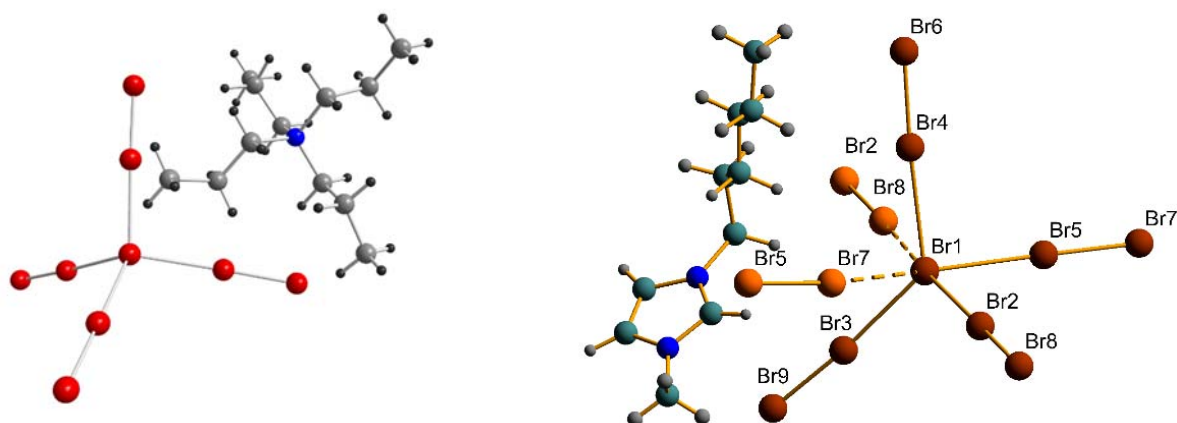


Figure 2.4 Molecular structures of $[\text{NPr}_4][\text{Br}_9]$ (left) and $[\text{HMIm}][\text{Br}_9]$ (right) in the crystal.

All nonabromide units are interconnected to form different kinds of networks. These kinds of network depend on the present cation. For the quaternary ammonium salts the general rule appears to be that smaller cations decrease the complexity of the network. So in $[\text{NMe}_4][\text{Br}_9]$ the nonabromide units are connected to chains, while in $[\text{NEt}_4][\text{Br}_9]$ they form layers. In $[\text{NPr}_4][\text{Br}_9]$ and $[\text{NBu}_4][\text{Br}_9]$ the nonabromide units are connected to three dimensional networks.

Finally the largest structurally known polybromide monoanion is $[\text{Br}_{11}]^-$ which is known as $[\text{PPN}][\text{Br}_{11}\cdot\text{Br}_2]$ (PPN = bis(triphenylphosphine)iminium) which has been structurally characterized in 2013 by Haller et al.,^[15] after $[\text{I}_{11}]^-$ had been detected in the gas phase by Groessl et al. in 2011.^[48] Analogous to the other polybromides the $[\text{Br}_{11}]^-$ anion exhibits a highly symmetrical structure. In the crystal the anion is shaped nearly perfectly like a square-based pyramid. Additionally to the structural characterization $[\text{Br}_{11}]^-$ has also been intensively investigated using quantum-chemical calculations.^[15] Even though the optimized structure using DFT functionals (e.g. B3LYP) shows a global minimum for a C_s -symmetrical structure that was already calculated for $[\text{I}_{11}]^-$, ab

initio methods (e.g. SCS-MP2) that proved to perform well in earlier investigations of polyhalides preferred the D_{3h} - and C_{4v} -symmetrical structures. In case of [PPN][Br₁₁·Br₂] the [Br₁₁][−] anion is forced into the nearly square-pyramidal structure by crystal packing effects, showing a τ -value of 0.^[49]

In contrary to the chemistry of polybromide monoanions which were mainly discovered in recent years, the investigation of polybromide dianions already began in 1959 as Strømme described the [Br₄]^{2−} dianion which is almost linear but exhibits bond lengths differing about 60 pm between the inner and the outer bonds.^[16] This is very similar to another polybromide dianion, namely [Br₁₀]^{2−}. This dianion is rectangularly shaped and consists of two [Br₃][−] units interconnected by two Br₂ units.^[18] The bond lengths within the [Br₃][−] units and between [Br₃][−] and Br₂ also differ about 60 pm. All bond lengths in this dianions are considerably elongated which emphasizes the coordination complex alike character of this dianion. Furthermore the [Br₈]^{2−} was first described in 1997 by Robertson et al.^[17] So far 3 crystal structures containing the [Br₈]^{2−} dianion are known.^[13,17,50] In all these structures [Br₈]^{2−} exists as a Z-shaped anion consisting of two [Br₃][−] units connected by one Br₂ unit. Another polybromide dianion is [Br₂₀]^{2−} which was characterized with two different counter ions by Feldmann et al..^[19] [Br₂₀]^{2−} possesses a very complex structure which can alternatively described as [(Br[−])₂·9(Br₂)]. The largest known polybromide dianion is [Br₂₄]^{2−} very recently reported by Maschmeyer et al.^[20] The structure resembles that of [Br₁₁·Br₂][−] very much it basically differs only by the orientation of the coordinated Br₂ molecule, making it possible to merge two [Br₁₁][−] units with a Br₂ unit thus resulting in a [Br₂₄]^{2−} dianion.

2.4.2 Applications

Due to the weakened Br – Br bond tribromides are a convenient, easy-to-handle bromination reagents in organic chemistry for over thirty years by now.^[51–53] Advantages are high selectivity along with good reactivity and low bromine vapor pressure. Further research by Belucci et al. suggested that the equilibrium of [Br₃][−] and [Br₅][−] might play a role in the formation of the intermediate bromonium ions in bromination reactions.^[54] Recently, first experiments for the use of nonabromides as

bromination reagents have been carried out with promising results. Especially concerning yield and selectivity $[\text{NPr}_4][\text{Br}_9]$ has quite an edge over elemental bromine and shows almost quantitative yields and good selectivity with lots of different organic compounds.^[55,56] Recent investigation on now accessible nonabromides showed that these substances exhibit an extremely high electrical conductivity.^[47] This is most likely accounted to a Grotthuss-type hopping mechanism for bromide anions.^[57] Therefore polybromides and especially nonabromides exhibit potential application in new redox-flow battery systems and could perhaps substitute polyiodides (especially the system $[\text{I}_3]^-/\text{I}^-$) in dye-sensitized solar cells. A recent study showed that the system $[\text{Br}_3]^-/\text{Br}^-$ exhibits a higher open circuit photo potential compared to the equivalent polyiodide system.^[58]

2.5 Polychlorides

2.5.1 Structures

As already mentioned polychlorides exhibit a much smaller diversity compared to the heavier homologues. The huge variety of polyiodides and nearly one hundred polybromides stand against five polychlorides that are structurally known. On the one hand this is probably due to the stronger electrostatic repulsion effects that arise from shorter bond lengths. On the other hand the unfavorable entropic balance caused by the gaseous state of Cl_2 at room temperature leads to a destabilization of the polychlorides compared to polybromides and polyiodides. The history of polychlorides started along with the polybromides in 1923 with the work of Chattaway and Hoyle.^[9] But in the following 80 years no other polychlorides than trichlorides were reported in literature. The four known crystal structures of trichlorides along with bond lengths and angles are listed in Table 2.2.

Table 2.2 Structurally known polychlorides.

Compound	Bond lengths ^[a]	Bonding angle ^[b]	Year of publication
[As(Ph) ₄][Cl ₃] (1)	222.7/230.5	177.5	1981 ^[21]
[(Me ₂ NC(Cl)N) ₂ SCI][Cl ₃] (2)	224.9/234.0	177.5	1985 ^[23]
[(Me ₂ N) ₂ C ₂ N ₄ S ₂ Cl][Cl ₃] (3)	218.3/239.3	177.7	1985 ^[22]
[P(Ph) ₄][Cl ₃] (4)	226.3/230.7	178.4	1995 ^[24]

^[a]: in pm; ^[b]: in °

As apparent in Table 2.2 none of the reported trichlorides is symmetrical. On the one hand that is surprising because in triiodides as well as in tribromides symmetric structures are common. On the other hand it might be an effect of the higher electric charge density on the surface of the molecule leading to stronger anion-cation interactions. This is in accordance with the observation, that the least asymmetrical trichlorides are salts of the weakly coordinating cations [As(Ph)₄]⁺ and [P(Ph)₄]⁺. All trichlorides are linear and exist as discrete anions in the crystal. These compound can be separated into two different structural categories. Compounds (**2**) and (**3**) consist of large cations mainly consisting of heteroatoms such as sulfur or nitrogen. In these compound the asymmetrical anions are placed parallel to one another not showing any signs of interanionic contacts as the distances are very long. Structures of the compounds (**1**) and (**4**) are very similar which is not remarkable as the cations [As(Ph)₄]⁺ and [P(Ph)₄]⁺ are just differing by their central atom. In these structures the [Cl₃]⁻ anions form long ranging zig-zag chains and even though interanionic distances exceed the sum of the van-der-Waals radii their positioning suggests weak interactions between the [Cl₃]⁻ anions. An example for both types is shown in Fig. 2.5.

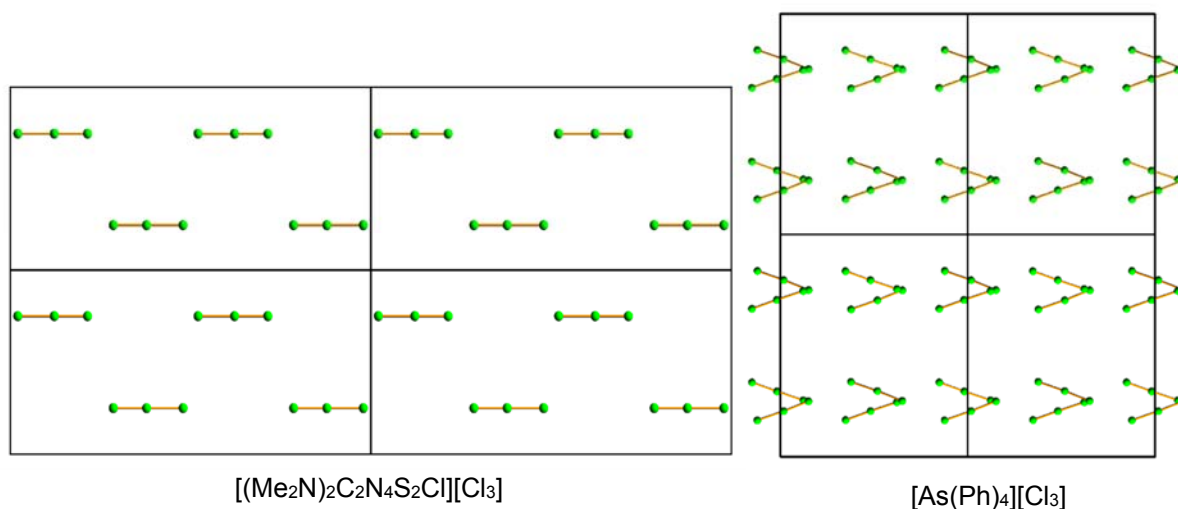


Figure 2.5 Comparison of the anion arrangement in **(3)** (left) and **(1)** (right) revealing parallel anion structure in **(3)** and zig-zag chains in **(1)**.

$[\text{PPh}_2\text{Cl}_2][\text{Cl}_3 \cdot \text{Cl}_2]$ was the only higher polychloride known so far and its structural proof was reported in 2003.^[25] This compound, sometimes referred to as “[Cl_5][−]”, consists of a highly asymmetric $[\text{Cl}_3]^-$ unit with a coordinated Cl_2 unit forming a “hockey-stick” like structure. Bond lengths in the $[\text{Cl}_3]^-$ unit differ by 27.5 pm and therefore exhibit a greater divergence than in any pure trichloride. The Cl_2 unit is loosely bound with a bond length of 317.1 pm which is well below the sum of the van-der-Waals radii of chlorine (350 pm)^[45] but considerably longer than other Cl–Cl bonds in polychlorides. In this compound the anions form a kind of 2D-network. The anions are arranged in strings made of rectangular units which are themselves stacked to layers, see Fig. 2.6.

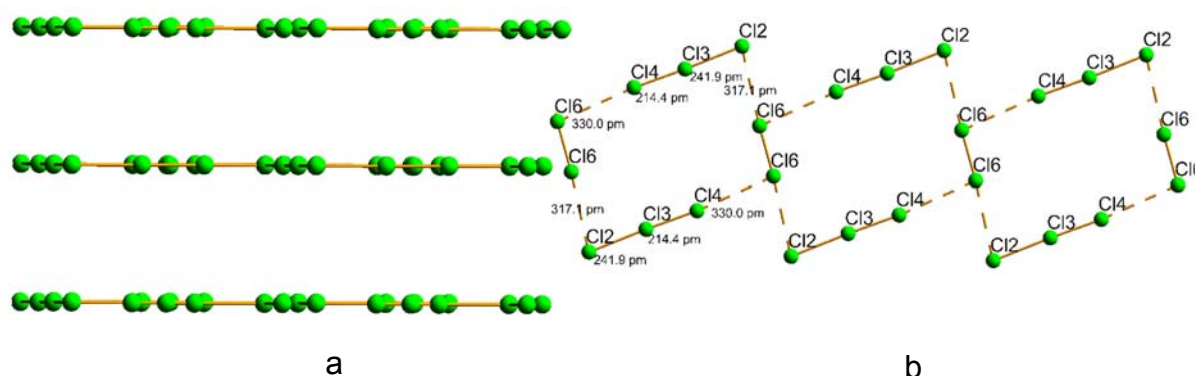


Figure 2.6 Details of the anionic arrangement in $[\text{PPh}_2\text{Cl}_2][\text{Cl}_3 \cdot \text{Cl}_2]$ showing layers (a) and top view (b) of an anionic string with displayed bond lengths.

Additionally the layers are connected among themselves as well by the chlorine atoms of the cations. These bonds (322.5 pm) are shorter than the sum of the van-der-Waals radii (350 pm).^[45] Considering the anion-cation-interactions the structure can be described as a network based on halogen bonding, see Fig. 2.7.

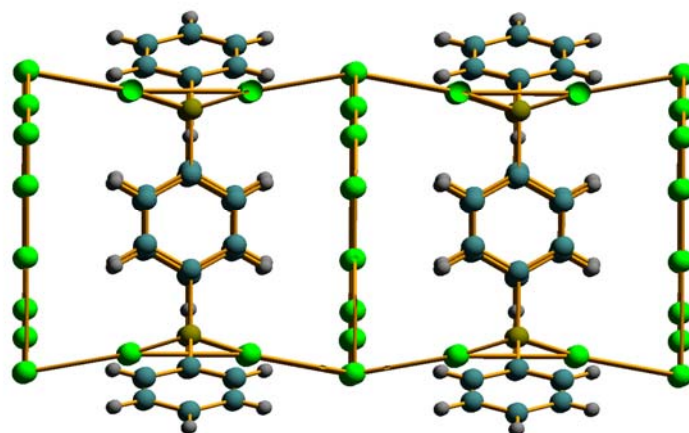


Figure 2.7 Detail of the crystal structure of $[PPh_2Cl_2][Cl_3 \cdot Cl_2]$ showing layers which are interconnected by Cl atoms of the cations.

2.5.2 Applications

In recent years more and more applications involving polyhalides have caught the interest of the scientific community. Several trichlorides are used as chlorinating agents.^[59] Especially tetraethylammoniumtrichloride has already been successfully tested as chlorinating and oxidizing agent for a variety of organic substrates.^[60] As most of these compounds exist as solids or liquids they bear several obvious advantages and even show higher selectivity compared to elemental chlorine.^[60]

2.6 Polyfluorides

For polyfluoride anions no structural proof is yet available. First reference concerning polyfluorides was issued in 1952 by Bode and Klesper who exposed alkaline metal chlorides to a flow of fluorine gas at 140°C – 220°C.^[61] They supposed the products to be MF₃ (M = Rb, Cs) with either an [F₃][−] anion or the alkaline metal in the oxidation state +III after analyzing them by gravimetry and powder diffraction. In 1961 however their results were doubted by Asprey et al. who identified similarly yielded products as fluorochlorates ([ClF₄][−]).^[62] First vibrational detection was made 1976 by Ault and Andrews under cryogenic conditions in argon matrices.^[27] They investigated alkaline metal fluorides by IR and Raman spectroscopy within an argon/fluorine matrix (ratio 400:1) at 15 K. Only one band could be observed in their IR spectra which was at 550 cm^{−1} and assigned to the asymmetric stretching mode of [F₃][−]. The band of the symmetric stretching mode could be observed at 461 cm^{−1} in the corresponding Raman spectra. They supposed a linear symmetric [F₃][−] anion in *D*_{∞h} symmetry in analogy to the other trihalides. Furthermore in mass-spectroscopic studies of [F₃][−] the bond dissociation energy has been determined to be 98±11 kJ·mol^{−1}.^[63] This is in well agreement with those of the trihalides of chlorine (99±5 kJ·mol^{−1})^[64], bromine (127±7 kJ·mol^{−1})^[64] and iodine (126±6 kJ·mol^{−1}).^[65] The isolated trifluoride anion could be detected in argon and neon matrices in 2010.^[28] In contrast to the previously known band at 550 cm^{−1} typical for cation-anion complexes, the isolated trifluoride anion shows IR bands at 510.6 cm^{−1} in argon and 524.7 cm^{−1} in neon matrices, respectively. However all attempts to prepare [F₃][−] in bulk or in solution yet failed.^[66] In 2010 it was also supposed that the [F₅][−] anion could indeed be a stable species as high level quantum-chemical calculations computed the elimination of F₂ from [F₅][−] forming [F₃][−] to be endothermic by 18.0 kJ·mol^{−1} at the CCSD(T)/aug-cc-pVTZ level.^[28] The optimized minimum structure of [F₅][−] at CCSD(T)/aug-cc-pVTZ level was surprisingly calculated to be the C_s symmetrical “hockey-stick” like structure already known from [PPh₂Cl₂]⁺ [Cl₃·Cl₂][−] being 6.2 kJ·mol^{−1} preferred over the regular V-shaped structure which is predicted for the heavier homologues [Cl₅][−], [Br₅][−] and [I₅][−],^[28] see Fig 2.8.

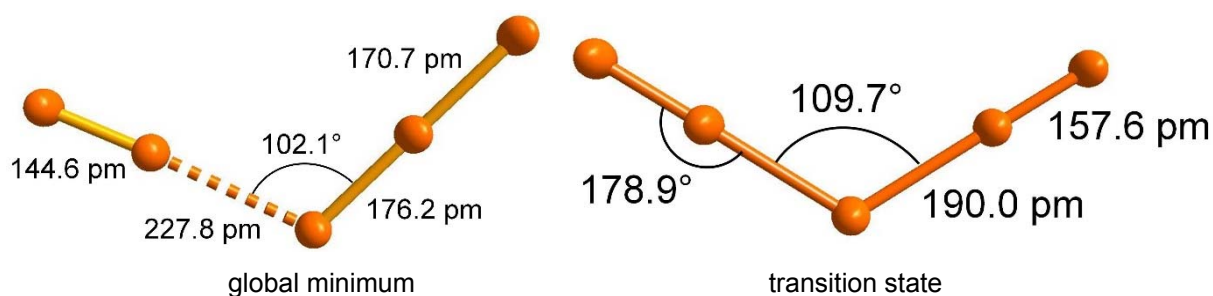


Figure 2.8 Structures of $[F_5]^-$ optimized at CCSD(T)/aug-cc-pVTZ level showing the global minimum hockey-stick structure (left) and V-shaped transition state (right).

Finally in 2015 the $[F_5]^-$ anion could be detected in Ne matrices at 4 K.^[30] The spectroscopic results suggest that the structure of the observed $[F_5]^-$ species is indeed C_{2v} symmetrical and therefore the $[F_5]^-$ anion possesses a regular V-shaped structure. This is thoroughly possible as for the hockey-stick structure a very shallow potential energy surface along the bending angle at the central F atom was found. Modification of the bending angle by 20° requires only around 1.5 kJ·mol⁻¹. Very recently new insights in polyfluoride chemistry have been reported concerning the use of neat fluorine as host material under cryogenic conditions^[67] as well as differences between free $[F_3]^-$ and MF_3 complexes (M = Rb, Cs).^[29]

2.7 Interhalide Anions

In addition to pure polyhalide anions also mixed polyhalides – the polyinterhalide anions exist. Considering these species we have to differentiate between “classical” and “non-classical” interhalide anions. Classical interhalide anions are well-known and built of an electropositive center surrounded by electronegative bonding partners, e.g. $[BrCl_2]^-$, $[ICl_4]^-$. A lot of works have been published concerning such compounds, see for example ^[68–70]. Apart from these classical interhalide anions we introduced the term of “non-classical” interhalide anions.^[31] In contrast these anions consist of an electronegative halide as center that coordinates one or more halogen or interhalogen molecules. Although very little examples are to be found in literature by now, this substantially increases the diversity of possible interhalide anions. One sort of these

non-classical interhalides are anions of the general formula $[X(YY)_n]^-$. Probably the most simple example is the $[I_2Cl]^-$ anion which consists of a diiodine molecule coordinated by a chloride anion. This species can be found in $[C_{12}H_9N]^+_2 [I_2Cl]^- [ICl_2]^-$ ($[C_{12}H_9N]^+ = \text{bis}(1,10\text{-phenanthroline-1-ium})$) for example.^[70] This compound contains the classical interhalide $[ICl_2]^-$ as well as the non-classical one $[I_2Cl]^-$ which form chains along one axis. The I–I bonds in this species are only slightly elongated and the I – Cl distances of 304.04 and 315.84 pm suggests covalent bonds. Another example is $[(H_5O_2)(I_2b15c5)_2][Cl(I_2)_4]$ that consists of a crown ether complex and the interhalide anion $[Cl(I_2)_4]^-$.^[71] Most remarkably about this anion is the square-planar coordination of the diiodine molecules which was expected to be tetrahedral.

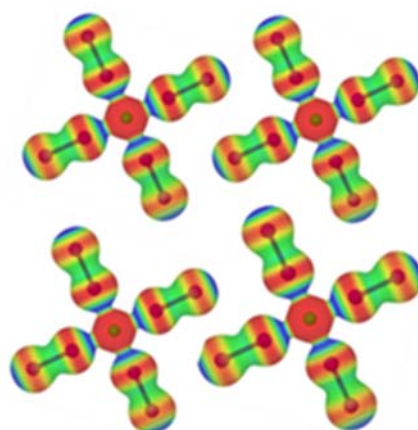


Figure 2.9 *Electrostatic potentials plot of $[Cl(I_2)_4]^-$ anions showing preferred arrangement allowing σ -hole interactions.*

Figure 2.9 clearly shows that the unexpected coordination sphere arises not only from packing effects but is stabilized by σ -hole interactions as well. The electrostatic potential plot nicely shows σ -holes (blue) and negative belts (red) of the coordinated iodine molecules. The energy gain through σ -hole interactions is greater than the energy loss because of the square-planar coordination. A related compound has been synthesized by Feldmann et al. in 2011.^[13] The $[Cl_2I_{14}]^{2-}$ anions in $[(Ph)_3PCl]_2[Cl_2I_{14}]$ consist of a central chloride which is almost exactly square-pyramidal coordinated by five iodine molecules. Four of them are directly bridging to the next chloride. A different kind of the non-classical interhalides are anions of the general formula $[X(YZ)_n]^-$. Known compounds exist for $X = Cl, Br$ and $YZ = IBr, ICl$. These compounds show

remarkable similarities to homonuclear polyhalides, especially concerning their structure. First vibrational studies and elemental analysis on those interhalides was carried out by Yagi and Popov in 1967.^[72] The first compound of this class which was structurally characterized was $[\text{Naph}_2][\text{I}_2\text{Cl}_3]$ ($[\text{Naph}_2]^+ = 2,2'$ -biquinoline) reported in 1979 by Parlow and Hartl.^[73] The anion can alternatively be described as $[\text{Cl}(\text{ICl})_2]^-$ and shows the same V-shaped structure as other pentahalide anions. The same can be observed for $[\text{I}_2\text{Br}_3]^-$ ($[\text{Br}(\text{IBr})_2]^-$) which was also characterized by Parlow and Hartl in 1985.^[74] Minkwitz et al. were able to crystallize $[\text{PPh}_4][\text{I}_3\text{Br}_4]$ from a mixture of IBr and $[\text{PPh}_4]\text{Br}$ or $[\text{PPh}_4]\text{Cl}$, respectively and therefore the first seven-membered polyinterhalide of this kind.^[75] They explained that triiodo-tetrabromide is formed from a reaction of a chloride with IBr is due to the presence of halogen-exchange reactions leading to the formation of $[\text{I}_3\text{Br}_4]^-$ rather than the less stabilized chloride containing species. This anion which can alternatively be described as $[\text{Br}(\text{IBr})_3]^-$ again is very similar to the heptahalides $[\text{Br}_7]^-$ and $[\text{I}_7]^-$ with exception of the $\text{I}-\text{Br}-\text{I}$ bonding angles which show large deviations from the ideal value of 109° which is probably due to repulsive interactions of the iodine lone pairs. The most significant difference in behavior of polyinterhalides compared to pure polyhalides is that the mixed species do not show high tendency to form multidimensional networks. Solely $[\text{PPh}_4][\text{I}_3\text{Br}_4]$ forms dimers in the crystal, while $[\text{I}_2\text{Br}_3]^-$ as well as $[\text{I}_2\text{Cl}_3]^-$ are only known as discrete anions. With respect to the redox potentials of neat halogens the formation of interhalides such as $[\text{I}-\text{Cl}-\text{Cl}]^-$ is very unlikely. Such species will most definitely undergo a rearrangement to form $[\text{Cl}-\text{I}-\text{Cl}]^-$ which is much more stabilized because of the oxidation state of Cl being -1 . To date there is only one non-classical interhalide dianion known. This is the $[\text{Cl}_2\text{I}_2]^{2-}$ dianion contained in the compound $[\text{C}_4\text{H}_5\text{N}_2\text{O}]_2[\text{I}_2\text{Cl}_2]^{2-}$, in analogy to other known tetrahalide dianions $[\text{Cl}_2\text{I}_2]^{2-}$ exhibits a linear structure with a central iodine molecule capped on both sides by chloride anions.^[76] Thus the central $\text{I}-\text{I}$ bond (272.6 pm) is only marginally elongated compared to elemental iodine (271.5 pm) while the terminal $\text{I}-\text{Cl}$ bonds are significantly elongated (306.5 pm) compared to the bond length observed in ICl . In consistency with remaining non-classical interhalides these anions exist as discrete dianions and do not form any kind of polyhalide network in the crystal.

2.8 Synthetic and Analytical Approaches

Almost all polyhalides of bromine and iodine can be synthesized in bulk by simply adding the specific elemental halogen to an appropriate halide. Increasing the amount of halogen added leads to the formation of higher polyhalides which is of course dependent on the stability of the desired polyhalide. Differences in the resulting polyhalide can also be made by choosing different reaction conditions or reaction media. Polyhalides can be synthesized in neat halogens, in organic solvents as well as in ionic liquids. Depending on the kind of halogen used different amounts of halogen content can be attained. The highest amount of halogen could be attained in polyiodides (e.g. $[I_{18}]^{2-}$ or $[I_{26}]^{4-}$). Although the structural diversity of polybromides is much smaller polybromides such as $[Br_{11}]^{-}$ or $[Br_{20}]^{2-}$ exhibit almost the same halogen content found in polyiodides. Regarding polychlorides the situation is quite different. Only the simple $[Cl_3]^{-}$ and $[Cl_5]^{-}$ have been proven to exist.^[26] Polychlorides with higher chlorine content could not be attained yet. As polyfluorides exhibits the lowest stability and due to the high reactivity of fluorine no polyfluorides could be synthesized in bulk yet. Polyfluorides observed in matrix isolation experiments were $[F_3]^{-}$ and $[F_5]^{-}$.^[28,30] In recent years an increasing number of polyhalides has been characterized due to new approaches in synthesis.^[31] The reaction of halide salts with neat elemental halogen has shown to be a promising route, especially for polybromides, as elemental bromine is liquid and can therefore be used as solvent.^[11,15] Furthermore, reactions in routine solvents and ionic liquids are quite successful.^[13,77,78] These approaches have yet only been applied to polyiodides and polybromides. Synthetic access to polyhalides of the lighter homologues chlorine and fluorine however, faces an essential challenge. As the elemental halogens Cl_2 and F_2 are gaseous at room temperature the degradation of polyhalides to the particular halogen and the correspondent halide is entropically favored. This is even more crucial regarding the fact that all polyhalides exhibit a tendency to the loss of elemental halogen which increases with higher halogen content. To yield higher polyhalides of chlorine and probably also fluorine synthetic work has to be carried out either at very low temperatures or in a stabilizing environment. The stability of polyhalides also depends on the physical properties of the considered halogen. The large variety of polyiodides is due to the good polarizability and donor properties of iodide anions as well as the fairly well acceptor

ability of elemental iodine. Iodine atoms are also known to form very strong halogen bonds which is due to the very distinct σ -hole they bear. Additionally polyiodides are stabilized by dispersive interactions. If polychlorides are considered it is quite obvious why the structural diversity is so much smaller. Due to the fact that chlorine atoms are much smaller, they exhibit a poor polarizability and the electric charge density on the surface of the chloride atom is much higher leading to a stronger electrostatic repulsion. These facts weaken possible bonds in polychlorides and therefore considerably increase the tendency to lose Cl_2 . Chlorine atoms have also been calculated to generate by far weaker σ -hole interactions compared to bromine and iodine.^[34] Nevertheless, polychlorides are able to form halogen bonded networks even though interactions are not as strong as in similar polyiodide structures. Furthermore, the stability in solution depends on the solvent. Interesting is the fact that in aprotic solvents the order of stability of the trihalides decreases with increasing atom weight. Which is literally opposite as expected. In water however this order is reversed.^[79] Due to their properties the preferable method to characterize polyhalides beside single crystal X-ray structure determination is vibrational spectroscopy. Almost all polyhalides show a strong Raman scattering effect and exhibit distinct bands that can be assigned to a certain polyhalide, especially when the investigations are accompanied by quantum-chemical calculations because they predict vibrational frequencies of different polyhalides very well.^[39] In case of interhalide anions also IR spectroscopy is of good use. Even homoatomic polyhalides show bands in IR spectra albeit with less intensity, due their electronic structure which can very well be explained using the example of the trichloride anion. At first the symmetric stretching mode of the trichloride does not seem to be IR-active as one would not expect the trichloride to exhibit a dipole momentum. Due to the unequal charge distribution within trichloride (see Section 2.2) the trichloride exhibits a very weak dipole momentum which is effected by the symmetric as well as the antisymmetric stretching mode of the trichloride anion, thus leading to IR-active modes and corresponding bands in the IR spectra.

3 Objective

The objective of this work is the synthesis and characterization of novel polychloride compounds. In doing so, convenient ways to synthesize and crystallize these types of anions, are to be developed. These newly synthesized compounds are studied by means of Raman- and IR- spectroscopy as well as x-ray single crystal structure determination. Vibrational and structural data is to be accompanied by and compared to quantum-chemical calculations at different levels of theory.

The stability of different counter ions against the exposure to elemental chlorine has to be examined. Symmetric and asymmetric ammonium salts of different sizes as well as different imidazolium and pyrrolidinium salts can be tested concerning their stability towards elemental chlorine as well as their potency to stabilize polychloride anions.

4 Results and Discussion

4.1 Quantum Chemical and Raman Spectroscopic Investigation of Polychloride Monoanions

This Section is mainly based on the manuscript submitted for final publication “Robin Brückner, Heike Haller, Mathias Ellwanger, Sebastian Riedel, Polychloride Monoanions from $[\text{Cl}_3]^-$ to $[\text{Cl}_9]^-$: A Raman Spectroscopic and Quantum Chemical Investigation, Chem. Eur. J., 2012, 18, 5741-5747 (DOI: 10.1002/chem.201103659) Copyright © 2012 WILEY-VCH Verlag GmbH & Co. KGaA, Weinheim [RB1] which can be found at the end of this work in Appendix A1. The presentation of the results has been shortened and complemented by previously unpublished data.

Main work of this publication has been carried out by Robin Brückner

Polychloride monoanions stabilized by quaternary ammonium salts were investigated using Raman spectroscopy and state-of-the-art quantum-chemical calculations. A regular V-shaped pentachloride was characterized for the $[\text{N}(\text{Me})_4][\text{Cl}_5]$ salt, whereas a hockey-stick-like structure was tentatively assigned for $[\text{N}(\text{Et})_4][\text{Cl}_2 \cdots \text{Cl}_3^-]$, suggesting that the $[\text{Cl}_5]^-$ anion can exist in two different forms, depending on the counter ion used, see Fig. 4.1.

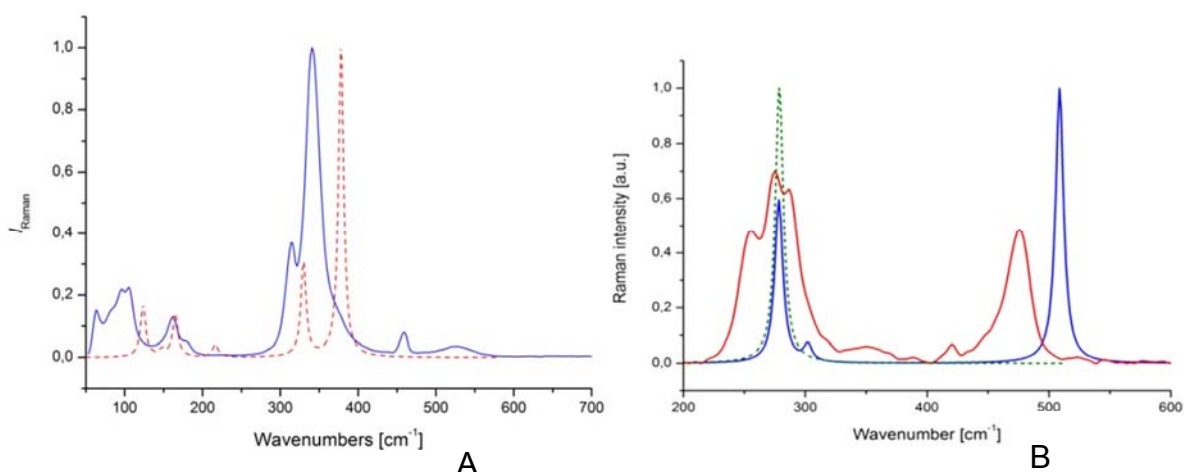


Figure 4.1 Comparison of the experimental and calculated Raman spectra of $[\text{N}(\text{Me})_4][\text{Cl}_5]$ (A) and $[\text{N}(\text{Et})_4][\text{Cl}_2 \cdots \text{Cl}_3^-]$ (B). (A: blue line: experimental, red line: computed at RI-MP2/def2-TZVPP level; B: red line: experimental, blue line: simulated spectra of $[\text{Cl}_3 \cdots \text{Cl}_2^-]$; green line: computed spectrum of $[\text{Cl}_3]^-$ at MP2/def2-TZVPP level).

Increasing the size of the cation to the quaternary ammonium salts $[\text{NPr}_4]^+$ and $[\text{NBu}_4]^+$ lead to the formation of the $[\text{Cl}_3]^-$ anion showing that increasing size of the cation probably leads to a lower chlorine content in the polychlorides generated.

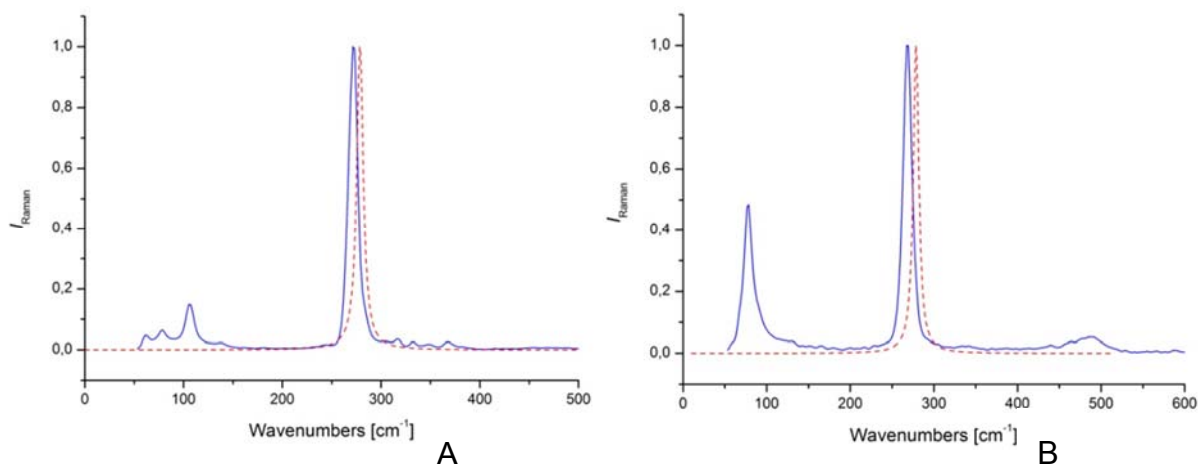


Figure 4.2 Comparison of the experimental and calculated Raman spectra of $[\text{NPr}_4][\text{Cl}_3]$ (A) and $[\text{NBu}_4][\text{Cl}_3]$ (B), (solid line: experimental, dotted line: computed at RI-MP2/def2-TZVPP level).

All compounds were obtained as powders, except $[\text{NBu}_4][\text{Cl}_3]$ which actually was found to be a pale yellow liquid at about 40 °C. Further to these observations, the existence of the novel $[\text{Cl}_9]^-$ anion could be proven by means of low-temperature Raman spectroscopy in conjunction with quantum-chemical calculations. Summary of all above mentioned Raman bands can be found in Table 4.1.

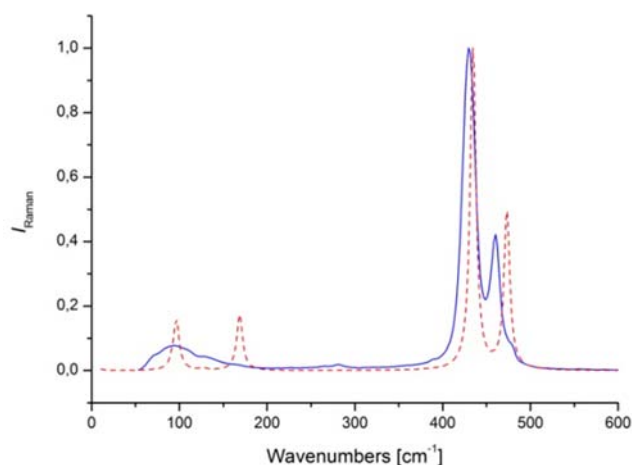


Figure 4.3 Experimental (solid line) and calculated (dotted line) Raman spectrum of $[\text{NEt}_4][\text{Cl}_9]$ (Experimental spectrum recorded at 70 K, calculated spectrum computed at RI-MP2/def2-TZVPP level).

Table 4.1 Experimental and calculated Raman frequencies of polychloride monoanions above 200 cm^{-1} .^[a]

Mode ^[b]	CCSD(T) ^[c]	MP2 ^[d]	[N(Me) ₄] ⁺	[N(Et) ₄] ⁺ ^[e]	[N(Pr) ₄] ⁺	[N(Bu) ₄] ⁺
ν_1 L-sh				475		
ν_1 [Cl ₅] [−]	371	378	341			
ν_2 [Cl ₅] [−]	321	330	315			
ν_1 [Cl ₃] [−]	262.4	278.7			272	268
ν_2 L-sh				287, 274, 255		
ν_3 [Cl ₅] [−]	196	216	162			
ν_1 [Cl ₉] [−]		473		460		
ν_2 [Cl ₉] [−]		435		429		

[a] Frequencies in cm^{-1} [b] ν Cl₂ band of the free Cl₂; ν_1 L-sh corresponds to the hockey stick like structure; ν_1 [Cl₅][−] corresponds to the V-shaped structure; ν_1 [Cl₃][−] computed for the free [Cl₃][−] [c] using aug-cc-pVTZ basis set [d] using def2-TZVPP basis set [e] Values of [N(Et)₄][Cl₂...Cl₃]^[26] measured in liquid CH₃CN: 482 cm^{-1} (Cl₂), 275 cm^{-1} ([Cl₃][−]) and values of [PPh₂Cl₂][Cl₂...Cl₃]^[25] measured in liquid CHCl₃: 466 cm^{-1} (Cl₂), 286 and 273 cm^{-1} ([Cl₃][−]).

All spectroscopic results were accompanied by quantum-chemical calculations confirming the results obtained. For all polychloride monoanions of the series [Cl₅][−], [Cl₇][−] and [Cl₉][−] structures were optimized at different levels of theory (see Figure 4.4) showing that the global minima for polychloride structures resemble those found for the corresponding polybromides.

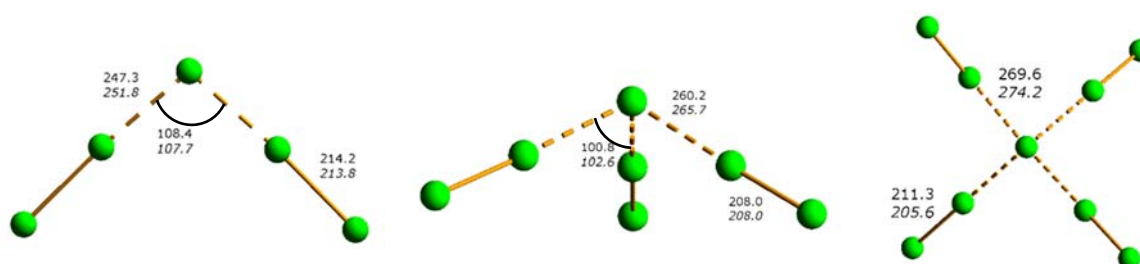


Figure 4.4 Optimized global minimum structures of [Cl₅][−], [Cl₇][−] and [Cl₉][−] at different level of theory. Normal text style: MP2/def2- TZVPP; italic: SCS-MP2/def2-TZVPP.

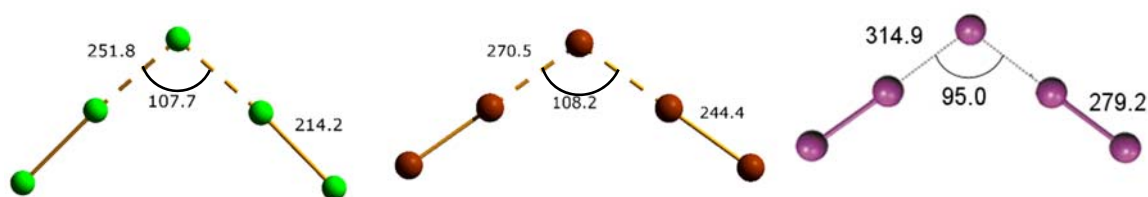


Figure 4.5 Calculated minimum structures of $[\text{Cl}_5]^-$, $[\text{Br}_5]^-$ and $[\text{I}_5]^-$ at SCS-MP2/def2-TZVPP level.

Figure 4.5 shows that the calculated structures of the pentahalides of chlorine, bromine and iodine exhibit the same V-shape with C_{2v} symmetry. Bond lengths of the outer bonds are elongated by 12 pm for iodine and 15 pm for bromine and chlorine which indicates that the weakening of the X–X bond is stronger in the pentabromide as well as in the pentachloride anion. Situation regarding the heptahalides $[\text{Cl}_7]^-$, $[\text{Br}_7]^-$ and $[\text{I}_7]^-$ is similar although no experimental proof indicating the existence of $[\text{Cl}_7]^-$ could be provided yet.

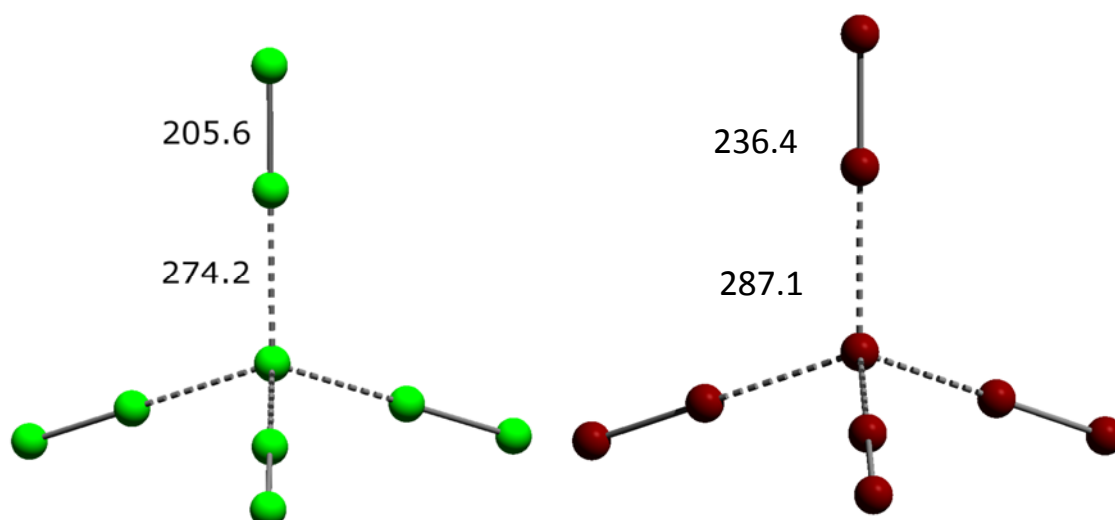


Figure 4.6 Calculated minimum structures of $[\text{Cl}_9]^-$ and $[\text{Br}_9]^-$ at SCS-MP2/def2-TZVPP level in T_d symmetry.

The minimum structures in Figure 4.6 show a very similar bond elongation on a relative basis, showing that $[\text{Cl}_9]^-$ as well as $[\text{Br}_9]^-$ consist of a central halide ion equally coordinating four dihalogen molecules. The corresponding nonaiodide $[\text{I}_9]^-$ however, exhibits a different structure with a distorted triiodide acting as the central unit end-on coordinating three iodine molecules.^[48] A picture of $[\text{I}_9]^-$ is displayed in Figure 4.7.

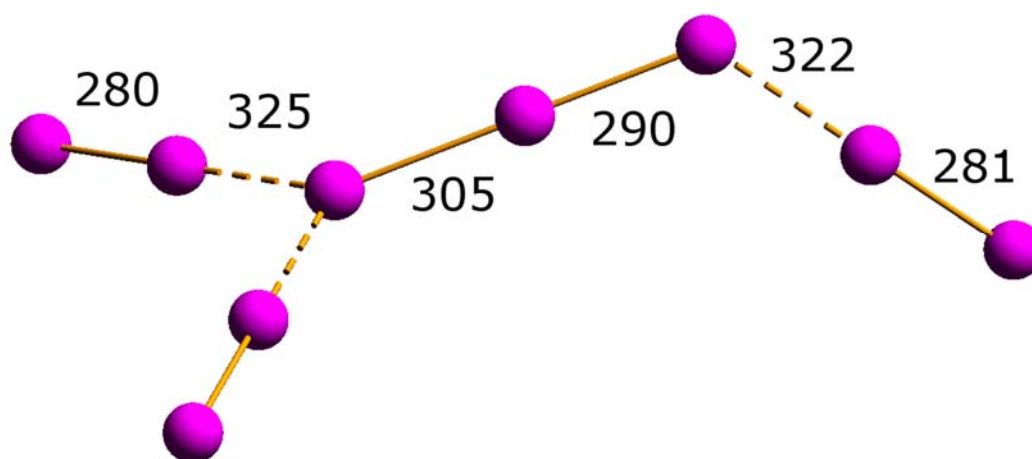


Figure 4.7 Structure of $[I_9]^-$ calculated at B3-LYP/aug-cc-pVTZ level.^[48] Structure was experimentally confirmed as well.^[80]

Despite all the similarities of the polyhalides especially of bromine and chlorine, a major difference is the fact that the $[Cl_3]^-$ anion does not seem to be a suitable building block for polychlorides. In contrast to the polyiodides and polybromides no polychloride containing a $[Cl_3]^-$ building block has yet been observed. If a $[Cl_3]^-$ unit is present, it is highly distorted representing more of an intermediate between a $[Cl_3]^-$ unit and a Cl_2 molecule coordinated to a Cl^- ion, see Section 4.4.3 and 4.4.4.

Additionally the Raman spectra for $[Cl_3]^-$, $[Cl_5]^-$, $[Cl_7]^-$, $[Cl_9]^-$ and Cl_2 have been calculated at RI-MP2/def2-TZVPP level, showing that all Raman bands of these polychlorides are situated between 270 cm^{-1} and 570 cm^{-1} , as could be expected, see Fig. 4.8.

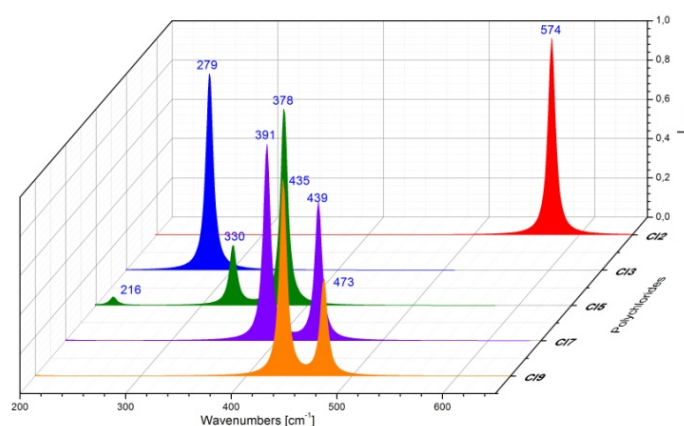


Figure 4.8 Calculated Raman-spectra at RI-MP2/def2-TZVPP level of the polychloride monoanions (Cl_2 (red), $[Cl_3]^-$ (blue), $[Cl_5]^-$ (green), $[Cl_7]^-$ (purple), $[Cl_9]^-$ (orange)).

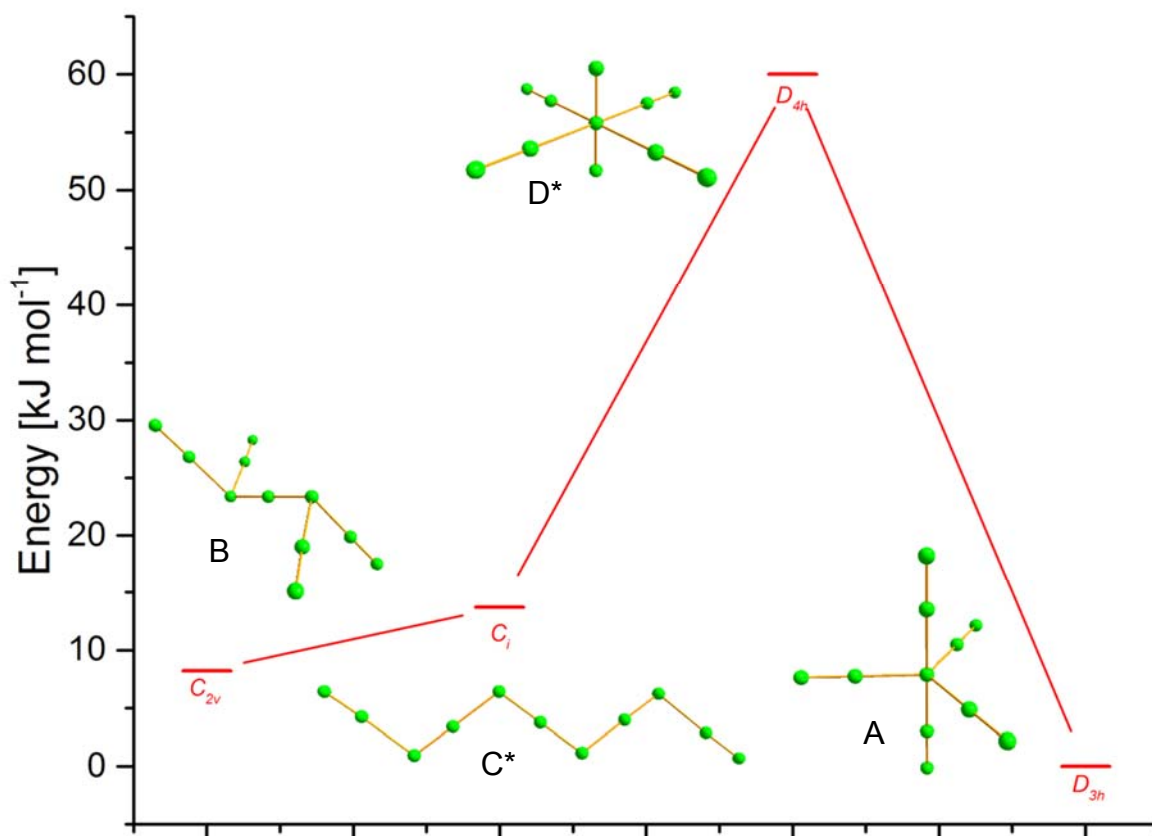
Furthermore structural parameters of $[\text{Cl}_3]^-$ were optimized using high level calculations (CCSD(T)/aug-cc-pVQZ) compared to calculations at lower levels and the experimental values. Table 4.2 shows that the tendency to overestimate dissociation energies and vibrational frequencies decreases with the use of higher basis sets and more precise methods.

Table 4.2 Optimized parameters of $[\text{Cl}_3]^-$ at different levels of theory.

Level	Bond Distance [pm]	$D_e [\text{Cl}_3]^- \rightarrow \text{Cl}_2 + \text{Cl}^-$ [kJ mol ⁻¹]	$\nu^{[a]}$ [cm ⁻¹]
MP2/def2-TZVPP	229.5	122.6	311 (540)
SCS-MP2/def2-TZVPP	230.6	112.0	294 (575)
CCSD(T)/aug-cc-pVDZ	238.5	108.6	268.0 264.5
CCSD(T)/aug-cc-pVTZ	232.8	102.9	262.4 259.7
CCSD(T)/aug-cc-pVQZ	231.3	102.4	
Exp.	222.7, 230.5 ^[b]	99 ± 5 ^[c]	268-271 ^[d]

[a]Values in *italic* are anharmonic frequencies, values in parenthesis are intensities. [b]Exp. bond distance, see Ref.^[21] [c]Experimental determined thermochemistry, see Ref.^[37] [d]Experimentally found Raman frequencies for $[\text{NPr}_4][\text{Cl}_3]$, $[\text{AsPh}_4][\text{Cl}_3]$ and $[\text{PPh}_4][\text{Cl}_3]$ (Ref.^[24])

In addition structures of $[\text{Cl}_{11}]^-$ and $[\text{Cl}_{13}]^-$ were optimized at B3-LYP/aug-cc-pVTZ level^[81,82] using the D3 dispersion correction by Grimme.^[83] Obtained minimum structures for $[\text{Cl}_{11}]^-$ are displayed in Figure 4.9. The global minimum of $[\text{Cl}_{11}]^-$ was found to be the D_{3h} symmetrical trigonal bipyramidal structure (A), the displayed bond lengths suggest it to be formed of a central chloride weakly coordinating five chlorine molecules with bond lengths being elongated by 8 and 9 pm, respectively. The C_{4v} symmetrical square-pyramidal conformation which was found in the $[\text{Br}_{11}]^-$ crystal structure always rearranged into the trigonal bipyramidal structure and is therefore not displayed in Fig. 4.9. The C_{2v} symmetrical chair-like conformation (B) lies about 8.2 kJ·mol⁻¹ higher in energy while the C_i symmetrical chain-like structure (C) is 13.7 kJ·mol⁻¹ higher. The same is accounted for the D_{4h} symmetrical distorted octahedral structure (D) which lies about 60 kJ·mol⁻¹ higher. This could be expected as it is very unlikely for a Cl_3 unit to coordinate chlorine molecules via the central Cl atom. The small energy difference between the structures A, B and C is somewhat surprising as no polyhalide structures containing a Cl_3 building block could be found yet. Especially structure C is surprisingly low in energy as the central Cl_3 building block would have to donate electron density across 3 Cl-atoms which does not seem very likely.



* For structures C and D a minimum could only be found without using the D3-dispersion correction

Figure 4.9 Calculated minimum structures of $[\text{Cl}_{11}]^-$ at B3-LYP/aug-cc-pVTZ level.

For $[\text{Cl}_{13}]^-$ only 2 minimum structures could be found which are displayed in Figure 4.10. The global minimum structure (E) exhibits octahedral symmetry showing bond lengths of 287.2 pm for the inner bonds and 206.9 pm for the outer bonds which is consistent with the assumption of this structure being made up of a central chloride coordinating six chlorine molecules. The D_{5h} symmetrical structure (F) lies $55.8 \text{ kJ} \cdot \text{mol}^{-1}$ higher in energy which is quite comprehensible as it seems unlikely for a Cl_3 unit to coordinate chlorine molecules via the central Cl atom as already mentioned above regarding structure D. This is reflected by the inner bond lengths of 321.9 pm which are very close to sum of the van-der-Waals radii of chlorine.^[45] A table displaying all bond lengths of the calculated $[\text{Cl}_{11}]^-$ and $[\text{Cl}_{13}]^-$ minima can be found in Appendix B.

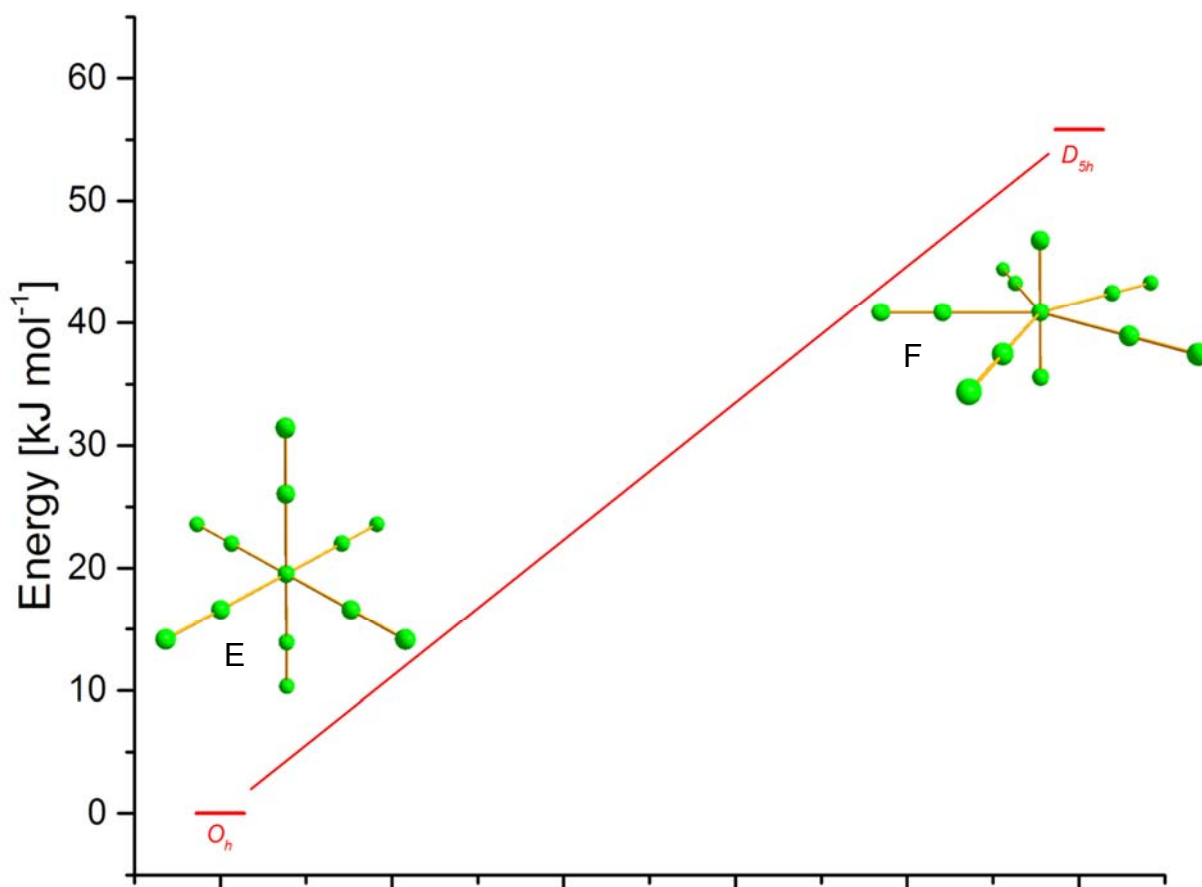


Figure 4.10 Calculated minimum structures for $[\text{Cl}_{13}]^-$ at B3-LYP/aug-cc-pVTZ level.

Table 4.3 Computed reaction enthalpies in $\text{kJ}\cdot\text{mol}^{-1}$ of higher polychlorides compared to those of the corresponding polybromides at different levels of theory.

Reaction	B3-LYP-D3	MP2	SCS-MP2 ^[a]	CCSD(T) ^[a]
a. ^[RB1] $[\text{Cl}_5]^- \rightarrow [\text{Cl}_3]^- + \text{Cl}_2$		44.8	36.2	37.8
b. ^[RB1] $[\text{Cl}_7]^- \rightarrow [\text{Cl}_5]^- + \text{Cl}_2$		37.1	32.1	
c. ^[RB1] $[\text{Cl}_9]^- \rightarrow [\text{Cl}_7]^- + \text{Cl}_2$		33.0	29.3	
d. $[\text{Cl}_{11}]^- \rightarrow [\text{Cl}_9]^- + \text{Cl}_2$	19.5			
e. $[\text{Cl}_{13}]^- \rightarrow [\text{Cl}_{11}]^- + \text{Cl}_2$	20.3			
d. ^[12] $[\text{Br}_5]^- \rightarrow [\text{Br}_3]^- + \text{Br}_2$		66.1	55.6	56.3
e. ^[12] $[\text{Br}_7]^- \rightarrow [\text{Br}_5]^- + \text{Br}_2$		51.1	43.0	43.6
f. ^[12] $[\text{Br}_9]^- \rightarrow [\text{Br}_7]^- + \text{Br}_2$		43.8	36.7	11.8
g. $[\text{Br}_{11}]^- \rightarrow [\text{Br}_9]^- + \text{Br}_2$		29.5	16.0	3.3
h. $[\text{Br}_{13}]^- \rightarrow [\text{Br}_{11}]^- + \text{Br}_2$		15.4		

^[a]Single-points at MP2/def2-TZVPP optimized structures.

Additionally calculations concerning the thermochemistry of the investigated polychloride monoanions up to $[\text{Cl}_9]^-$ have been performed at different levels of theory. The preferred decomposition channel of almost all polyhalides is the loss of halogen to form the next smaller polyhalide or – in case of the trihalide – the halide. For all the polychloride monoanions investigated here the decomposition reaction energies are calculated to be endothermic. Table 4.3 shows that the bond energies of the polychlorides is roughly two thirds of those calculated for the corresponding polybromides. Of course polychlorides are additionally destabilized for entropic reasons as well which is emphasized by the values displayed in Table 4.4.

Table 4.4 *Boiling points and vaporization enthalpies of the halogens.**

	$T_B / ^\circ\text{C}$ [84]	$\Delta_{\text{vap}}H / \text{kJ}\cdot\text{mol}^{-1}$ [84]
F_2	-188.1	6.62
Cl_2	-34.0	20.41
Br_2	58.8	29.96
I_2	184.4	41.57

* At has been excluded for obvious reasons

4.2 Stability of Cations Against Elemental Chlorine

Most important for the successful synthesis of polychloride salts is the choice of a proper cation. Working with Cl_2 gas provides special requirements regarding chemical stability of potential reagents because Cl_2 gas is known to be a corrosive and reactive gas able to react with a lot of organic substructures substituting hydrogen atoms under generation of HCl gas which is even more aggressive and corrosive. Due to the quite weak nature of bonds in polyhalides in general and particularly in polychlorides the most promising option is the use of large cations with a quite equally distributed charge on its surface.

4.2.1 Ammonium Cations

Preceding work concerning polybromides suggested symmetric quaternary ammonium salts with chain lengths of the organic rests up to four carbon atoms to be promising candidates as they yielded a couple of new polybromide salts.^[6] Reaction of the corresponding chloride salts with elemental chlorine yielded different polychlorides as yellow powders or liquids, see Section 4.1. The use of quaternary ammonium salts to yield polychlorides is limited because the stability against chlorination fades with elongation of the organic chains. ^1H -NMR spectra of solutions containing $[\text{NMe}_4]^+$, $[\text{NEt}_4]^+$ or $[\text{NPr}_4]^+$ show no signals indicating chlorination after treatment with Cl_2 . Solutions of $[\text{NBu}_4]^+$ do not seem to be sensitive against Cl_2 , a reaction occurs however if Cl_2 is added to solid $[\text{NBu}_4]\text{Cl}$ even though the reaction speed is quite slow. Figure 4.11 shows an ^1H -NMR spectrum recorded directly after the addition of Cl_2 to $[\text{NBu}_4]\text{Cl}$.

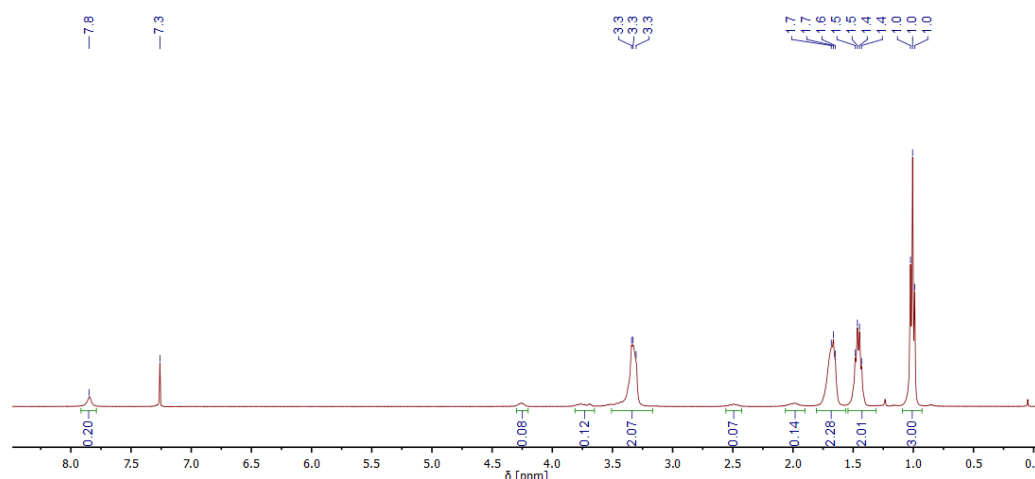


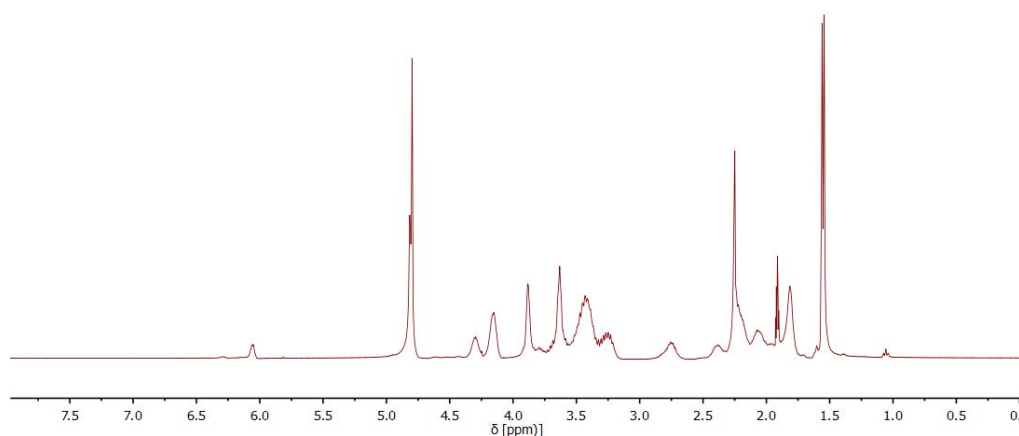
Figure 4.11 ^1H -NMR spectrum of $[\text{NBu}_4]\text{Cl}$ after the addition of Cl_2 (10 min.).

The spectrum shows the expected signals for the $[\text{NBu}_4]^+$ cation (Tab. 4.5). Additionally very small broad signals are visible deriving from partially chlorinated CH_2 - and CH_3 -groups of the cation. Another result of the partial chlorination is the comparatively bad resolution of the spectrum. The peak at 7.8 ppm is due to $[\text{Cl}-\text{H}-\text{Cl}]^-$ which is the secondary reaction product of the chlorination.^[85] Although the peaks of chlorinated side products are very small the spectrum shows that the $[\text{NBu}_4]^+$ cation is indeed affected by elemental chlorine.

Table 4.5 List of ^1H -NMR signals, multiplicity, integrals and associated C-atoms of the spectrum above.

δ /[ppm]	Multiplicity	Integral (rel.)	C-atom
1.0	t	3.00	1
1.4-1.5	tq (not fully split-up)	2.01	2
1.6-1.7	tt (not fully split-up)	2.28	3
1.9-2.0	t	0.14	1
2.4-2.5	m	0.07	2
3.3	t	2.07	4
3.6-3.7	m	0.12	2, 3
4.2	t	0.08	4
7.8	s	0.20	$[\text{Cl}-\text{H}-\text{Cl}]^-$

This observation was emphasized by the following spectrum (Fig. 4.12).

**Figure 4.12** ^1H -NMR spectrum of a mixture of $[\text{NBu}_4]\text{Cl}$ and excess Cl_2 after 3 months.

The spectrum shows a large number of signals indicating significant non-selective chlorination of the butyl chains. Assignment and further analysis of the spectrum was not performed due to the very number of signals, suggesting that most of the conceivable chlorination products are present. Therefore ammonium cations with alkyl chain longer than four carbon atoms have not been investigated further.

Additionally to the symmetric ammonium salts which possess a higher tendency to crystallize asymmetric salts were used. The asymmetric salts used were $[\text{Et}_3\text{MeN}]\text{Cl}$, $[\text{Et}_3\text{PrN}]\text{Cl}$ and $[\text{PhMe}_3\text{N}]\text{Cl}$ which represents the only exception in number of C atoms as the phenyl ring is predicted to be stable against chlorination by elemental chlorine. Most interesting the salts $[\text{Et}_3\text{MeN}]\text{Cl}$, $[\text{Et}_3\text{PrN}]\text{Cl}$ and $[\text{NBu}_4]\text{Cl}$ liquefy almost

immediately after addition of excess Cl_2 . Mass balances of the reactions of $[\text{Et}_3\text{MeN}]\text{Cl}$, $[\text{Et}_3\text{PrN}]\text{Cl}$ and $[\text{NBu}_4]\text{Cl}$ with excess chlorine are listed in Table 4.6.

Table 4.6 Mass balances of reactions of different ammonium salts with excess chlorine.

	$[\text{NBu}_4]\text{Cl}$	$[\text{Et}_3\text{MeN}]\text{Cl}$	$[\text{Et}_3\text{PrN}]\text{Cl}$
n [mmol]	0.89	1.40	1.08
n (Cl_2)* [mmol]	2.07	2.57	2.46
equiv. (Cl_2)	2.32	1.83	2.27

* Cl_2 was condensed on the sample, then the sample was warmed to r.t. and the pressure was released until chlorine evaporation stopped.

The values in Table 4.6 show that approx. 2 equivalents of chlorine are consumed during the reaction with the ammonium salts. This would suggest the formation of pentachlorides. The Raman spectra, however indicate a variety of polychloride species which cannot certainly be determined without a doubt, see Fig. 4.13.

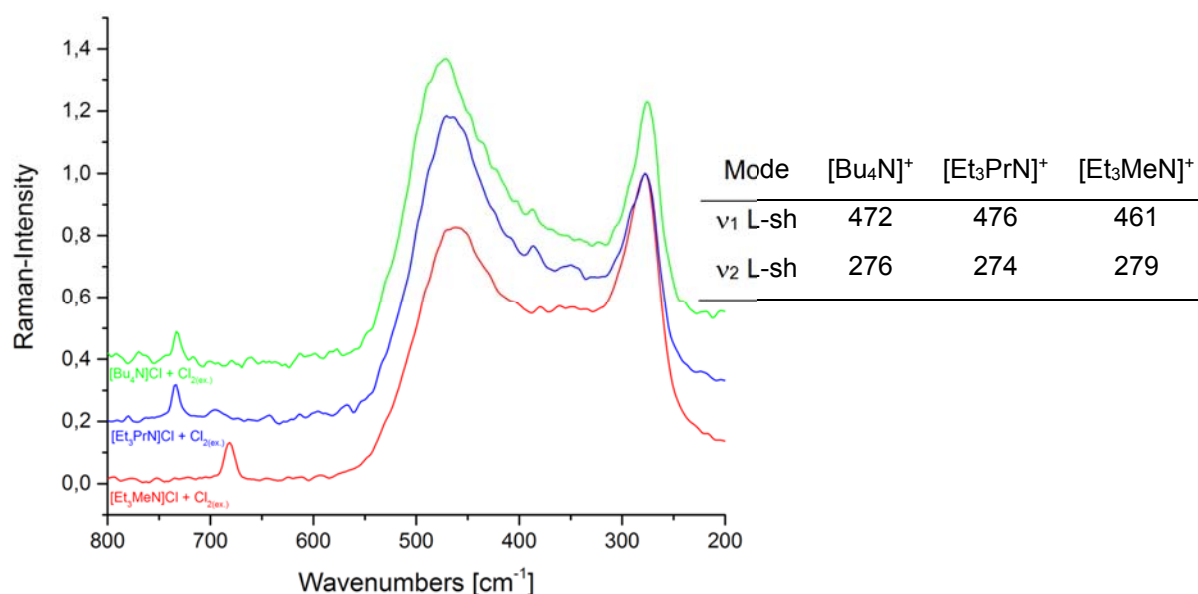


Figure 4.13 Raman spectra of the compounds yielded from the reactions in Table 4.6.

Fig 4.13 shows a broad band centered at 465 cm^{-1} which can be assigned to coordinated Cl_2 molecules in agreement with earlier publications.^[25] As the band in Fig 4.13 is very broad, the formation of a hockey-stick-like pentachloride does not seem likely. A more probable assumption would be the formation of a large number of undefined polychloride species with a variable number of coordinated Cl_2 molecules. In particular cases this band can be eliminated by keeping the liquid product under

reduced pressure for several hours. This works very well in case of $[\text{NBu}_4]\text{Cl}$ which also contains higher polychloride species after chlorine has been added. If the pressure is reduced the mixture starts to degas quickly while the viscosity increases finally resulting in a highly viscous residue which could be identified as pure $[\text{NBu}_4][\text{Cl}]_3$, see Fig. 4.14).

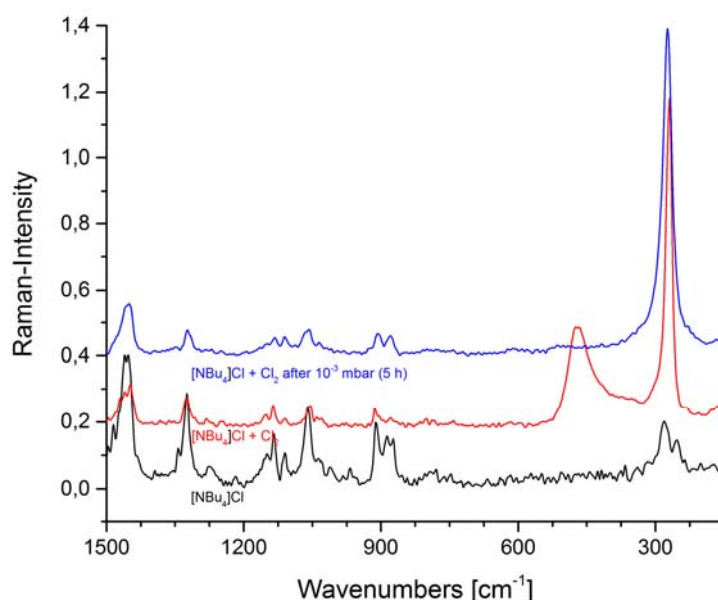


Figure 4.14 Raman spectra of $[\text{NBu}_4]\text{Cl}$ before (black) and after addition of Cl_2 (red) and after keeping the mixture at dynamic vacuum for 5 hours (blue).

In case of $[\text{Et}_3\text{MeN}]\text{Cl}$ and $[\text{Et}_3\text{PrN}]\text{Cl}$ however no loss of Cl_2 gas can be observed under reduced pressure. These compounds form stable liquids with low vapor pressure at room temperature and can therefore be described as room temperature ionic liquids (RTILs). Generally these observations suggest that liquid products tend to dissolve considerable amounts of elemental chlorine which makes them interesting materials for potential application as e. g. chlorine storage materials.

4.2.2 Other N-based Cations

A different approach towards the preparation of polychlorides is the synthesis in ionic liquids. As these substances exhibit a very high potential to dissolve gases the solvation of chlorine in ionic liquids could be a crucial factor as it lowers the negative impact of entropic effects on the formation of polychlorides. Thus, different ionic liquids had to be tested regarding their stability towards liquid chlorine. Already the coloring of a solution of chlorine can give an important hint towards the stability of tested cation. By solving chlorine in an ionic liquid (e.g. [HMiM]Cl or [BMP]Cl) a yellow solution is formed. Ionic liquids containing an imidazolium cation show decolorization of the solution after several minutes, indicating that Cl₂ is consumed upon substitution or addition reactions with the cation. For an example Figure 4.15 shows an ¹H-NMR spectrum of 1-hexyl-3-methyl-imidazolium chloride ([HMiM]Cl) after repeated addition of chlorine – always followed by decolorization.

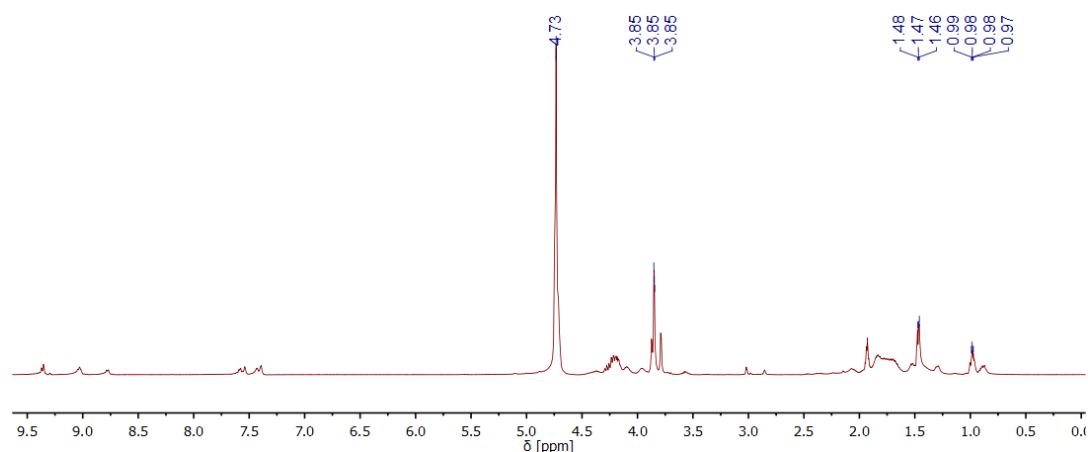


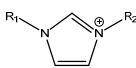
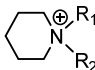
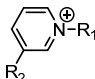
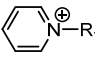
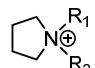
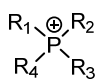
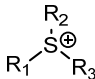
Figure 4.15 ¹H-NMR spectrum of [HMiM]Cl after repeated addition of Cl₂.

The spectrum in Figure 4.15 shows a very large number of peaks suggesting significant and non-selective chlorination of the hexyl-chain as well as the imidazolium ring. Only major peaks were picked for clarity. Unfortunately this result lead to the uselessness of the most commonly used ionic liquids on the basis of imidazolium cations.

Based on these results two major structural requirements for ionic liquids to withstand elemental chlorine were identified. [NBu₄]Cl as well as [HMiM]Cl were mainly chlorinated on the long alkyl chains so first of all the cation must not contain alkyl chains of more than four carbon atoms. Concerning [HMiM]Cl chlorine was also added to the C–C double bond of the imidazolium ring. That is why non-aromatic rings must not

have any unsaturated carbon-carbon bonds. So a screening of different IL cations was setup. Results are displayed in Table 4.7. Ammonium-based ILs were neglected as the different ammonium chlorides were already discussed above. Ammonium ILs containing a different counter ion than Cl⁻ were not applied.

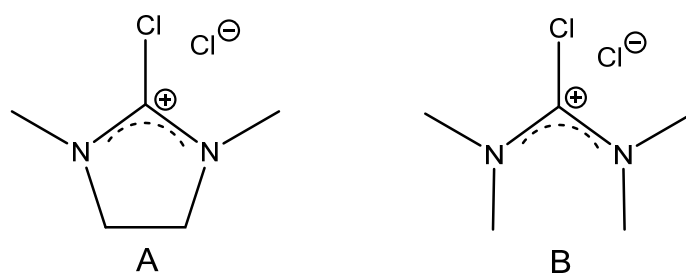
Table 4.7 List of tested ILs towards their stability against elemental chlorine.

Cation	R ₁	R ₂	R ₃	R ₄	Anion ^[a]	Suitability
	Me, Et, nBu, nHe	Me	--	--	[Cl] ⁻ , [NTf ₂] ⁻ , [OTf] ⁻	n
	Me, nBu	Me, nPr	--	--	[Cl] ⁻ , [NTf ₂] ⁻ , [OTf] ⁻	y
	Et, nPr, nBu	Me	--	--	[Cl] ⁻ , [NTf ₂] ⁻ , [OTf] ⁻	y
	Et, nPr, nBu	--	--	--	[Cl] ⁻ , [NTf ₂] ⁻ , [OTf] ⁻	y
	Me, Et, nBu	Me, nPr	--	--	[Cl] ⁻ , [OTf] ⁻	y
	Et, Ph, nBu	Ph, nBu	Ph, nBu	Ph, nBu, Cl	[Cl] ⁻	n
	Me, Et	Et	Et	--	[NTf ₂] ⁻	n

^[a]Due to commercial availability, not all possible combinations could be tested

Table 4.7 shows that a lot of widely used ionic liquids are suitable for being used as solvents or – in case of chloride ILs – even as possible starting materials for the synthesis of polychlorides. Surprisingly n-butyl-chains attached to pyridinium and pyrrolidinium ring do not seem to undergo a reaction with Cl₂. Unfortunately none of the chloride salts used as starting materials was soluble in pyridinium- and piperidinium-based ILs, therefore no reaction occurred. On the other hand a wide range of salts showed good solubility in pyrrolidinium-based ILs. Further investigation and resulting compounds will be discussed in Section 4.3.

Finally a third kind of cations was tested. Tetramethylchloroamidiniumchloride ([CCl(NMe₂)₂]⁺Cl⁻) and N,N'-dimethyl-2-chloroimidazoliniumchloride ([C₅H₁₀N₂Cl]⁺Cl⁻) were chosen (see Scheme 4.1), because they both fit to the above mentioned requirements.



Scheme 4.1 Structural formula of *N,N'*-dimethyl-2-chloroimidazoliniumchloride (A) and tetramethylchloroamidiniumchloride (B).

4.2.3 Other Cations

According to previous work on polychlorides^[24] also the P-based cations $[\text{PPh}_4]^+$ and $[\text{PPh}_3\text{Cl}]^+$ were tested whereas $[\text{PPh}_3\text{Cl}]^+$ was prepared by carefully streaming chlorine over PPh_3 leading to a highly exothermic reaction yielding PPh_3Cl_2 which in solution exists in its ionic form $[\text{PPh}_3\text{Cl}]^+ [\text{Cl}]^-$.^[86–89] The same reaction was performed using $\text{P}(\text{C}_6\text{F}_5)_3$ instead of PPh_3 . Unfortunately $\text{P}(\text{C}_6\text{F}_5)_3$ does not possess enough reactivity to voluntarily undergo a reaction with Cl_2 . Nevertheless reaction takes place if Cl_2 is condensed onto $\text{P}(\text{C}_6\text{F}_5)_3$ at -78°C . In this case signals indicating a $[\text{Cl}_3]^-$ anion could be observed at -78°C which unfortunately decomposed upon warming.

$[\text{PPh}_4][\text{Cl}]$ was displayed in Table 4.7 even though it is technically speaking not an IL. Other P-based cation that were tested are displayed in Table 4.7. Although the phosphonium cation itself is quite stable against Cl_2 the alkyl chain attached to the phosphorous atom seem to lack stability as $[\text{PBu}_4][\text{Cl}]$ is chlorinated even faster than $[\text{NBu}_4][\text{Cl}]$. Therefore phosphonium-based ILs cannot be considered as suitable solvents for a polychloride synthesis. Also sulfonium-based ILs seem to undergo a reaction with Cl_2 as they turn brown upon contact with Cl_2 . The generated products were not investigated further. Additionally the P-N-P-based cation bis(triphenylphosphine)iminium (PPN) was tested and proved to be stable against Cl_2 .

4.3 Investigation of Suitable Conditions for the Convenient Crystallization of Polychloride Salts

For the synthesis of polybromides at which Br_2 can be used both as reactant and solvent at room temperature, performing the reaction in neat halogen is fairly easy. In the case of polychlorides on the other hand, synthesis in neat chlorine bears a couple of challenges, due to the gaseous state and high reactivity of elemental chlorine. Therefore a suitable way to crystallize polychlorides had to be found. Difficulties arise from keeping the products at low temperatures which is essential especially for higher polychlorides as those substances exhibit a high tendency to loose Cl_2 . This is surely due to the gain in entropy if chlorine is set free. As almost no references concerning higher polychlorides exist,^[25] many different methods of crystallization were tested.

As some of the used chlorides yielded liquid products with Cl_2 – substances that can be described as room temperature ionic liquids (RTILs) – the first idea was to cool the substances until crystallization occurs. Almost all of the liquids obtained formed amorphous glassy solids rather than crystals when cooled, independent to the cooling rate. Whenever crystals were obtained the crystallization product was the chloride due to incomplete conversion or the crystals were so disordered that no solvable data set could be received from x-ray diffraction.

As crystallization in substance could not be achieved, the next approach was recrystallization of the obtained products from organic solvents. Unfortunately all products showing bands of higher polychlorides dissolved upon loss of Cl_2 shown by yellow coloring of the solvent. Therefore recrystallization mostly was unsuccessful. If crystallization occurred only the (mono)chloride salt could be detected. Only one attempt of recrystallization was successful. The reaction product of N,N-dimethyl-2-chloroimidazoliniumchloride and Cl_2 was recrystallized from CH_2Cl_2 at $-22\text{ }^\circ\text{C}$. The obtained crystals were investigated by single crystal X-ray structure determination and Raman spectroscopy and could be identified as N,N'-dimethyl-2-chloroimidazoliniumtrichloride (**5**). Full discussion of the structure as well as the corresponding Raman spectrum can be found in Section 4.4.1.

Alternatively the starting materials were dissolved in a particular solvent and the solution was saturated with chlorine. Tests of this method were performed using a couple of different solvents. The results showed that the used organic solvents cannot stabilize higher polychlorides than $[\text{Cl}_3]^-$. Nevertheless this synthetic approach yielded another crystal structure which unfortunately was the same as the one already recrystallized from CH_2Cl_2 .

In order to find a way to stabilize higher polychlorides in solution, crystallize them and thus being able to determine the structure via x-ray diffraction a different approach had to be made. As working in organic solvents failed to yield higher polychlorides the next setup was using liquefied chlorine as solvent. This can be realized either by cooling the sample below $-34.6\text{ }^\circ\text{C}$ which is the boiling point of Cl_2 .^[90] Normally this is done by just condensing chlorine onto the sample at $-78\text{ }^\circ\text{C}$ and keeping the sample at this temperature. The second way is to condense a great excess of chlorine into a pressure vessel containing the sample and letting it warm to room temperature. This procedure leads to liquefied chlorine which has a vapor pressure of 6.7 atm at room temperature. At low temperature most chloride salt were insoluble. Therefore suspensions were obtained in the first instance. During warming up the sample to room temperature most of the chlorides dissolved temporarily. Further warming lead to the formation of a stable two phase system at room temperature. Usually consisting of a heavier phase of a liquefied polychloride and a lighter phase of liquid chlorine, see Fig. 4.16. The spectra in Figure 4.16 both show a strong band at 548 cm^{-1} with a shoulder at 542 cm^{-1} which is a typical shift and pattern of elemental chlorine, indicating that Cl_2 also is dissolved in the polychloride phase. The band of the lower phase spectrum is shifted by about 6 cm^{-1} which is probably an effect caused by the solvation in the polychloride. The spectrum of the lower phase spectrum shows two additional bands at 491 cm^{-1} and 458 cm^{-1} which we assigned to the $[\text{Cl}_9]^-$ anion.

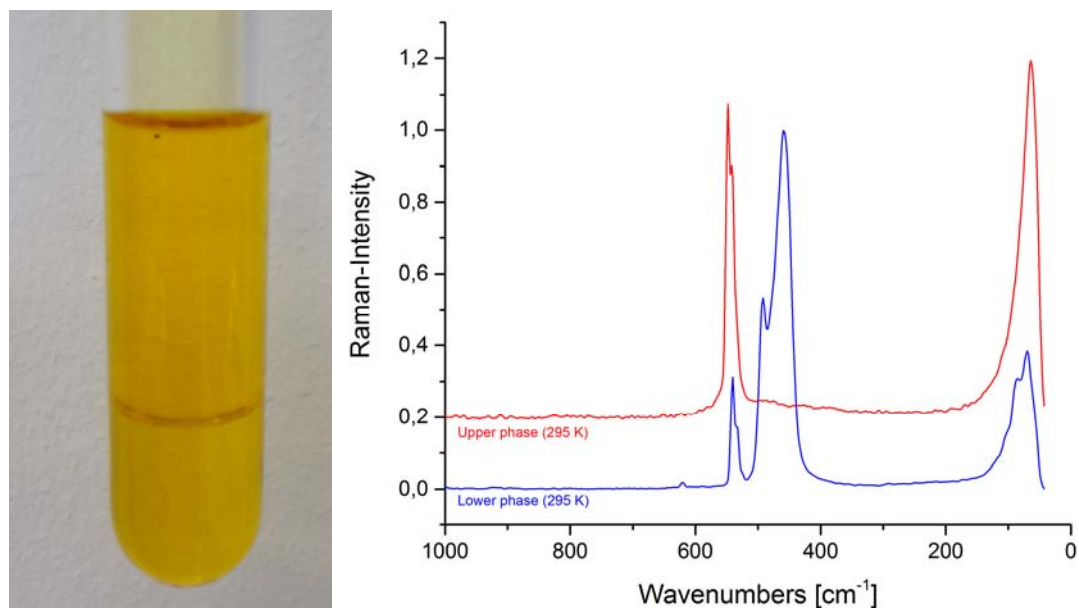


Figure 4.16 Raman spectra of the two phase system of $[\text{CCl}(\text{NMe}_2)_2][\text{Cl}]$ and liquid chlorine.

By slowly decreasing the temperature to $-27\text{ }^\circ\text{C}$ light yellow crystals of this compound could be obtained. At this temperature the vessel is still pressurized and has therefore to be cooled further. At $-40\text{ }^\circ\text{C}$ chlorine has a vapor pressure of approx. 1 atm, so the vessel can be opened to remove some crystals. Unfortunately, the crystals are very fragile and start losing chlorine immediately after being removed from the mother liquor. So far, this could neither be prevented by low temperatures nor by keeping the crystals under inert gas at all times. So no structural data could yet be acquired. Similar behavior can be found for a couple of other cations (see Table 4.8) but no structural trend concerning nonachloride formation could be observed.

Table 4.8 List of nonachlorides including cations, Raman frequencies, measurement temperature and temperature of crystallization (if available) (calculated frequencies given for comparison).

Cation	$\nu_1 [\text{cm}^{-1}]$	$\nu_2 [\text{cm}^{-1}]$	$T_{\text{Raman}} [\text{K}]$	$T_{\text{cryst.}} [\text{K}]$
RI-MP2/def2-TZVPP ^[a]	474.5	435.9	--	--
$[\text{NEt}_4]^+$	460	430	70 K	--
$[\text{PhNMe}_3]^+$	475	448	295 K	--
$[\text{Et}_3\text{MeN}]^+$	463	437	295 K	--
$[\text{CCl}(\text{NMe}_2)_2]^+$	458	437	70 K	246
$[\text{C}_5\text{H}_{10}\text{N}_2\text{Cl}]^{+[\text{b}]}$	491	458	70 K	$>195; <253^{[\text{c}]}$

^[a] Calculation level, ^[b]*N,N'*-dimethyl-2-chloro-imidazolinium, ^[c]exact crystallization temperature could not yet be determined

Upon release of chlorine and decompression of the sample the polychloride phase solidifies and the corresponding trichloride is formed quantitatively, see Fig.4.17.

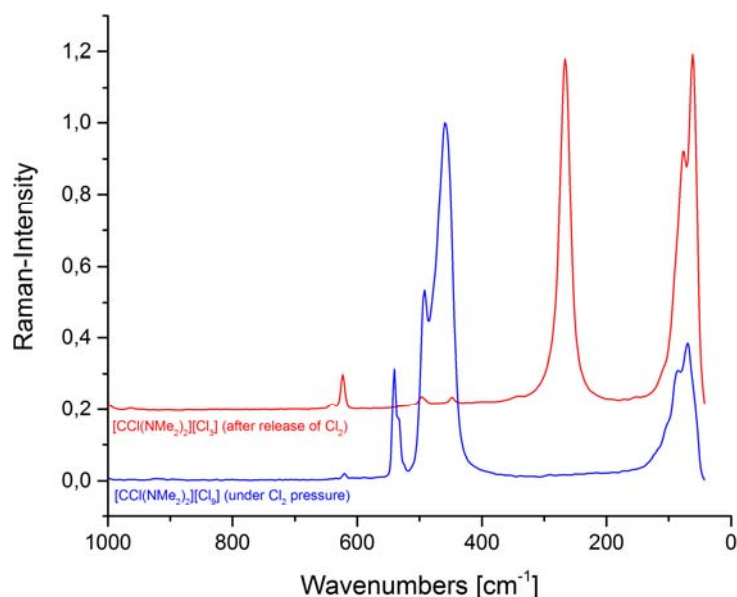


Figure 4.17 Raman spectrum of $[\text{CCl}(\text{NMe}_2)_2][\text{Cl}]$ and liquid chlorine before (blue) and after (red) the release of chlorine.

As already mentioned a different approach towards the crystallization of polychlorides was the use of ionic liquids as solvent. This approach had already been successfully applied for synthesizing polybromides by Feldmann et al. in 2011.^[77] Another advantage of the approach is the avoidance of the entropically unfavorable transition of gaseous Cl₂ to a solid polychloride or rather the preferred loss of gaseous Cl₂ from the solid polychloride. This is the case because Cl₂ exhibits a very high solubility in most of the ionic liquids tested and will so be available in solution already so that a chlorine saturated environment can be created in solution.

First attempt were adapted from the already mentioned polybromide synthesis.^[77] The use of the $[\text{C}_{10}\text{MP}]^+$ cation was avoided as legitimate doubt regarding the stability against elemental chlorine was given. N-butyl-N-methylpyrrolidiniumchloride ($[\text{BMP}]\text{Cl}$) was used instead to form an eutectic mixture of $[\text{BMP}]\text{Cl}$ and N-butyl-N-methylpyrrolidiniumtriflate ($[\text{BMP}]\text{OTf}$). That is a crucial point to successfully perform this synthetic approach as $[\text{BMP}]\text{Cl}$ exhibits a melting point of 124 °C while $[\text{BMP}]\text{OTf}$ has a melting point of 4 °C. Indeed an equimolar mixture of both ionic liquids formed more of a slush than a liquid but remained fluid down to 0 °C. Addition of gaseous Cl₂

lead to a further significant drop of the melting point as well as the viscosity and a clear, bright yellow solution of low viscosity with a melting point of around $-30\text{ }^{\circ}\text{C}$ was formed. Cooling of the solution below $-30\text{ }^{\circ}\text{C}$ lead to the formation of colorless crystals of [BMP]OTf. Although these solutions contained different polychlorides according to the Raman spectrum, no polychloride crystals could be obtained.

Because crystallization with the given cation was not successful another chloride salt was added to the reaction mixture. As for the symmetric quaternary ammonium salts the only salt that showed sufficient solubility at room temperature after addition of Cl_2 was [NEt₄]Cl. [NMe₄]Cl was completely insoluble at all temperatures while [NPr₄]Cl and [NBu₄]Cl formed a microcrystalline precipitate which could be dissolved by slightly warming the reaction mixture to about $40\text{ }^{\circ}\text{C}$. Upon cooling both mixtures containing the heavier ammonium cations again a microcrystalline precipitation occurred, but no suitable crystals could be obtained. In the mixture containing [NEt₄]Cl however, crystallization could be observed below $-15\text{ }^{\circ}\text{C}$.^[RB2] The crystallized compound was characterized to be [Et₄N]₂[(Cl₃)₂·Cl₂] (**7**), see Section 4.4.3.

The P-based compounds PPh₃, P(C₆H₅)₃, [PPh₄]Cl and [PPN]Cl showed the same insolubility as [NMe₄]Cl. In contrast, the asymmetric ammonium salts [Et₃MeN]Cl, [Et₃PrN]Cl and [PhMe₃N]Cl showed very high solubility before as well as after addition of Cl_2 . On the other hand those mixtures showed no crystallization even if cooled below $-25\text{ }^{\circ}\text{C}$. By cooling below $-30\text{ }^{\circ}\text{C}$ crystals of [BMP]OTf were obtained.

The same procedure was applied to tetramethylchloroamidiniumchloride ([CCl(NMe₂)₂]Cl) and N,N'-dimethyl-2-chloroimidazoliniumchloride ([C₅H₁₀N₂Cl]Cl) which showed good solubility in the eutectic mixture of ILs and Cl_2 . Crystallization could be achieved for both compounds. In case of [C₅H₁₀N₂Cl]Cl the same trichloride already obtained in Section 4.3.2 was crystallized. In case of [CCl(NMe₂)₂]Cl also the trichloride was crystallized and [CCl(NMe₂)₂][Cl₃] (**6**) was characterized via single crystal X-ray structure determination as well as Raman spectroscopy, for detailed information and full discussion of the crystal structure see Section 4.4.2.

An interesting fact concerning the reaction mixtures of [BMP]Cl, [BMP]OTf, Cl_2 and a variety of different chloride salt, is that those mixtures show no noticeable difference in the characteristic range of their Raman spectra from $600\text{ to }300\text{ cm}^{-1}$, see Figure 4.18.

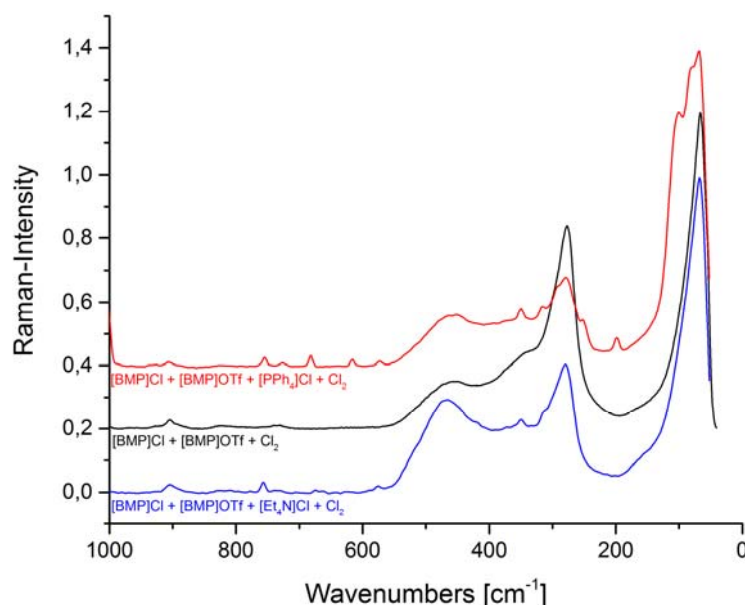


Figure 4.18 Raman spectra of reaction mixtures in the eutectic mixture of [BMP]Cl and [BMP]OTf.

As displayed in Figure 4.18 all spectra show the same characteristics. A distinct band at 278 cm^{-1} which can be assigned to the $[\text{Cl}_3]^-$ anion, a broad band centered at 463 cm^{-1} that has already been assigned to different coordinated Cl_2 species and finally two minor bands at 313 cm^{-1} and 350 cm^{-1} that derive from the triflate anion which is contained in the ionic liquids used as solvent.^[91] This suggests that the same anionic species are present in these solutions, independent from the cation used. Separation into specific polychlorides can be achieved via crystallization.

The above mentioned starting materials were also used for crystallization using the ILs [BMP]Cl and [BMP]OTf on their own as solvent. This was found to be possible as both ILs form liquid solutions of Cl_2 exhibiting melting points below $-30\text{ }^\circ\text{C}$. Unfortunately $[\text{C}_5\text{H}_{10}\text{N}_2\text{Cl}]\text{Cl}$ was found to be insoluble in the [BMP]Cl/ Cl_2 mixture. In a [BMP]OTf/ Cl_2 mixture crystals of $[\text{C}_5\text{H}_{10}\text{N}_2\text{Cl}][\text{Cl}_3]$ (**5**) could be obtained. $[\text{CCl}(\text{NMe}_2)_2]\text{Cl}$ was found to be well soluble in both mixtures. While $[\text{CCl}(\text{NMe}_2)_2]\text{Cl}$ in a [BMP]Cl/ Cl_2 mixture yielded the trichloride $[\text{CCl}(\text{NMe}_2)_2][\text{Cl}_3]$ (**6**) already obtained from the eutectic mixture mentioned above. Finally $[\text{CCl}(\text{NMe}_2)_2]\text{Cl}$ in a [BMP]OTf/ Cl_2 mixture yielded coffin-lid shaped pale yellow crystals at $-25\text{ }^\circ\text{C}$ which were investigated by single crystal X-ray structure determination and Raman spectroscopy and could be identified as $[\text{CCl}(\text{NMe}_2)_2]_2[\text{Cl}_8]$ (**8**) being the first structural proof for a polychloride dianion, see Section 4.4.4.

4.4 Crystal Structures

4.4.1 *N,N'*-Dimethyl-2-Chloroimidazoliniumtrichloride

N,N'-dimethyl-2-chloroimidazoliniumtrichloride (**5**) crystallizes in the orthorhombic space group *Pbca*. The structure represents a typical trichloride being linear and slightly asymmetric with bond lengths of 231.0(1) pm and 227.1(1) pm. With a difference of only 3.9(1) pm between the Cl–Cl bonds (**5**) is the most regular trichloride to be reported up to now. The compound exhibits a layered structure every layer consisting of anions and cations being arranged in columns which are themselves arranged alternately (Fig.4.19). Cation arrangement is repeated in every second layer while the arrangement of the anions is recurred in every fourth layer forming a layered structure with an ABA'B' sequence.

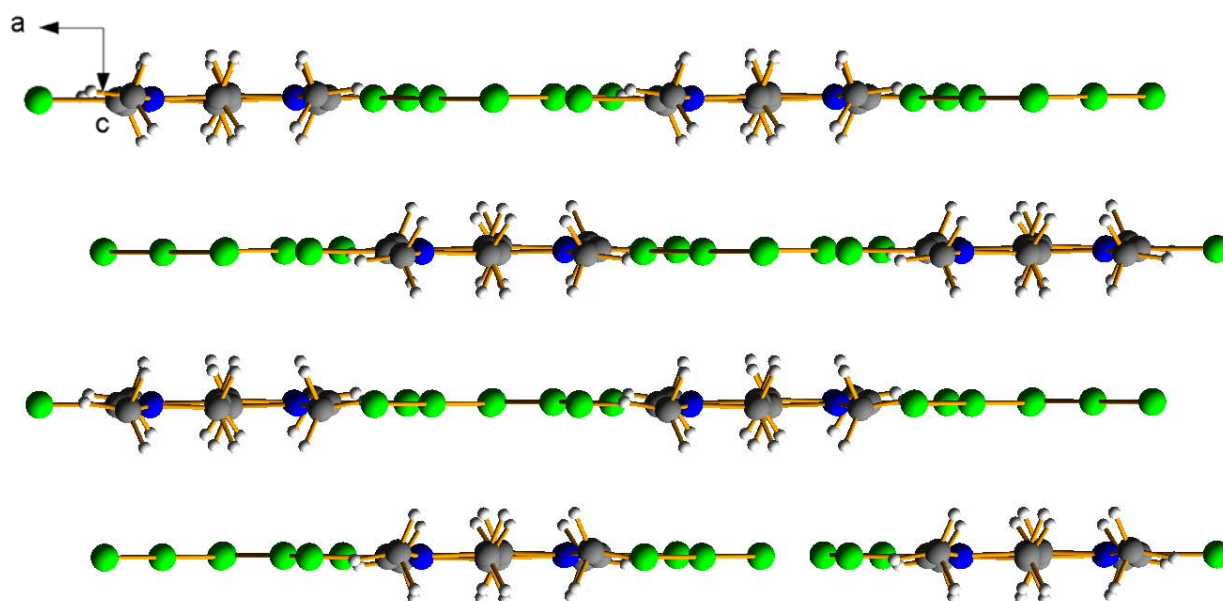


Figure 4.19 Crystal structure of (**5**) viewed along *b*-axis showing layers as well as anionic and cationic columns.

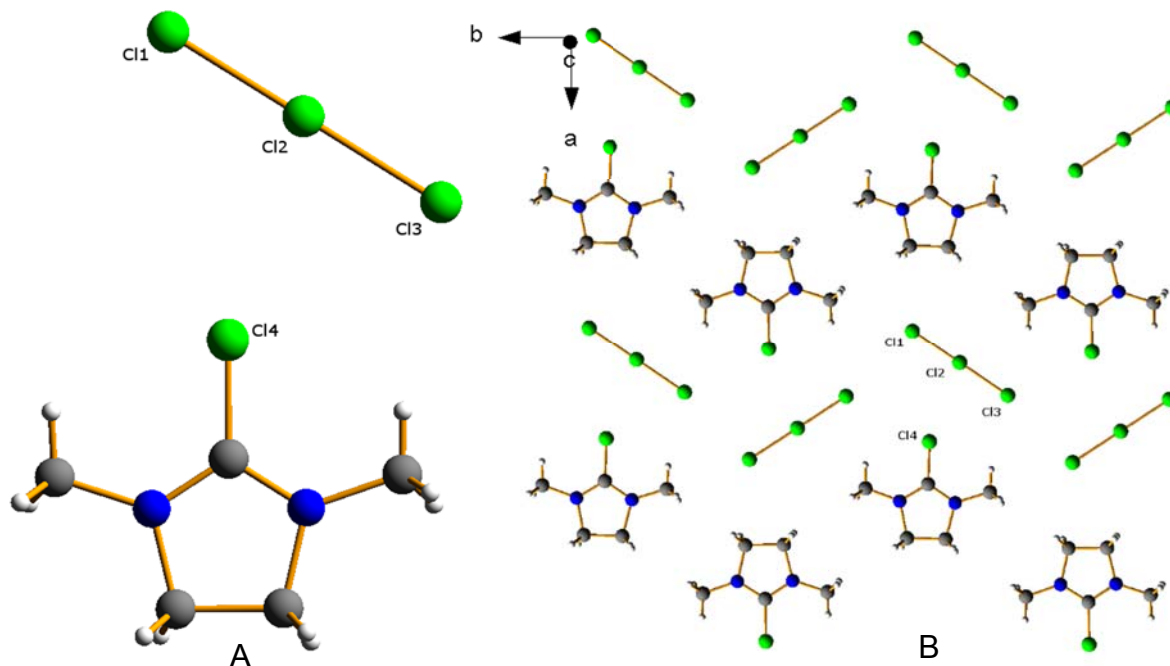


Figure 4.20 Labelled molecular structure of (5) (A) and arrangement of anions and cations viewed along *c*-axis (B).

Figure 4.20 shows the arrangement of the ions revealing that the $[\text{Cl}_3]^-$ anions form infinite zig-zag chains within the layer. Even though Cl–Cl distances (371.0 pm) are higher than the sum of the van-der-Waals radii of chlorine (350 pm)^[45] these anions interact with one another. Another hint suggesting interactions between the anions lies within the angles formed by the zig-zag chains of the $[\text{Cl}_3]^-$ anions. The angle in which the $[\text{Cl}_3]^-$ anions are situated to one another is $100.9(1)^\circ$. This angle suggests that σ -hole interactions could play a role in directing the structure of the compound. Those zig-zag chains have also been observed in other trichloride structures, such as $[\text{AsPh}_4][\text{Cl}_3]$ ^[21] although the distances between the $[\text{Cl}_3]^-$ anions tend to be longer.

Table 4.9 Comparison of bond lengths and angles of (5), $[\text{PPh}_4][\text{Cl}_3]$ ^[24] (4) and $[\text{AsPh}_4][\text{Cl}_3]$ ^[21] (1).

Bond/Angle ^[a]	(5)	(4)	(1)
r_{12}	227.1(1)	226.3(1)	230.5(3)
r_{23}	231.0(1)	230.7(1)	222.7(4)
$r_{31'}$	371.0(1)	> 500	397.8(2)
r_{24}	336.5(1)	-	-
α_{123}	179.8(1)	178.4(1)	177.5(2)

^[a]Bond lengths in [pm] and angles in [°]

Table 4.9 shows the bond lengths and angles of **(5)** compared to those of $[\text{PPh}_4][\text{Cl}_3]$ (**4**) and $[\text{AsPh}_4][\text{Cl}_3]$ (**1**) which are the trichloride structures with the most regular Cl–Cl bond distances besides the presented one.^[21,24] Comparing these structures it is even more surprising that the $[\text{Cl}_3]^-$ anions in **(5)** are more regular than in **(4)** because the interanionic distances in **(4)** are very long, so no interaction can be assumed between the $[\text{Cl}_3]^-$ anions. **(1)** has a more comparable distance between the anions but shows a higher irregularity than both of the other structures. Observing the structure of **(4)** shows that the more loosely bond Cl-atom has lots of close contacts to the surrounding cations while the other terminal Cl-atom has no such contacts. This might well be the explanation for the greater difference in the bond lengths of **(4)**. Also the almost perfect linearity of the $[\text{Cl}_3]^-$ anion is rather surprising as the structure **(5)** exhibits very close contacts between the central Cl-atom of the anion (Cl2) and the Cl-atom of cation (Cl4) (336.5 pm) being even below the sum of the van-der-Waals radii of chlorine.

The Raman spectrum in Figure 4.21 shows the expected band at at 266 cm^{-1} which was assigned to the $[\text{Cl}_3]^-$ anion. The other band belong to the cation. Solvent peaks are not present because the Raman spectrum of the crystal was recorded on a Raman microscope.

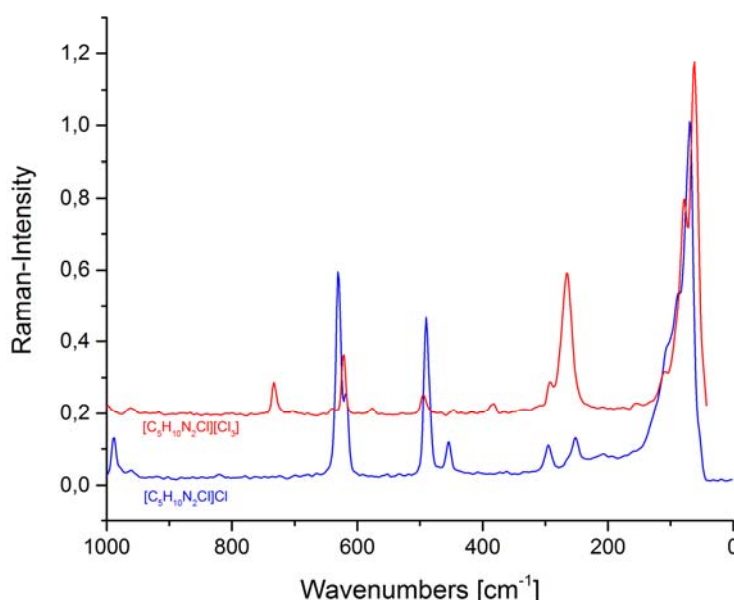


Figure 4.21 Raman spectra of **(5)** (red) and the starting material $[\text{C}_5\text{H}_{10}\text{N}_2\text{Cl}]\text{Cl}$ (blue).

4.4.2 Tetramethyl-Chloro-Amidinium Trichloride $[\text{CCl}(\text{NMe}_2)_2][\text{Cl}_3]$

Tetramethyl-chloro-amidinium trichloride (**6**) also crystallized in the orthorhombic space group *Pbca*. In general structural parameters the structures (**5**) and (**6**) are very similar (see crystallographic data). (**6**) also represents a typical linear trichloride and the difference of Cl–Cl bond lengths ($\Delta r = 5.9$ pm) is only slightly bigger than in (**5**). Thus, (**6**) is also a very regular trichloride and the Cl–Cl bond lengths of 225.9(1) pm and 231.8(1) pm are almost matching those of (**5**). This compound also exhibits a layered structure with layers that consist of anions as well as of cations, see Fig.4.22. Even though the cations of (**5**) and (**6**) are very similar the structural composition within the layers is quite different. In contrast to (**5**) this structure is much more separated as the cations and anions are stacked alternately to pillars that do not seem to have much contact to one another, see Fig.4.23.

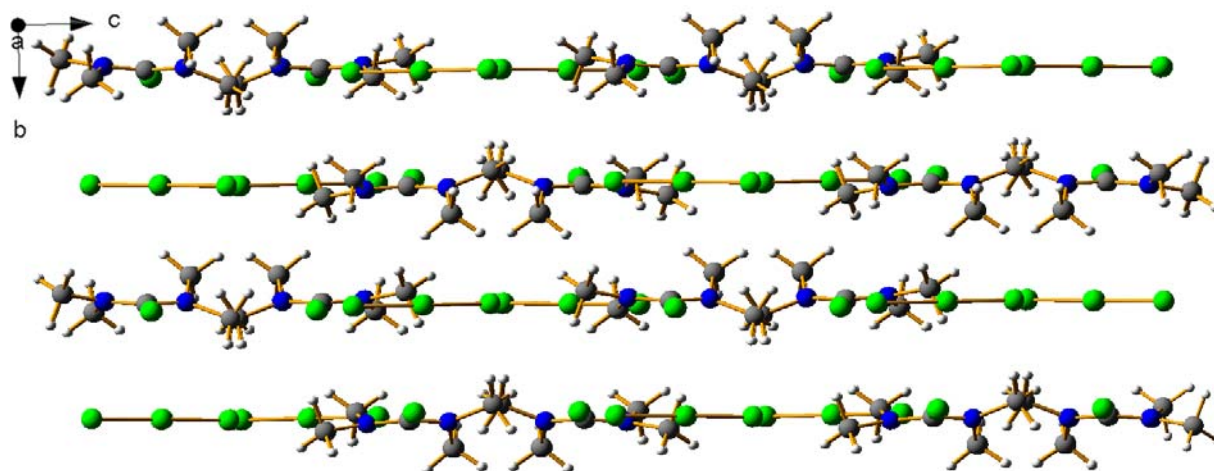


Figure 4.22 Crystal structure of (**6**) viewed along *a*-axis exhibiting layers made up of cations and anions.

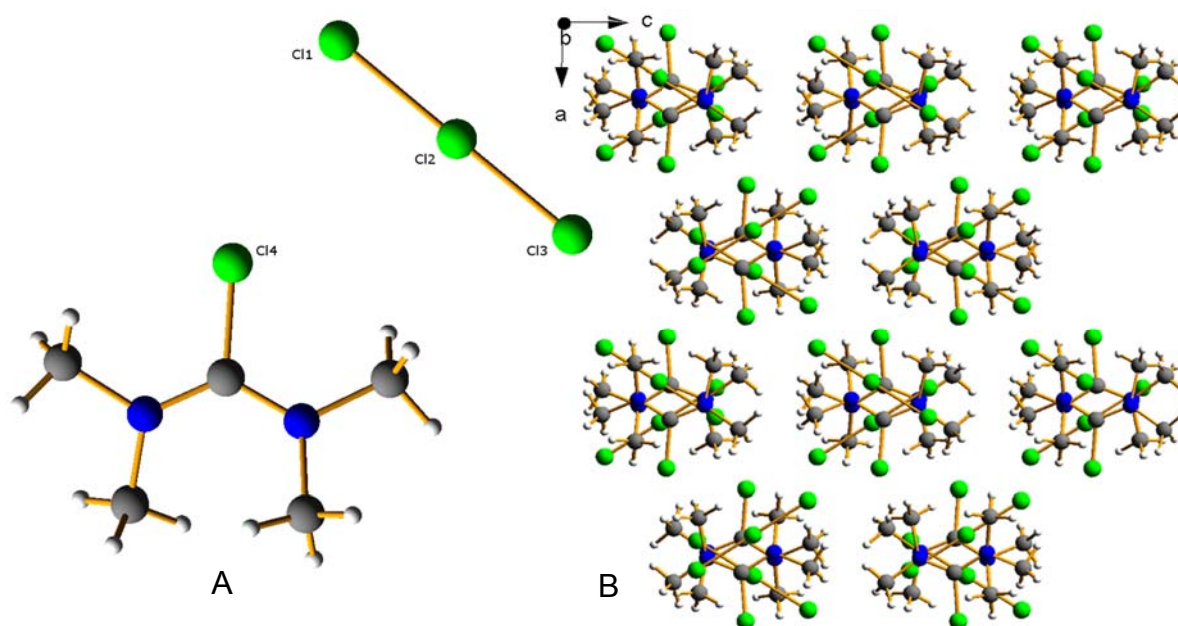


Figure 4.23 Labeled *molecular structure of (6)* (A) *top view of the layers along b-axis showing isolated pillars* (B).

Although it is not as obvious as in **(5)** the $[\text{Cl}_3]^-$ anions in **(6)** are also arranged in zig-zag chains which are much more wide-meshed here. A view of anions is displayed in Figure 4.24 showing the zig-zag chains. Distances along the chains ($r_{13'}$) are 511.0(1) pm which is not the shortest interanionic distance being 470.1(1) pm ($r_{12'}$). Both distances are marked in Figure 4.24. Selected bond lengths and angles of both **(5)** and **(6)** are listed in Table 4.10.

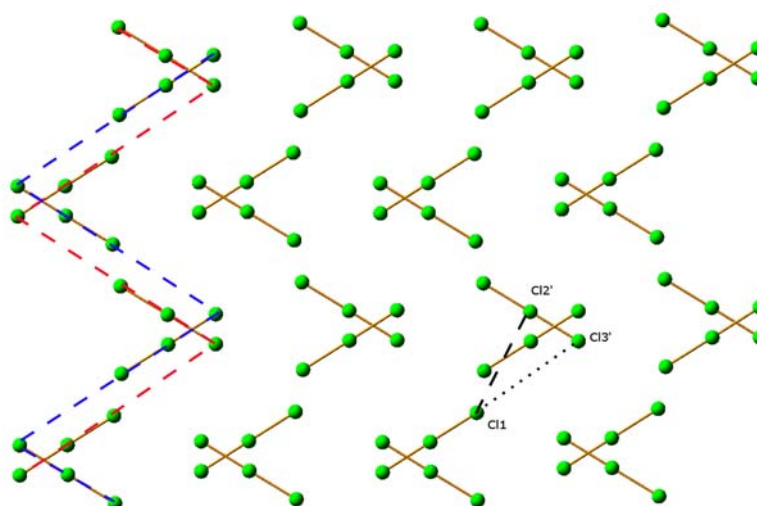


Figure 4.24 *Projection showing two layers of anions exhibiting zig-zag chains (dashed blue and red lines) as well as the shortest interanionic contact (dashed black line).*

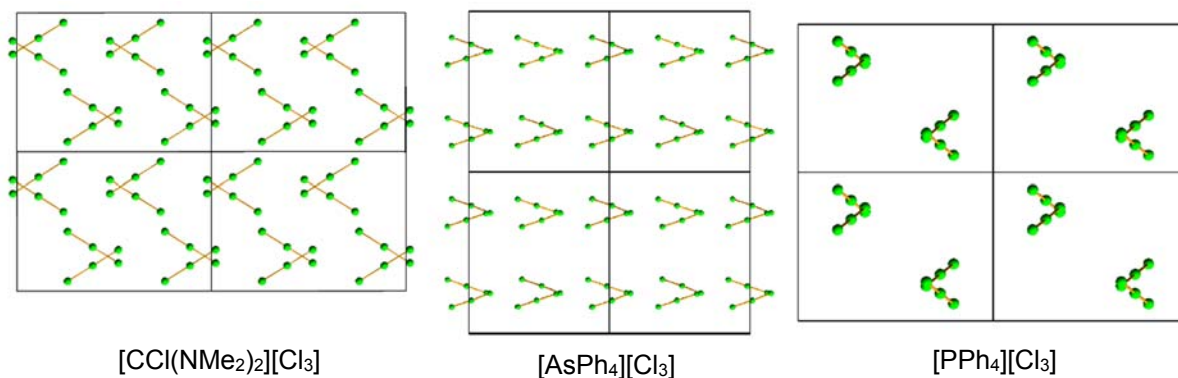


Figure 4.25 Comparison of the anionic arrangements of $[\text{CCl}(\text{NMe}_2)_2][\text{Cl}_3]$, $[\text{AsPh}_4][\text{Cl}_3]$ ^[21] and $[\text{PPh}_4][\text{Cl}_3]$.^[24]

Figure 4.25 shows that the positioning of the $[\text{Cl}_3]^-$ anions in the displayed crystal structures resemble each other very much. All three show the same arrangement of the anions enabling very weak contacts in forming wide meshed zig-zag chains. Only the arrangement of structure (B) differs as the orientation of the $[\text{Cl}_3]^-$ anions is not alternating but regular. Furthermore in Figure 4.26 a comparison of anion arrangement in structures (5) and (6) is shown, revealing that (5) exhibits a very similar structural motive.

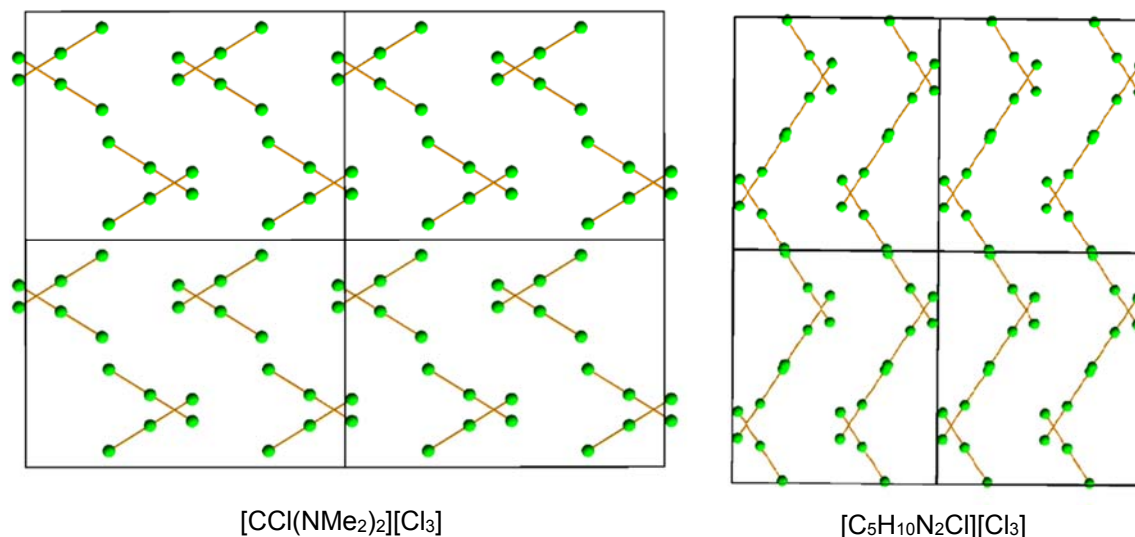


Figure 4.26 Anionic arrangement of $[\text{CCl}(\text{NMe}_2)_2][\text{Cl}_3]$ and $[\text{C}_5\text{H}_{10}\text{N}_2\text{Cl}][\text{Cl}_3]$ also showing similarities.

Table 4.10 Comparison of bond lengths and angles of (5) and (6).

Bond/Angle ^[a]	(5)	(6)
r ₁₂	227.1(1)	225.9(1)
r ₂₃	231.0(1)	231.8(1)
r _{31'}	371.0(1)	511.0(1)
r _{21'}	599.1(1)	470.1(1)
r ₂₄	336.5(1)	381.1(1)
r ₁₄	447.1(1)	369.5(1)
α ₁₂₃	179.8(1)	179.6(1)

^[a]Bond lengths in [pm] and angles in [°]

A Raman spectrum of the solution of [BMP]Cl and [BMP]OTf from which (6) was crystallized was recorded as well as a spectrum of a crystal of (6) employing a Raman-microscope. As shown in Figure 4.27 the spectra show significant differences, emphasizing that the compound crystallized is not necessarily the only species present in the solution of the ILs. Both spectra show the well-known band assigned to the [Cl₃][−] anion at 278 cm^{−1} (in solution) and 270 cm^{−1} (in the crystal). The only additional bands the spectrum of the crystal shows are those belonging to the cation. The spectrum of the solution shows most notably the broad band centered at 465 cm^{−1} which can be assigned to coordinated Cl₂ molecules. Additionally the spectrum shows the smaller bands already assigned to the triflate anion.^[91]

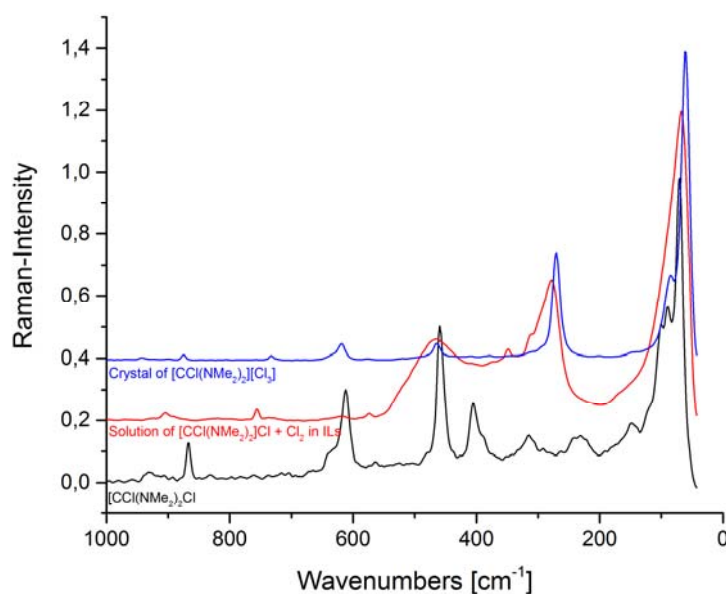


Figure 4.27 Raman spectra of [CCl(NMe₂)₂]Cl (black), [CCl(NMe₂)₂][Cl₃] in solution (red) and a crystal of [CCl(NMe₂)₂][Cl₃] (blue).

4.4.3 $[\text{Et}_4\text{N}]_2[(\text{Cl}_3)_2\cdot\text{Cl}_2]$: A 2D Polychloride Network Held Together by Halogen–Halogen Interactions

This chapter is based on the manuscript submitted for final publication “Robin Brückner, Heike Haller, Simon Steinhauer, Carsten Müller, and Sebastian Riedel. A 2D Polychloride Network Held Together by Halogen–Halogen Interactions, Angew. Chem. Int. Ed., 2015, 54, 15579–15583.” (DOI: 10.1002/anie.201507948) [RB2] which can be found at the end of this work in Appendix A2. Copyright © 2015 WILEY-VCH Verlag GmbH & Co. KGaA, Weinheim.

Main work of this publication has been carried out by Robin Brückner, refinement of the structural data has been carried out by Heike Haller, solid-state calculations have been carried out by Carsten Müller.

$[\text{Et}_4\text{N}]_2[(\text{Cl}_3)_2\cdot\text{Cl}_2]$ (**7**) exhibits a quite different structure than the above described trichlorides. The compound crystallized in the monoclinic space group $\text{C2}/m$. Like other polyhalides, the structure consists of three different building blocks: Cl^- and $[\text{Cl}_3]^-$ as Lewis bases and Cl_2 as Lewis acid. A central Cl^- (5) and one bridging Cl_2 unit in two differing crystallographic positions form a linear chain, see Fig. 4.28. The bond lengths of the coordinated chlorine molecules (1–1' and 8–8') are only slightly elongated by 5 pm compared to that found in the crystal structure of Cl_2 (199.4(2) pm).^[92] This is already known from coordinated Cl_2 units.^[25] An additional Cl_2 unit (6–7) is coordinating end-on; that is, orthogonally to the chain. This coordination is much stronger (255.7(6) pm) than for the bridging units and we may indeed consider this as a distorted $[\text{Cl}_3]^-$ anion ($\beta\text{-Cl}_3$). The bond lengths between this $[\text{Cl}_3]^-$ group and the two coordinated Cl_2 molecules are 301.9(1) pm and 291.9(5) pm, respectively, and so considerably longer than normal Cl–Cl bonds, but still noticeably shorter than the sum of the van-der-Waals radii of chlorine (350 pm).^[45]

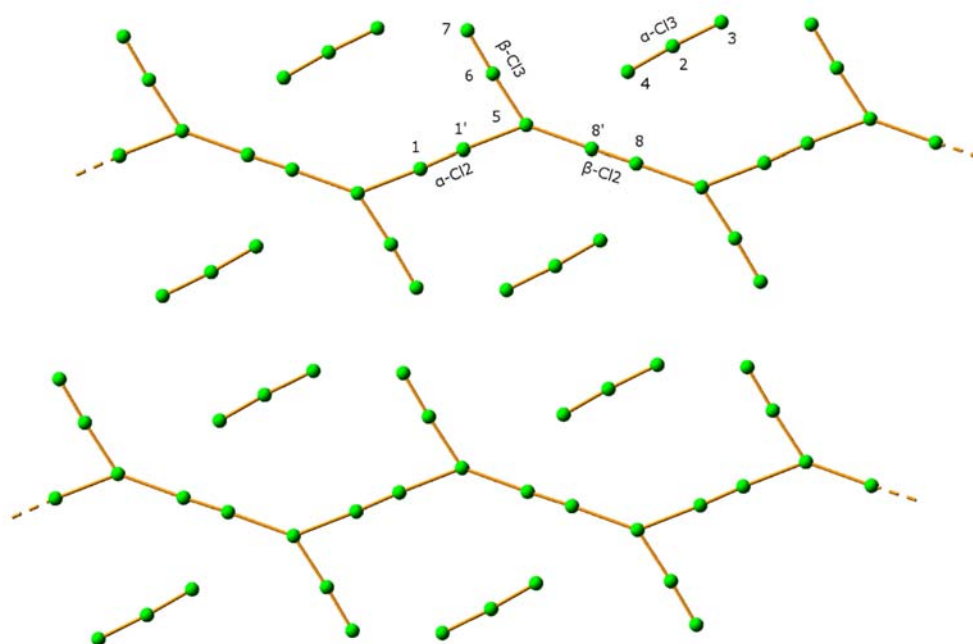


Figure 4.28 Structure of the anionic layer in the crystal. Selected bond lengths [pm] and angles[°]: r_{56} 255.8(3), r_{67} 211.0(3), r_{23} 223.2(2), r_{24} 234.6(2), $r_{11'}$ 202.3(3), $r_{88'}$ 203.7(4), r_{15} 301.9(2), r_{58} 292.0(3); a_{567} 177.4(2), a_{423} 176.5(1).

The parallel chains are stacked to planar layers, see Fig. 4.29. Embedded within the planar layers, we find an additional $[\text{Cl}_3]^-$ group ($\alpha\text{-Cl}_3$). This does not show any coordinating contacts to the chlorine framework. The cations are situated between the anionic layers.

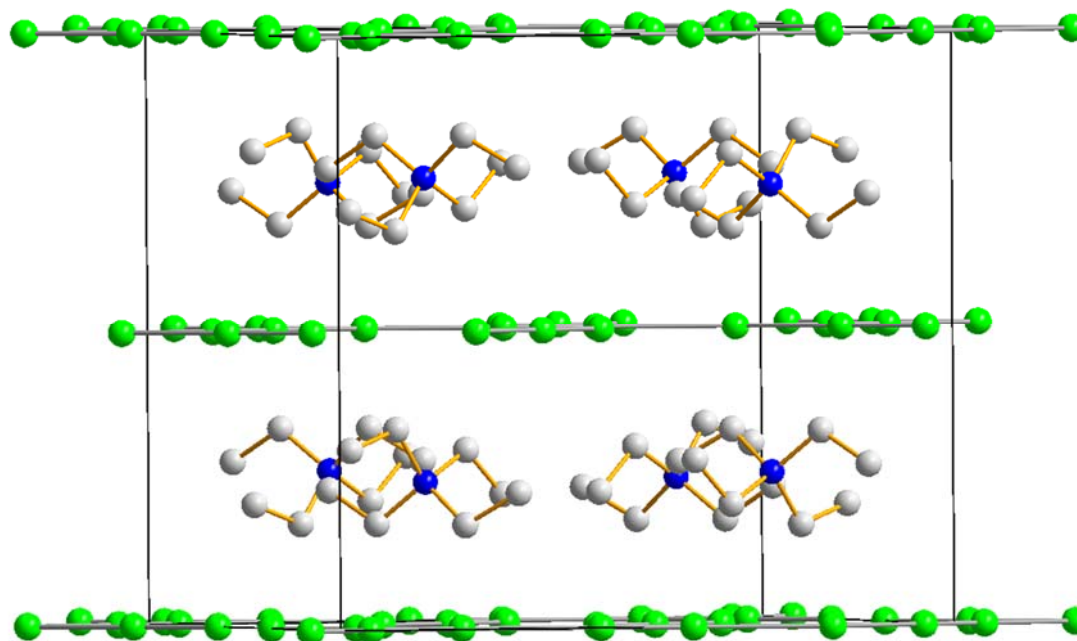


Figure 4.29 Projection of the unit cell of (7) showing the anionic layers and cations situated in between.

Structure optimization of the internal coordinates (fixed unit cell) at DFT level using the B3LYP functional in combination with dispersion correction (D2 according to Grimme)^[83] was used to verify the structure determination from the above discussed X-ray diffraction data, simulate IR and Raman spectra, and further analyze the bonding character in the polychloride layers. Counter ions were neglected because their influence on the properties of the polychloride network is expected to be minor.

Table 4.11 Calculated and experimental structure parameters.^[a]

Compound	X-Ray	B3LYP-D2	Fragment
r _{11'}	202.3(3)	207.4	α-Cl ₂
r _{88'}	203.7(4)	211.2	β-Cl ₂
r ₅₆	255.8(3)	243.6	β-Cl ₃
r ₆₇	211.0(3)	219.7	β-Cl ₃
r ₂₃	223.2(2)	228.5	α-Cl ₃
r ₂₄	234.6(2)	231.2	α-Cl ₃
r ₁₅	301.9(2)	294.7	
r ₈₅	292.0(3)	280.1	
α ₅₆₇	177.4(2)	179.1	β-Cl ₃
α ₄₂₃	176.5(1)	179.8	α-Cl ₃

^[a]Bond lengths in pm and angles in °.

A comparison of the most relevant bond distances and angles shows that the result from the B3LYP-D2 structure optimization agrees well with the experimental structure shown above (Table 4.11). Only the very weak interactions between the Cl₂ and [Cl₃]⁻ anion in the Cl₃–Cl₂ chains appear to be overestimated, leading to distances that are too small, an effect which is very likely related to the well-known exaggeration of dispersion effects by the D2 correction method in solids.^[17] Comparison with calculations for isolated Cl₂ (r= 200.4 pm) and [Cl₃]⁻ (r=230.3 pm) molecules at the same level of theory show that the two Cl₂-like and the isolated Cl₃- like groups (α-Cl₃) in the polychloride layer are only slightly perturbed from their equilibrium structure in vacuum. The second Cl₃-like group (β -Cl₃) is much more perturbed and appears to resemble an intermediate between [Cl₃]⁻ and a Cl₂ bound to a Cl⁻. Such bonding situations can be further investigated by vibrational spectroscopy. Raman spectroscopy in particular is a very powerful technique, as the present system shows a strong Raman-scattering effect (Figure 4.30).

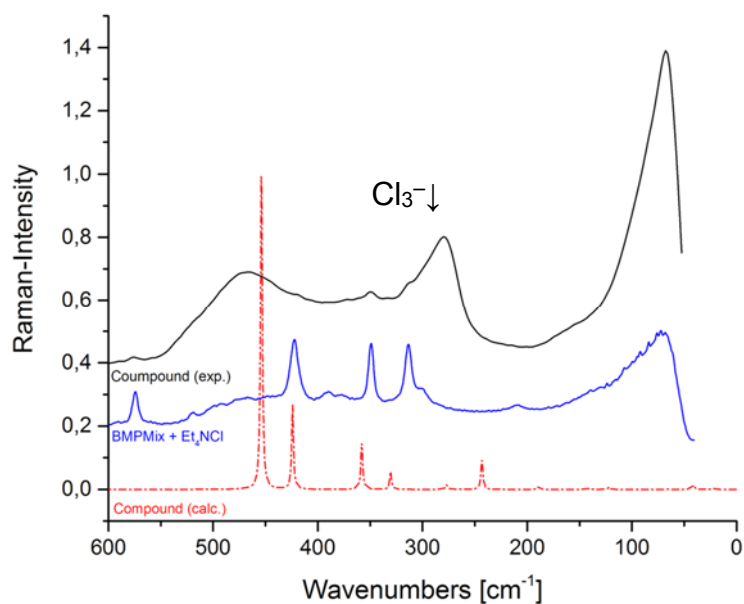


Figure 4.30 Calculated (red) and experimental (black) *Raman spectra of (7)*. *Raman spectrum of solution without Cl₂ (blue) is given for comparison.*

The measured Raman spectrum shows a strong band at 280 cm⁻¹ (calc. 277 cm⁻¹) belonging to the symmetric stretching vibration of the [Cl₃]⁻ ion. This is in good agreement with the bands observed in our previous powder spectra of [Et₄N]⁺[Cl₃⋯Cl₂]⁻ (274 cm⁻¹) and [Pr₄N]⁺[Cl₃]⁻ (272 cm⁻¹). Another intense broad Raman band centered at 465 cm⁻¹ (calc. 454 cm⁻¹) is assigned to the stretching mode of one Cl₂ unit.^[25] Furthermore, we found a less intense Raman band at 420 cm⁻¹ (calc. 424 cm⁻¹) that can be assigned to the Cl–Cl stretching mode of the other Cl₂ unit. At 350 cm⁻¹ and 313 cm⁻¹, two bands with lower intensity occur belonging to the triflate anion,^[91] which was part of the ionic liquids used as solvent. The large band below 100 cm⁻¹ belongs to longitudinal vibrations of the compound. Along with the Raman spectrum, a far-IR spectrum was measured (Figure 4.31 and Table 4.12). The spectrum shows two broad bands of the symmetric and antisymmetric stretching mode of [Cl₃]⁻ at 277 and 228 cm⁻¹, respectively.^[26]

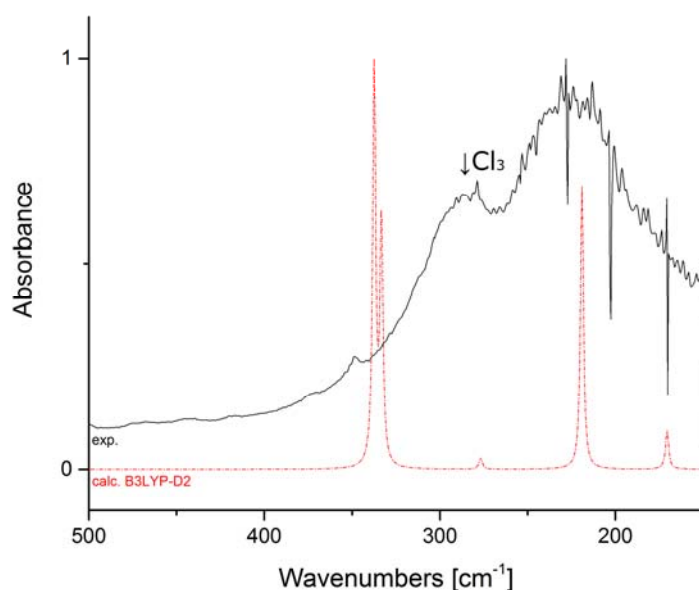


Figure 4.31 Experimental (black) and at B3LYP-D2 level calculated IR spectrum (red, dashed line).

Table 4.12 Experimental and computed vibrational frequencies of $[Et_4N]_2[(Cl_3)_2 \cdot Cl_2]$.

Mode ^[a]	Raman ^[b]	IR	Calc.(Raman) ^[c]	Calc.IR ^[c]	Lit. ^[25,45]
$\nu_s [Cl_3]^-$		228.5		219.1	232
$\nu_1 [Cl_3]^-$	279.8	278.6	278.7	276.8	275
$2\nu_2 [Cl_3]^-$	333.2		330.4	333.3	330
$\nu_s [Cl_3 \cdots Cl_2]^-$			358.0	337.4	
$\nu_1 [Cl_3 \cdots Cl_2]^-$	420.3		424.1		
ν_1 L-sh	465.7		453.8		466

^[a]Frequencies in cm^{-1} , ^[b]calculated band at 358 probably overlain by OTf band, ^[c]calculated at B3LYP-D2 level

For a qualitative characterization of the bonding pattern in the Cl-layers, Mulliken charges were calculated from the Hartree-Fock wave function taking into account the experimental crystal structure, see Table 4.13. The entire unit cell of the isolated Cl-network has a charge of -4 a.u. The network consists of stronger bound Cl_3-Cl_2 chains with Mulliken charges of -0.990 and $-0.090 / -0.136$ a.u., respectively, and looser bound $[Cl_3]^-$ ions with a Mulliken charge of -0.998 a.u.. For further analysis, the electrostatic potential was calculated within the plane. Figure 4.32 shows a combined contour-rainbow plot of the electrostatic potential with one additional (bold) contour indicating the electron density value of 0.001 e/bohr^3 , which is the value suggested by Bader et al. for exploring features in the electrostatic potential around a molecule.^[93] Most remarkable in this map are the regions of less negative potentials along the extension of the bond axis in the $\alpha-Cl_3$ units – known as σ -holes – and the related belts

of negative potential perpendicular to the bond axis at both lateral chlorine atoms. The atoms within the $\text{Cl}_2\text{-Cl}_3$ -chains are too close to each other to observe σ -holes, but the belts are visible to less extent for the $\beta\text{-Cl}_2$ and $\beta\text{-Cl}_3$ units as well. Thus one also observes a weak σ -hole interaction between $\beta\text{-Cl}_2$ and $\alpha\text{-Cl}_3$ units, as well as between the $\beta\text{-Cl}_3$ and $\alpha\text{-Cl}_3$ units. These halogen-halogen interactions lead to further stability of the negatively charged polychloride network.

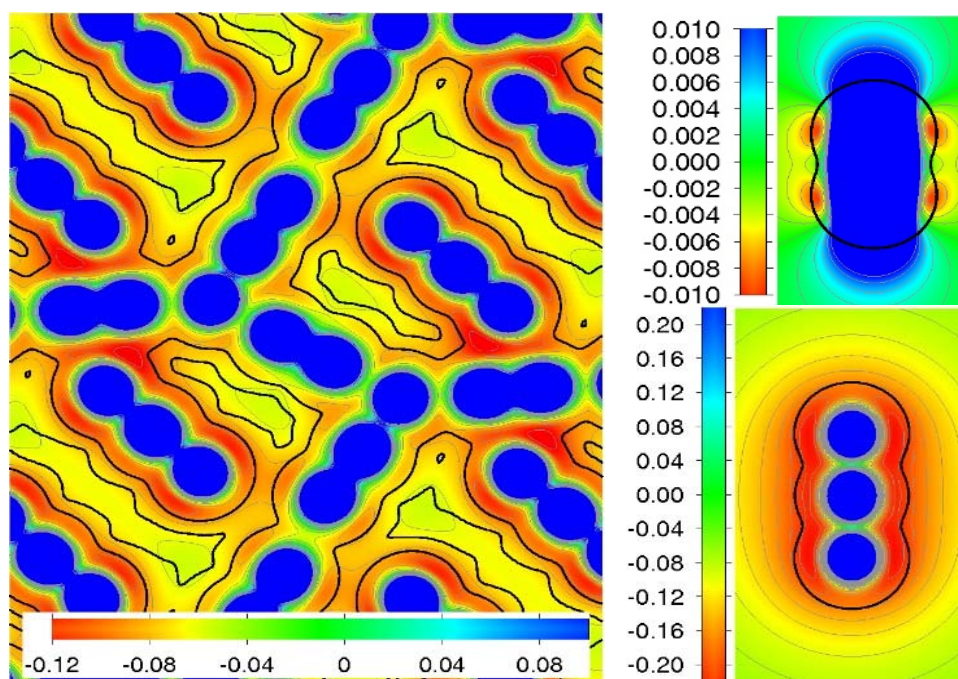
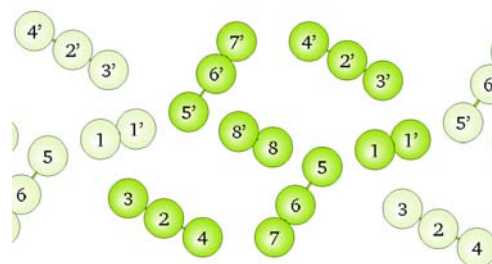


Figure 4.32 Plot of the electrostatic potential (in a.u.) of the polychloride network as well as for the isolated Cl_2 and $[\text{Cl}_3]$ molecules. The bold black line indicates the electron density contour line of 0.001 e/bohr^3 . Thin grey contours show equi-electrostatic potentials as indicated in the color bar with intervals of 0.02 (Cl-layer, $[\text{Cl}_3]$) and 0.002 a.u. (Cl_2).

Table 4.13 Computed Mulliken charges of the polychloride network calculated for the experimental structure at the HF level.

Atom number	Charge	Fragment
1	-0.045	$\alpha\text{-Cl}_2$
2	-0.021	$\alpha\text{-Cl}_3$
3	-0.415	"
4	-0.562	"
5	-0.658	$\beta\text{-Cl}_3$
6	-0.009	"
7	-0.222	"
8	-0.068	$\beta\text{-Cl}_2$



4.4.4 Tetramethyl-Chloro-Amidinium Octachloride $[\text{CCl}(\text{NMe}_2)_2]_2[\text{Cl}_8]$: Structural Proof for the First Dianion of a Polychloride

This chapter is based on the manuscript submitted for final publication “Robin Brückner, Patrick Pröhm, Anja Wiesner, Simon Steinhauer, Carsten Müller, Sebastian Riedel. Structural Proof for the First Dianion of a Polychloride: Investigation of $[\text{Cl}_8]^{2-}$, Angew. Chem. Int. Ed., 2016.” (DOI: 10.1002/anie.201604348) [RB3] which can be found at the end of this work in Appendix A3. Copyright © 2016 WILEY-VCH Verlag GmbH & Co. KGaA, Weinheim.

Main work of this publication has been carried out by Robin Brückner, refinement of the structural data has been carried out by Anja Wiesner, solid-state calculations have been carried out by Carsten Müller.

Tetramethylchloroamidiniumoctachloride $[\text{CCl}(\text{NMe}_2)_2]_2^+[\text{Cl}_8]^{2-}$ (**8**) is – to the best of our knowledge – the first compound exhibiting a polychloride dianion to be described so far. The compound was crystallized at $-22\text{ }^\circ\text{C}$ from a solution of tetramethylchloroamidiniumchloride ($[\text{CCl}(\text{NMe}_2)_2]\text{Cl}$) and chlorine in N-butyl-N-methylpyrrolidiniumtriflate ($[\text{BMP}]\text{OTf}$). After addition of chlorine this mixture solidifies below $-30\text{ }^\circ\text{C}$. This kind of polyhalide synthesis was first used by Feldmann et al. in 2011^[19] and also recently by our group.^[RB2] As the solubility of elemental chlorine in $[\text{BMP}]\text{OTf}$ is 3.6 wt.% (13.1 mol%) the chlorine is consumed by the reaction mixture via the formation of polychloride salts of $[\text{CCl}(\text{NMe}_2)_2]^+$. Storing the mixture at $-22\text{ }^\circ\text{C}$ leads to the formation of small coffin lid shaped crystals after several days. The salt crystallizes in the monoclinic space group $P 2_1/c$. As it is known from $[\text{Br}_8]^{2-}$ ^[17] and most of the $[\text{I}_8]^{2-}$ structures^[94] the $[\text{Cl}_8]^{2-}$ anions are composed of two distorted $[\text{Cl}_3]^-$ units which are bridged by a Cl_2 molecule. Bonding angles are $149.7(3)^\circ$ for $(\text{Cl}(2)-\text{Cl}(3)-\text{Cl}(4))$ and $177.4(4)^\circ$ for $(\text{Cl}(1)-\text{Cl}(2)-\text{Cl}(3))$. The shortest interanionic distance is 350.5 pm and so just the sum of the van-der-Waals radii (350 pm). Therefore we can speak of discrete $[\text{Cl}_8]^{2-}$ dianions, because the interactions between the different anions is very weak and can be more or less neglected. Fig.4.33 shows the crystal structure along the b-axis exhibiting that the anions are arranged parallel. Observed along the c-axis however (Fig.4.34) the anions are arranged crosswise and so cavities are formed in which the cations are situated in two different orientations.

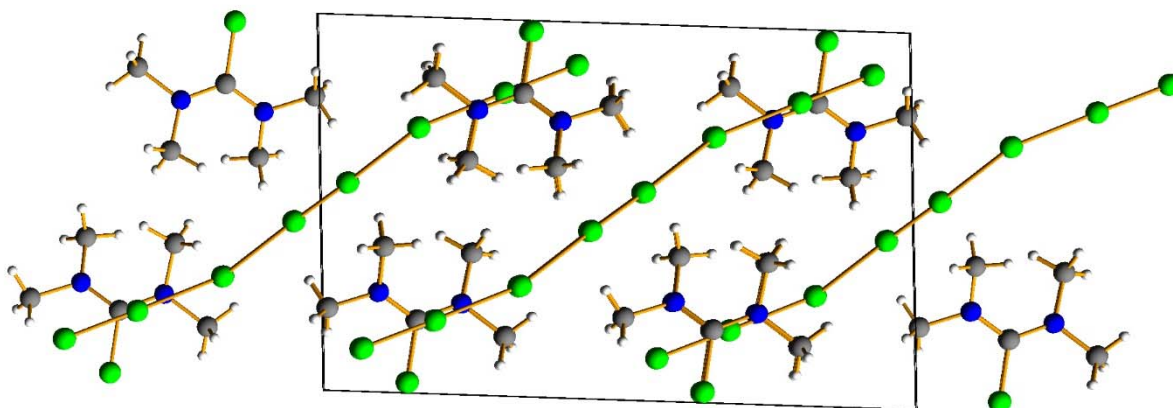


Figure 4.33 Crystal structure of (8) shown along *b*-axis.

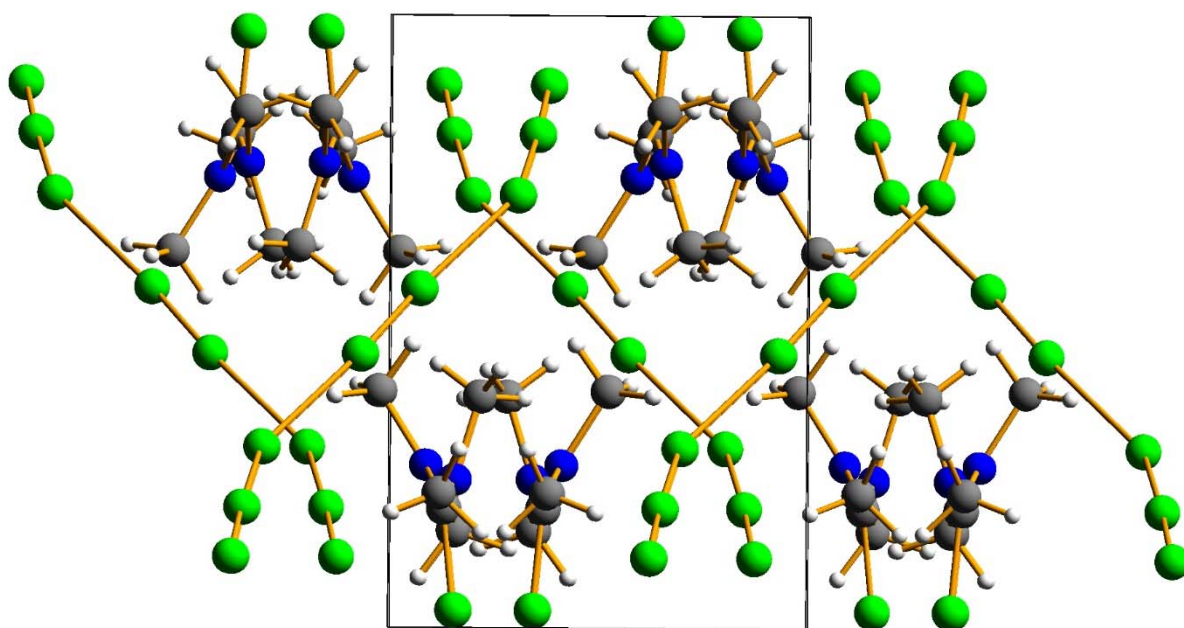


Figure 4.34 Crystal structure of (8) shown along *c*-axis.

When taking a closer look at the chlorine-chlorine distances Cl(1)–Cl(2) and Cl(4)–Cl(4') which are elongated by only 13 pm and 5 pm, respectively compared to the bond of free Cl₂ (199 pm),^[92] it is obvious that the structure has a considerable character of a [Cl₂–Cl–Cl₂–Cl–Cl₂] motive. On the other hand the bond lengths between the inner Cl₂ group and the distorted [Cl₃][–] units ($r_{34} = 293.9(3)$ pm) are considerably longer than the ones within the [Cl₃][–] units ($r_{23} = 253.7(3)$ pm). This bonding situation also resembles the one observed in [PPh₂Cl₂]⁺[Cl₃⋯Cl₂][–] published by Taraba and Zak in 2003.^[25] So the [Cl₃][–] units can be considered as an intermediate between a [Cl₃][–] and a Cl₂ coordinated to a Cl[–]. The values of the bonding angles in the crystal structure leads to the assumption that the bonding situation does not depend so much on σ -

hole interaction as it is assumed for $[\text{Br}_8]^{2-}$ and $[\text{I}_8]^{2-}$ because that is reflected by preferred bonding angles around 90° . This is probably due to the higher electron density around the Cl atoms, for more details see discussion *vide infra*. Interestingly the bond lengths and angles of the $[\text{Cl}_8]^{2-}$ anion are almost exactly matching to a motive found in the recently published polychloride network $[\text{Et}_4\text{N}]_2[(\text{Cl}_3)_2\cdot\text{Cl}_2]$,^[RB2] see Table 4.14.

Table 4.14. Selected bond lengths and angles in $[\text{Et}_4\text{N}]_2[(\text{Cl}_3)_2\cdot\text{Cl}_2]$ (7) and $[\text{CCl}(\text{NMe}_2)_2]_2[\text{Cl}_8]$ (8), including deviations from (7) and (8) as well as calculated values of the gas phase structure of $[\text{Cl}_8]^{2-}$ at RI-MP2/aug-cc-pVTZ level (9).

Bond/Angle ^[a]	(7)	(8)	Δ	(9)
r_{12}	211.0(3)	212.1(5)	1.1	224.5
r_{23}	255.8(3)	253.7(3)	2.1	231.4
r_{34}	292.0(3)	293.9(3)	1.9	299.1
$r_{44'}$	203.7(4)	204.9(4)	1.2	202.6
α_{123}	177.4(2)	177.4(4)	0.0	179.6
α_{234}	143.2(3)	149.7(3)	6.5	83.4

^[a]Bond lengths in pm and angles in $^\circ$.

Further analysis of the bonding situation was carried out by vibrational spectroscopy. Especially Raman spectroscopy is a very powerful technique as most polyhalide systems show a strong Raman-scattering effect. The Raman spectrum of a single crystal of $[\text{CCl}(\text{NMe}_2)_2]_2[\text{Cl}_8]$ shows three major bands (Fig. 4.35). The intense band at 446 cm^{-1} is assigned to the symmetric stretching vibration of the $\text{Cl}(4)\text{--Cl}(4')$ bond and was calculated to appear at 424 cm^{-1} while the broad band at 340 cm^{-1} is assigned to the stretching vibration of the $\text{Cl}(1)\text{--Cl}(2)$ bond (calc. 322 cm^{-1}). The small band at 271 cm^{-1} is assigned to the symmetric stretching vibration of the $\text{Cl}(2)\text{--Cl}(3)$ bond (calc. 237 cm^{-1}). Although these bands show a general shift of approximately 5 %, they are in good agreement with our solid-state calculations (B3-LYP-D2) and previous investigations of polychlorides, as coordinated Cl_2 molecules often show broad bands around 450 cm^{-1} .^[25] Additionally the band at 271 cm^{-1} is where we expect a $[\text{Cl}_3]^-$ anion.^[26] An analysis of the calculated vibrational modes supports this assignment.

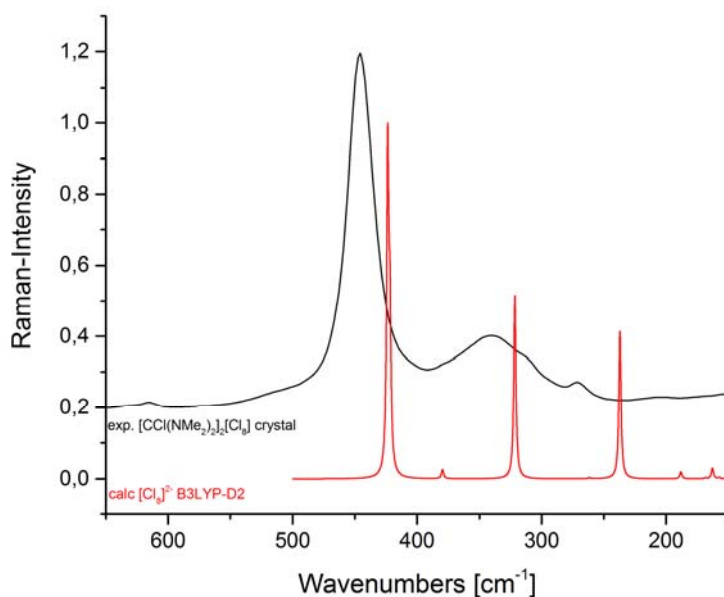


Figure 4.35 Raman spectrum of a single crystal of $[\text{CCl}(\text{NMe}_2)_2]_2[\text{Cl}_8]$ (black) and the solid state calculated spectrum of $[\text{Cl}_8]^{2-}$, respectively.

For comparison the gas-phase structures of $[\text{Cl}_8]^{2-}$ and $[\text{Br}_8]^{2-}$ were calculated at B3-LYP and RI-MP2 level using Dunning's aug-cc-pVTZ basis set^[95] and the Grimme D3 correction.^[83] Calculations for $[\text{Cl}_8]^{2-}$ at DFT level show spontaneous dissociation which can be expected because of the well-known Coulomb explosion for dianions in the gas phase.^[96] When the COSMO^[97] model ($\epsilon = 100$) is applied to mimic a stabilizing effect of a surrounding crystal a Z-shaped minimum structure results, see Figure 4.36.

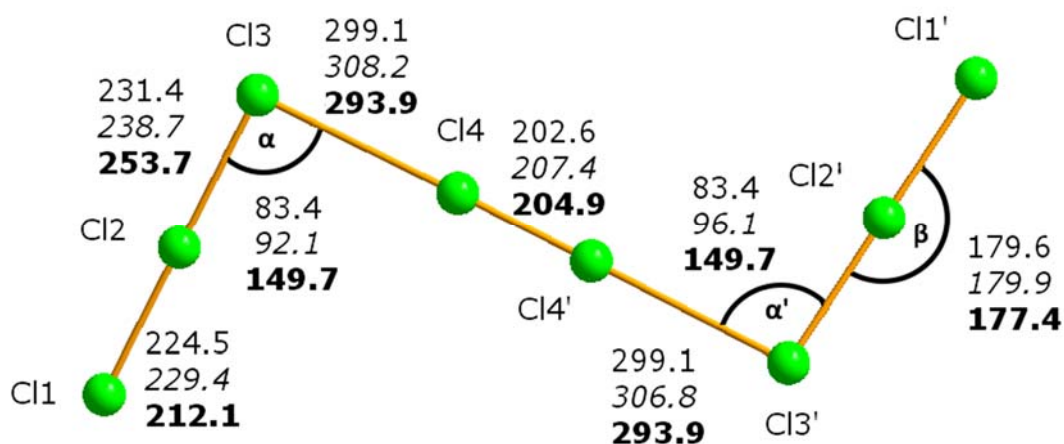


Figure 4.36 Calculated gas phase structure of $[\text{Cl}_8]^{2-}$ bond lengths [pm] and angles [°] are given (normal text style: RI-MP2, italic: B3-LYP). For comparison experimental data is given (bold text style).

The structure of the free $[\text{Cl}_8]^{2-}$ calculated at B3LYP/aug-cc-pVTZ and RI-MP2/aug-cc-pVTZ level shown in Figure 4.35 exhibits significant similarities to the experimentally found Z-shaped structures of $[\text{Br}_8]^{2-}$ and $[\text{I}_8]^{2-}$.^[13,17,50,94] Of course gas phase calculations do not include other interactions e.g. packing effects so bonding angles around 90° are preferred because of σ -hole interactions known from halogen bonding. This is well demonstrated by the electrostatic potentials maps around a $[\text{Cl}_8]^{2-}$ unit cut out from the experimental crystal structure and the isolated $[\text{Cl}_8]^{2-}$ optimized, see Figure 4.37.

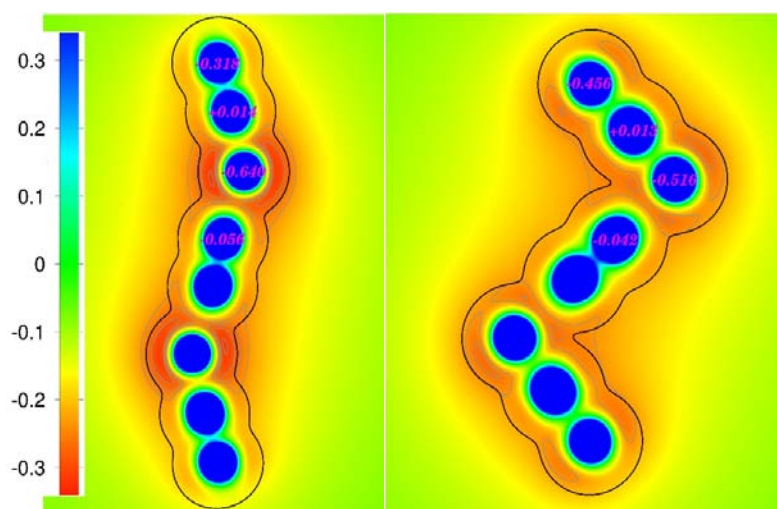


Figure 4.37 Plot of the electrostatic potential (in a.u.) calculated from a RHF wavefunction of an isolated $[\text{Cl}_8]^{2-}$ in the crystal structure (left) and the optimized vacuum structure (B3-LYP-D3) (right). The bold black line indicates the electron density contour line of 0.001 e/bohr^3 . Thin grey contours are drawn in the range of -0.34 to -0.24 a.u. with intervals of 0.02 a.u. The numbers in magenta are the atomic Mulliken charges calculated from the RHF wavefunction.

The atomic Mulliken charges (here calculated from the RHF wave function with a special basis set for condensed chloride systems) for the isolated molecules in Figure 4.37 show, that the $[\text{Cl}_8]^{2-}$ anion can indeed be interpreted as an intermediate between a $[\text{Cl}_3^- - \text{Cl}_2 - \text{Cl}_3^-]$ and a $[\text{Cl}_2 - \text{Cl}^- - \text{Cl}_2 - \text{Cl}^- - \text{Cl}_2]$; the latter character being more emphasized in the crystal structure as observed from the lateral charges of the Cl_3^- units. The electrostatic potentials show that the interactions between the $[\text{Cl}_3^-]$ units and the Cl_2 molecule in the crystal are not much controlled by σ -hole interactions, see above. As seen for the optimized free structure, σ -hole interactions force the molecule into a zig-zag shape with 90° angles, ensuring a good geometric match of the Cl_2 - σ -hole and the $[\text{Cl}_3^-]$ charge-belts and gaining about $16 \text{ kJ}\cdot\text{mol}^{-1}$ in energy compared to the crystal structure.

Two independent periodic calculations were performed mainly to verify the experimentally recorded spectra, *vide infra*: Periodic RHF and B3LYP calculations using the Crystal14 program^[98] and periodic PAW-PBE calculations using the VASP program.^[99] The Crystal14 program has the advantage that the calculations are very fast, allow for using the generally very reliable B3LYP functional and have IR and Raman intensities implemented. However, with atomic basis functions, it was not possible to perform calculations including the cation, due to linear dependencies in the basis set. Hence as for a previously studied periodic polychloride network, calculations of the $[\text{Cl}_8]^{2-}$ sub-lattice were performed with a uniform positive background charge replacing all cations. However, due to the absence of the cations, this calculation yields insights into the packing effects.

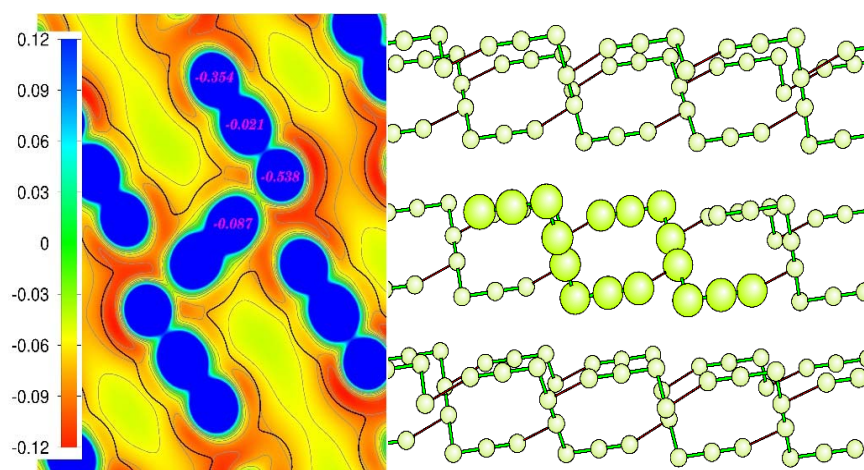


Figure 4.38 Optimized structure of the periodic $[\text{Cl}_8]^{2-}$ sub-lattice with a uniform charge background (left) and electrostatic potential (in a.u.) calculated from a RHF wavefunction. The bold black line indicates the electron density contour line of 0.001 e/bohr³. Thin grey contours are drawn in the range of -0.34 to -0.24 a.u. with intervals of 0.02 a.u. The numbers in magenta are the atomic Mulliken charges calculated from the RHF wavefunction.

Apparently, the purpose of the cations is first of all to prevent the $[\text{Cl}_8]^{2-}$ anions from adopting the thermodynamically more stable, σ -hole interaction driven zig-zag shape. Indeed the optimized crystal structure differs not much from that for the isolated $[\text{Cl}_8]^{2-}$ anion in vacuum. A second purpose of the cations appears to be to prevent the layers of $[\text{Cl}_8]^{2-}$ anions to merge due to inter-layer σ -hole interactions between two different $[\text{Cl}_8]^{2-}$ anions. The latter effect, which is nicely illustrated in yet another electrostatic potential map (Figure 4.38) of the optimized $[\text{Cl}_8]^{2-}$ sub-lattice stabilizes the lattice structure by about 38 kJ·mol⁻¹ compared to the experimental crystal structure. This

leads to the conclusion that the experimentally found chain-like geometry of the $[\text{Cl}_8]^{2-}$ anions in the crystal structure of (**8**) is due to packing effects and cannot be ascribed to the generally weak interactions between chlorine atoms.

Due to the use of plane-waves in the VASP program, the cations can be included in the calculations as well, however, the B3-LYP functional is unfeasible, and IR/Raman intensities are not implemented. An optimization of the experimental structure with fixed lattice parameters leads to only slight distortions of the atomic positions. Applying AIM analysis we observe that the anions don't seem to form any halogen-halogen bonds between one another. The electron density on bond critical point between $[\text{Cl}_8]^{2-}$ ions is one to two orders of magnitude smaller than the electron density on bond critical point within $[\text{Cl}_8]^{2-}$ ions. This is very surprising due to the great resemblance between the present structure and (**7**) in which halogen-halogen bonding is the driving force. In contrast to the experimental structure the calculations assume the terminal $[\text{Cl}_3]^-$ units to be much more regular. This is consistent with the overestimated bond lengths between the $[\text{Cl}_3]^-$ units and the central Cl_2 -unit. So the gas phase structure describes rather a $[(\text{X}_3)^-(\text{X}_2)(\text{X}_3)^-]$ adduct, which is also found in specific crystal structures of e.g. $[\text{Br}_8]^{2-}$ [13,50] instead of our present $[\text{Cl}_2-\text{Cl}^--\text{Cl}_2-\text{Cl}^--\text{Cl}_2]$ like structure.

Table 4.15 Comparison of bond dissociation energies (in $\text{kJ}\cdot\text{mol}^{-1}$) at different levels of theory.

	ΔE (B3-LYP) ^a	ΔE (RI-MP2) ^a	ΔE (CCSD(T))
$\text{Cl}_8^{2-} \rightarrow \text{Cl}_5^- + \text{Cl}_3^-$	2.0	-37.5	-
$\text{Cl}_8^{2-} \rightarrow \text{Cl}_2 + 2\text{Cl}_3^-$	15.8	-25.0	-
$\text{Cl}_8^{2-} \rightarrow 3\text{Cl}_2 + 2\text{Cl}^-$	84.6	-145.1	-
$\text{Cl}_5^- \rightarrow \text{Cl}_2 + \text{Cl}_3^-$	13.8	-60.1	40.6
$\text{Cl}_3^- \rightarrow \text{Cl}_2 + \text{Cl}^-$	34.4	12.6	102.9

^a Basis set: aug-cc-pVTZ, [9] for B3-LYP and RI-MP2 the continuous solvent model COSMO was applied ($\epsilon = 100$).

Table 4.15 shows for all degradation processes at DFT level no spontaneous dissociation while at RI-MP2 level however decomposition channels are computed to be exothermic, except the degradation of $[\text{Cl}_3]^-$. This inconsistency is probably due to the use of the COSMO^[97] solvent model, which is known for overestimating the solvation energies of small fragments.^[100] This can also be proved as earlier calculations without the COSMO model came to opposite results regarding the energy

values of MP2 calculations.^[RB1] Nevertheless these results confirm that polychloride anions are species depending on very weak interactions.

4.4.5 Summarized Crystallographic Data

Table 4.16 *Crystal data and structure refinement for N,N'-dimethyl-2-chloroimidazoliniumtrichloride.*

Name	N,N'-dimethyl-2-chloroimidazoliniumtrichloride
Identification code	n/a
Empirical formula	C ₅ H ₁₀ Cl ₄ N ₂
Formula weight	237.95
Temperature	100(2) K
Wavelength	0.71073 Å
Crystal system	Orthorhombic
Space group	P b c a
a [Å]	11.6135(9)
b [Å]	12.8276(10)
c [Å]	13.1227(8)
α [°]	90
β [°]	90
γ [°]	90
Volume	1954.9(2) Å ³
Z	8
Density (calculated)	1.362 Mg/m ³
Absorption coefficient	0.479 mm ⁻¹
F(000)	852
Crystal size/mm ³	0.250 x 0.490 x 0.180
Theta range for data collection	2.830 to 27.534°.
Index ranges	-15<=h<=15, -16<=k<=16, -15<=l<=17
Reflections collected	71343
Independent reflections	2253 [R(int) = 0.1087]
Completeness to theta = 26.000°	100.0 %
Absorption correction	Semi-empirical from equivalents
Max. and min. transmission	0.7456 and 0.6006
Refinement method	Full-matrix least-squares on F ²
Data / restraints / parameters	2253 / 0 / 140
Goodness-of-fit on F ²	1.100
Final R indices [I>2sigma(I)]	R1 = 0.0369, wR2 = 0.0789
R indices (all data)	R1 = 0.0582, wR2 = 0.0884
Largest diff. peak and hole	0.390 and -0.530 e.Å ⁻³

Table 4.17 *Crystal data and structure refinement for tetramethylchloroamidiniumtrichloride.*

Name	Tetramethylchloroamidiniumtrichloride
Identification code	n/a
Empirical formula	C ₅ H ₁₂ Cl ₄ N ₂
Formula weight	239.95
Temperature	100(2) K
Wavelength	0.71073 Å
Crystal system	Orthorhombic
Space group	P b c a
a [Å]	10.6432(5)
b [Å]	13.3086(8)
c [Å]	14.9014(8)
α [°]	90
β [°]	90
γ [°]	90
Volume	2110.7(2) Å ³
Z	8
Density (calculated)	1.523 Mg/m ³
Absorption coefficient	1.067 mm ⁻¹
F(000)	992
Crystal size/mm ³	0.280 x 0.130 x 0.070
Theta range for data collection	2.734 to 27.512°.
Index ranges	-13<=h<=13, -17<=k<=17, -19<=l<=19
Reflections collected	42094
Independent reflections	2424 [R(int) = 0.2673]
Completeness to theta = 26.000°	100.0 %
Absorption correction	Semi-empirical from equivalents
Max. and min. transmission	0.7456 and 0.6798
Refinement method	Full-matrix least-squares on F ²
Data / restraints / parameters	2424 / 0 / 148
Goodness-of-fit on F ²	0.923
Final R indices [I>2sigma(I)]	R1 = 0.0346, wR2 = 0.0691
R indices (all data)	R1 = 0.0583, wR2 = 0.0740
Largest diff. peak and hole	0.360 and -0.360 e.Å ⁻³

Table 4.18 *Crystal data and structure refinement for Bis-(tetraethylammonium) bis-(trichloride) – dichlorine .*

Name	<i>Bis-(tetraethylammonium) bis-(trichloride) – dichlorine</i>
Identification code	CCDC 1416833
Empirical formula	C ₈ Cl ₄ NH ₂₀
Formula weight	252.02
Temperature/K	100(2)
Crystal system	monoclinic
Space group	C2/m
a [Å]	14.4823(9)
b [Å]	12.7020(8)
c [Å]	15.0044(10)
α [°]	90.00
β [°]	102.343(3)
γ [°]	90.00
Volume/Å ³	2696.3(3)
Z	8
ρ _{calc} /cm ³	1.242
μ/mm ⁻¹	0.838
F(000)	985.0
Crystal size/mm ³	0.12 × 0.28 × 0.05
Radiation	MoKα (λ = 0.71073)
2Θ range for data collection/°	4.78 to 52.74
Index ranges	-18 ≤ h ≤ 18, -15 ≤ k ≤ 15, -18 ≤ l ≤ 18
Reflections collected	37047
Independent reflections	2877 [R _{int} = 0.0971, R _{sigma} = N/A]
Data/restraints/parameters	2877/0/134
Goodness-of-fit on F ²	0.993
Final R indexes [I ≥ 2σ (I)]	R ₁ = 0.0672, wR ₂ = 0.1537
Final R indexes [all data]	R ₁ = 0.0820, wR ₂ = 0.1616
Largest diff. peak/hole / e Å ⁻³	0.97/-0.99

Table 4.19 *Crystal data and structure refinement for tetramethylchloroamidiniumoctachloride.*

Name	Tetramethylchloroamidiniumoctachloride
Identification code	CCDC 1456573
Empirical formula	C ₅ H ₁₂ N ₂ Cl ₅
Formula weight	277.42
Temperature/K	100.0
Crystal system	monoclinic
Space group	P2 ₁ /c
a [Å]	10.2477(9)
b [Å]	6.9908(6)
c [Å]	16.1400(11)
α [°]	90
β [°]	92.845(3)
γ [°]	90
Volume/Å ³	1154.84(16)
Z	4
ρ _{calc} /cm ³	1.596
μ/mm ⁻¹	1.210
F(000)	564.0
Crystal size/mm ³	0.21 × 0.52 × 0.22
Radiation	MoKα (λ = 0.71073)
2θ range for data collection/°	5.054 to 55.114
Index ranges	-13 ≤ h ≤ 13, -9 ≤ k ≤ 9, -20 ≤ l ≤ 20
Reflections collected	39262
Independent reflections	2649 [R _{int} = 0.0728, R _{sigma} = 0.0249]
Data/restraints/parameters	2649/0/157
Goodness-of-fit on F ²	1.005
Final R indexes [I ≥ 2σ (I)]	R ₁ = 0.0242, wR ₂ = 0.0550
Final R indexes [all data]	R ₁ = 0.0346, wR ₂ = 0.0577
Largest diff. peak/hole / e Å ⁻³	0.29/-0.26

4.5 Conductivity Measurements

Based on the very promising results considering the conductivity of liquid polybromides, especially nonabromides (see Section 2.4.2), conductivity measurements were made on some of the liquid products obtained from the polychloride synthesis. The first substance tested was the product from [BMP]Cl and one equivalent of Cl_2 was obtained as a bright yellow liquid with low viscosity and identified to be pure [BMP][Cl_3] by Raman spectroscopy. Another substance was [BMP][Cl_3] in which 0.5 equiv. of Cl_2 were dissolved. Additionally [Et₃MeN][Cl_3] was prepared from [Et₃MeN]Cl and one equiv. of Cl_2 and tested as well. For comparison [BMP][Br₃] was prepared from [BMP]Br and Br₂ and measured as well, see Fig. 4.38.

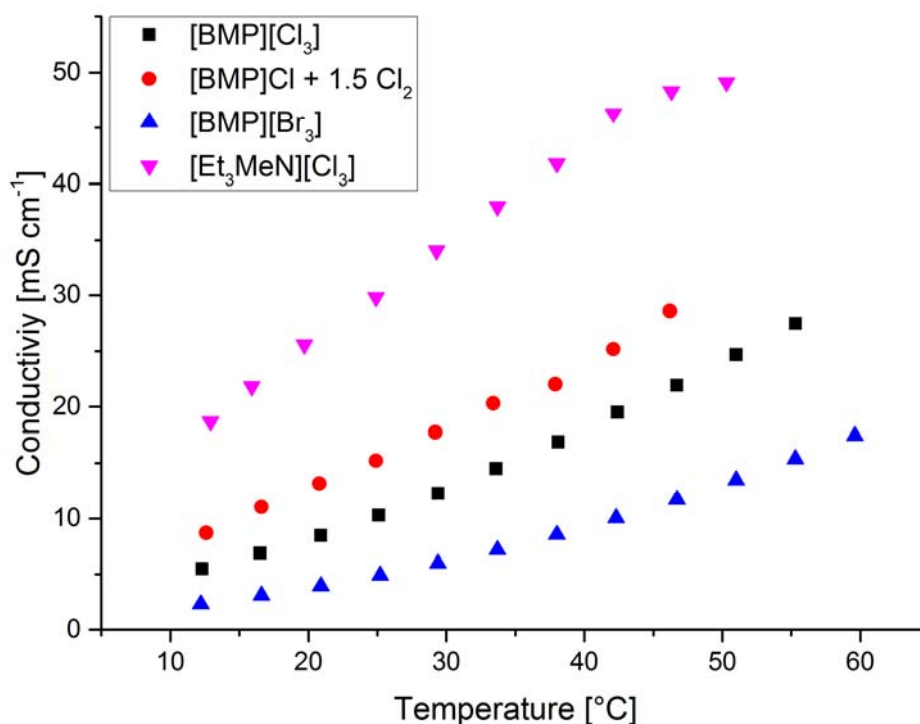


Figure 4.39 Conductivity of the tested polyhalides plotted against temperature.

As apparent in Fig. 4.39 the conductivity of the measured trichlorides is significantly higher than that of the corresponding tribromide. At 21 °C [BMP][Cl_3] exhibits a conductivity of 8.5 $\text{mS}\cdot\text{cm}^{-1}$ which can be increased up to 13.2 $\text{mS}\cdot\text{cm}^{-1}$ by dissolving additional Cl_2 in the trichloride. The corresponding tribromide [BMP][Br₃] on the other hand, shows a conductivity of only 4.0 $\text{mS}\cdot\text{cm}^{-1}$. [Et₃MeN][Cl_3] even showed a conductivity

of $25.6 \text{ mS}\cdot\text{cm}^{-1}$ at 20°C . This is already in same dimension as those of nonabromides, such as $[\text{Pr}_4\text{N}][\text{Br}_9]$ or $[\text{N}_{1225}][\text{Br}_9]$ that show conductivities of $22.8 \text{ mS}\cdot\text{cm}^{-1}$ and $27.9 \text{ mS}\cdot\text{cm}^{-1}$ at 25°C , respectively.^[12] Polychlorides might indeed be even more applicable than the polybromides, because of their lower molecular weight saves a lot of mass which could be a significant advantage, especially for use in redox-flow batteries, for example. Challenges arise from the lower temperature stability of polychlorides. Polychlorides higher than the trichloride start losing chlorine at around 40°C which could be very risky if closed systems are considered. Fortunately this does not apply on trichlorides tested which were temperature stable up to at least 60°C .

5 Summary and Conclusion

In this thesis a number of novel polychloride salts were synthesized including the first 2-dimensional polychloride network as well as the first polychloride dianion to be reported in literature. Additionally a variety of ionic liquids were tested towards their stability against elemental chlorine. In order to properly analyze the synthesized compounds a convenient way to match the specific requirements for the crystallization of polychlorides was found.

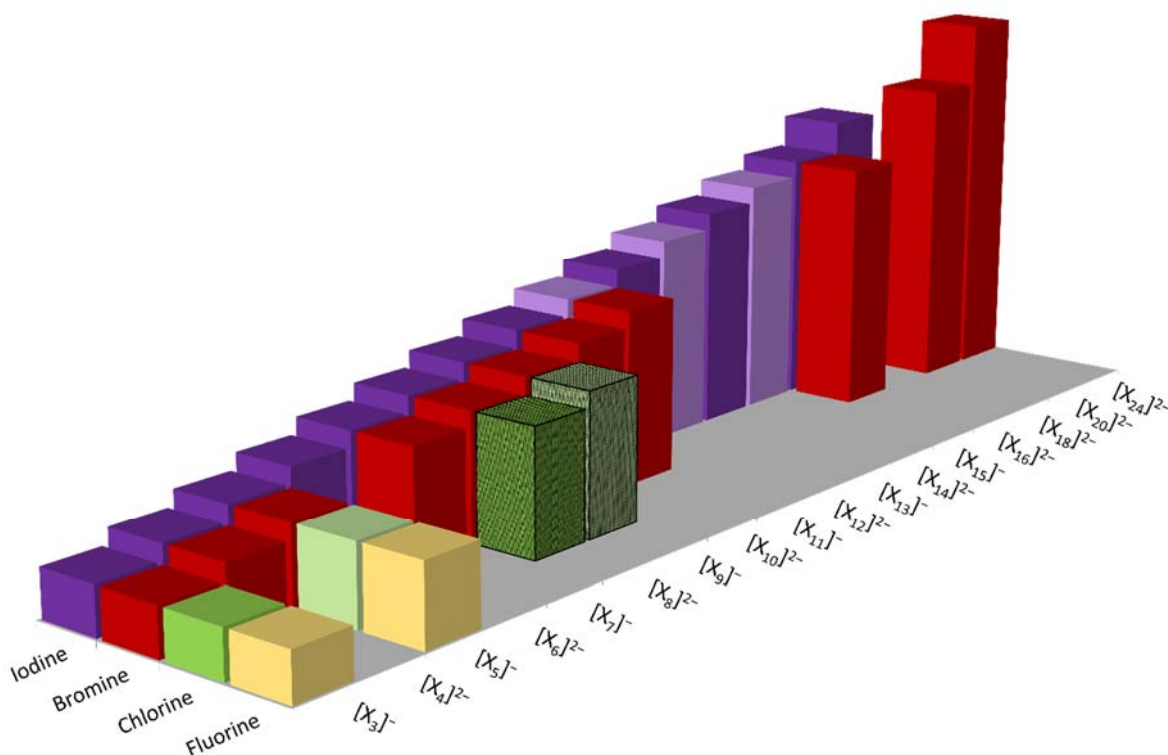


Figure 5.1. Diagram of known polyhalide mono- and dianions, pale colored items represent those only known by spectroscopic evidence, polychloride anions first evidence was found for in this work are marked (updated version of Figure 1 in ^[31]).

The synthesized compounds were characterized by vibrational spectroscopy and single crystal X-ray structure determination. Results were supported and confirmed by quantum-chemical calculations concerning structure, vibrational frequencies as well as thermochemical properties.

By means of reaction with neat chlorine without the use of any solvent the polychloride salts $[\text{NMe}_4][\text{Cl}_5]$, $[\text{NEt}_4][\text{Cl}_3 \cdots \text{Cl}_2]$, $[\text{NPr}_4][\text{Cl}_3]$ and $[\text{NBu}_4][\text{Cl}_3]$ were synthesized at room temperature as well as $[\text{NEt}_4][\text{Cl}_9]$ at 77 K and characterized by Raman spectroscopy.

Results were accompanied by quantum-chemical calculations predicting vibrational frequencies at RI-MP2/def2-TZVPP level. Thermochemical properties of the polychloride anions $[\text{Cl}_9]^-$ and $[\text{Cl}_7]^-$ were computed at MP2 and SCS-MP2 level, for the anions $[\text{Cl}_5]^-$ and $[\text{Cl}_3]^-$ properties were additionally calculated at CCSD(T) level. Furthermore minimum structures for the monoanions $[\text{Cl}_3]^-$, $[\text{Cl}_5]^-$, $[\text{Cl}_7]^-$ and $[\text{Cl}_9]^-$ were determined at MP2/def2-TZVPP and SCS-MP2/def2-TZVPP level. For $[\text{Cl}_{11}]^-$ and $[\text{Cl}_{13}]^-$ as well as for the dianion $[\text{Cl}_8]^{2-}$ minimum structures were calculated at B3LYP - D3/aug-cc-pVTZ level.

The polychloride compounds N,N'-dimethyl-2-chloroimidazoliniumtrichloride ($[\text{C}_5\text{H}_{10}\text{N}_2\text{Cl}][\text{Cl}_3]$), tetramethylchloroamidiniumtrichloride ($[\text{CCl}(\text{NMe}_2)_2][\text{Cl}_3]$), Bis-(tetraethylammonium) bis-(trichloride) – dichlorine ($[\text{Et}_4\text{N}]_2[(\text{Cl}_3)_2\cdot\text{Cl}_2]$) and tetramethylchloroamidiniumoctachloride ($[\text{CCl}(\text{NMe}_2)_2]_2[\text{Cl}_8]$) were successfully crystallized and characterized by single crystal X-ray structure determination as well as vibrational spectroscopy. $[\text{C}_5\text{H}_{10}\text{N}_2\text{Cl}][\text{Cl}_3]$ being the most regular trichloride compound yet to be reported with deviations of the bond lengths by only 3.9 pm. $[\text{Et}_4\text{N}]_2[(\text{Cl}_3)_2\cdot\text{Cl}_2]$ was crystallized from a eutectic mixture of ionic liquids allowing higher polychlorides to be formed in solution. $[\text{Et}_4\text{N}]_2[(\text{Cl}_3)_2\cdot\text{Cl}_2]$ crystallized in a layered structure exhibiting pure polychloride layers forming an infinite 2-dimensional network made up of isolated $[\text{Cl}_3]^-$ anions and chains of highly asymmetric $[\text{Cl}_3]^-$ anions interconnected via Cl_2 units. This structure emphasizes the assumption that halogen bonding is strong enough to act as a driving force even in species solely consisting of chlorine atoms. $[\text{CCl}(\text{NMe}_2)_2]_2[\text{Cl}_8]$ is the first polychloride dianion to be synthesized and characterized so far. $[\text{CCl}(\text{NMe}_2)_2]_2[\text{Cl}_8]$ was crystallized from the ionic liquid $[\text{BMP}]\text{OTf}$ exhibiting a structure made up of discrete $[\text{Cl}_8]^{2-}$ dianions showing no tendency to form networks which is even more surprising as the structure highly resembles that of the former mentioned network $[\text{Et}_4\text{N}]_2[(\text{Cl}_3)_2\cdot\text{Cl}_2]$. The unusual structure of the anion that significantly differs from the bromide and iodide analogs arises from packing effects preventing the anion from taking up the preferred Z-shaped structure observed for $[\text{Br}_8]^{2-}$ and $[\text{I}_8]^{2-}$. Ionic liquids containing the N-butyl-N-methylpyrrolidinium cation were found to be excellent solvents for synthesizing and crystallizing higher polychloride compound as they possess the ability to solve high amounts of chlorine gas and form eutectic mixtures with one another as well as with Cl_2 leading to melting points below $-30\text{ }^\circ\text{C}$.

In addition conductivity measurements were performed for the liquid polychloride compounds $[\text{BMP}][\text{Cl}_3]$, $[\text{Et}_3\text{MeN}][\text{Cl}_3]$ and $\{[\text{BMP}][\text{Cl}_3] \cdot \frac{1}{2}\text{Cl}_2\}$ and compared to polybromide analogs. Results were promising and show that additionally to their use as chlorinating agents, polychlorides exhibit potential applications comparable to those of the polybromide compound, e. g. electrolyte materials in redox-flow batteries.

6 Experimental Section

6.1 Preparation of [Et₃MeN]Cl and [Et₃PrN]Cl

Triethylamine (15.0 g, 148.3 mmol) was dissolved in acetonitrile (100 ml), *n*-alkyl iodide (30.0 g, 211.4 mmol) was added in about 60 min and the reaction mixture was heated to reflux overnight. During heating the corresponding ammonium iodide formed as a white precipitate. The precipitate was filtered and washed three times with diethyl ether (Et₂O). The resulting ammonium iodide was dissolved in degassed water and freshly prepared silver hydroxide (AgOH) was added. Upon contact light yellow silver iodide (AgI) was formed. AgOH was added until no formation of AgI could be observed. AgI was removed and the solution was neutralized with aqueous HCl. The water was then removed and the product was dried in high vacuum.^[101]

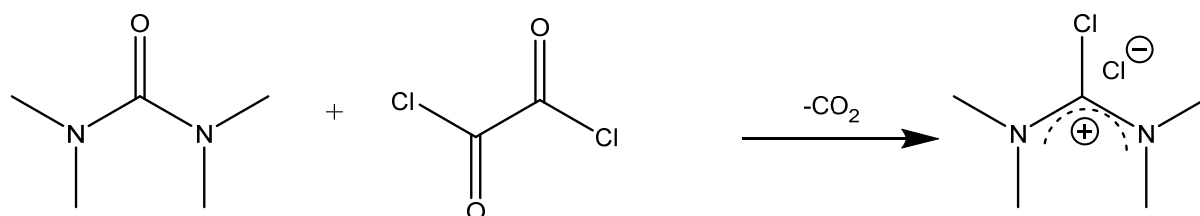
6.2 Methods of Crystallization

Crystallization was carried out using various techniques.

If organic solvents were applied crystallization was tried to achieve by cooling (down to -80 °C), by slow evaporation of the solvent, by concentration of the solution in vacuum, by addition of nonpolar solvents such as *n*-pentane and by combination of two or more of these techniques. Same experiments were applied on samples dissolved in liquefied chlorine, except the addition of a different solvent for obvious reasons. Samples dissolved in one or more ionic liquids were simply cooled at different temperatures until crystallization occurred.

6.3 Preparation of Tetramethylchloroamidiniumtrichloride

Tetramethylchloroamidiniumchloride synthesis was carried out as reported in literature.^[102]



Scheme 6.1 Reaction of tetramethylurea and oxalyl chloride to tetramethylchloroamidiniumchloride.^[102]

[BMP]Cl (780 mg; 4.4 mmol) and [BMP]OTf (1320 mg; 4.4 mmol) were mixed in a Schlenk tube flushed with argon and stirred for about 2 h until a milky white viscous liquid formed. Thereafter insoluble tetramethyl-chloro-amidinium chloride was added (373 mg; 2.2 mmol), then Cl₂ gas was passed through the tube. Upon contact with the Cl₂ gas, the color of the mixture turned from colorless to bright yellow and the turbid liquid cleared. After passing the Cl_{2(g)} through the tube for about 5 min the amidiniumchloride was fully dissolved in the yellow liquid, forming a clear bright yellow solution. To complete the reaction Cl_{2(g)} was passed through the reaction mixture for another approx. 5 min. Then the vessel was closed and stirred at room temperature overnight. On the next day the tube was stored at -22 °C. After 24 h small colorless crystals formed.

As the trichlorides of almost all used corresponding chloride salts can be obtained quantitatively by just passing chlorine gas over the chloride a yield obtained from crystallization was not determined.

6.4 Preparation of N,N-dimethyl-2-chloroimidazoliniumtrichloride

Preparation of N,N-dimethyl-2-chloroimidazoliniumchloride:

Under inert conditions 1,3-dimethyl-2-imidazolidone (5.45 g; 47.0 mmol) was dissolved in absolute (abs.) THF (20 ml). Oxalyl chloride (4.73 ml, 55.1 mmol) was added at room temperature during 5 min. The mixture was then refluxed for 20 h whereas a white precipitate was formed. The precipitate was filtered, washed with diethyl ether and dried under reduced pressure. The product was obtained as a colorless solid (2.91 g; 36 %).

Preparation of N,N-dimethyl-2-chloroimidazoliniumtrichloride:

Cl₂ (approx. 5 ml) was condensed on N,N-dimethyl-2-chloroimidazoliniumchloride (175 mg) in a schlenk tube equipped with a teflon valve at –80 °C. The vessel was closed and left to warm to ambient temperature. Then, the valve was slowly opened to remove pressurized Cl₂. After all of the Cl₂ evaporated a light yellow solid remained. The solid was dissolved in a small quantity of warm CH₂Cl₂ and was then stored at –22 °C until small light yellow crystals were formed.

6.5 Obtaining Vibrational and Crystal Data

The Raman spectra were recorded on a Bruker Vertex 70 spectrometer equipped with a RAM II module using a liquid nitrogen cooled Ge detector (1064 nm, 50 mW, resolution 4 cm⁻¹) and on a Bruker MultiRAM II equipped with a similar Ge-detector. Single-crystal Raman spectra have been recorded at –30 °C (1064 nm, 350 mW, resolution 4 cm⁻¹) using a Bruker RamanScope III equipped with a Linkam stage cooling unit. Conventional Raman spectra were recorded (backscattering mode) at r.t. as well as with cooling to liquid nitrogen temperature in flame sealed glass capillaries and as well as schlenk tubes. NMR-spectra were taken on a JEOL type JNMECA400II spectrometer at 400 MHz.

Data for the crystal structures were collected on a Bruker D8 Venture CMOS area detector diffractometer with Mo-K_α radiation. A single crystal was coated with perfluoroether oil at –30 °C and mounted on a 0.1 mm Micromount. The structure was

solved by direct methods in SHELXTL^[103] and refined by least squares on weighted F² values for all reflections using OLEX2.^[104] The hydrogen atoms were included in the refinement in calculated positions by a riding model. The graphical representations were prepared with Diamond 3.1.^[105]

6.6 Quantum Chemical Calculations

If not labelled differently all gas-phase calculations were performed at RI-MP2 level and at DFT level using the B3-LYP hybrid functional and the Dunning correlated consistent basis set [triple- ζ (aug-cc-pVTZ)] for all calculations and atoms.^[81,82] The calculations were carried out using the Turbomole V7.0.1 program and the herein implemented analytical and numerical gradient methods, the D3 dispersion correction by Grimme and the COSMO dielectric solvation model.^[83,97,106,107] Thermochemistry was provided without any further BSSE or zero-point corrections.

7 References

- [1] J. Pelletier, J. B. Caventou, *Ann. Chim. Phys.* **1819**, 142–177.
- [2] S. M. Jørgensen, *J. Prakt. Chem.* **1870**, 2, 433–458.
- [3] A. I. Popov, *MTP Int. Rev. Sci.: Inorg. Chem., Ser. One* **1972**, 53–84.
- [4] A. I. Popov, *Halogen Chem.* **1967**, 1, 225–264.
- [5] A. I. Popov, R. E. Buckles, *Inorg. Synth.* **1957**, 5, 167–175.
- [6] K.-F. Tebbe, *Homoat. Rings, Chains Macromol., Main-Group Elem.* **1977**, 551–606.
- [7] P. H. Svensson, L. Kloo, *Chem. Rev.* **2003**, 103, 1649–1684.
- [8] L. Kloo, in *Comprehensive Inorganic Chemistry II, Vol. 1. Catenated Compounds - Group 17 - Polyhalides*. (Eds.: J. Reedijk, K. Poeppelmeier), Elsevier, **2013**.
- [9] F. D. Chattaway, G. Hoyle, *J. Chem. Soc., Trans.* **1923**, 123, 654–662.
- [10] J. C. Evans, G. Y.-S. Lo, *Inorg. Chem.* **1967**, 6, 1483–1486.
- [11] H. Haller, M. Ellwanger, A. Higelin, S. Riedel, *Angew. Chem. Int. Ed.* **2011**, 50, 11528–11532.
- [12] H. Haller, M. Ellwanger, A. Higelin, S. Riedel, *Z. anorg. allg. Chem.* **2012**, 638, 553–558.
- [13] M. Wolff, A. Okrut, C. Feldmann, *Inorg. Chem.* **2011**, 50, 11683–11694.
- [14] V. Vitske, H. Herrmann, M. Enders, E. Kaifer, H.-J. Himmel, *Chem. Eur. J.* **2012**, 18, 14108–14116.
- [15] H. Haller, J. Schröder, S. Riedel, *Angew. Chem. Int. Ed.* **2013**, 52, 4937–4940.
- [16] K. O. Strømme, *Acta Chem. Scand.* **1959**, 13, 2089–2100.
- [17] K. N. Robertson, P. K. Bakshi, T. S. Cameron, O. Knop, *Z. anorg. allg. Chem.* **1997**, 623, 104–114.
- [18] C. W. Cunningham, G. R. Burns, V. McKee, *Inorg. Chim. Acta* **1990**, 167, 135–137.

- [19] M. Wolff, J. Meyer, C. Feldmann, *Angew. Chem. Int. Ed.* **2011**, *50*, 4970–4973.
- [20] M. E. Easton, A. J. Ward, T. Hudson, P. Turner, A. F. Masters, T. Maschmeyer, *Chem. Eur. J.* **2015**, *21*, 2961–2965.
- [21] M. P. Bogaard, J. Peterson, A. D. Rae **1981**, *37*, 1357–1359.
- [22] R. T. Boéré, A. W. Cordes, R. T. Oakley, R. W. Reed, *J. Chem. Soc., Chem. Commun.* **1985**, 655–656.
- [23] T. Chivers, J. F. Richardson, N. R. M. Smith, *Inorg. Chem.* **1985**, *24*, 2453–2458.
- [24] M. Jansen, S. Strojek, *Z. Naturforsch., B: Chem. Sci.* **1995**, *50*, 1171–1174.
- [25] J. Taraba, Z. Zak, *Inorg. Chem.* **2003**, *42*, 3591–3594.
- [26] J. C. Evans, G. Y.-S. Lo, *J. Chem. Phys.* **1966**, *44*, 3638–3639.
- [27] B. S. Ault, L. Andrews, *J. Am. Chem. Soc.* **1976**, *98*, 1591–1593.
- [28] S. Riedel, T. Köchner, X. Wang, L. Andrews, *Inorg. Chem.* **2010**, *49*, 7156–7164.
- [29] F. A. Redeker, H. Beckers, S. Riedel, *RSC Adv* **2015**, *5*, 106568–106573.
- [30] T. Vent-Schmidt, F. Brosi, J. Metzger, T. Schlöder, X. Wang, L. Andrews, C. Müller, H. Beckers, S. Riedel, *Angew. Chem. Int. Ed.* **2015**, *54*, 8279–8283.
- [31] H. Haller, S. Riedel, *Z. anorg. allg. Chem.* **2014**, *640*, 1281–1291.
- [32] P. Metrangolo, G. Resnati, *Halogen bonding*, Springer, **2008**.
- [33] T. Clark, M. Hennemann, J. S. Murray, P. Politzer, *J. Mol. Model* **2007**, *13*, 291–296.
- [34] M. H. Kolář, P. Hobza, *Chem. Rev.* **2016**, *116*, 5155–5187.
- [35] G. Cavallo, P. Metrangolo, R. Milani, T. Pilati, A. Priimägi, G. Resnati, G. Terraneo, *Chem. Rev.* **2016**, *116*, 2478–2601.
- [36] L. C. Gilday, S. W. Robinson, T. A. Barendt, M. J. Langton, B. R. Mullaney, P. D. Beer, *Chemical reviews* **2015**, *115*, 7118–7195.
- [37] G. A. Landrum, N. Goldberg, R. Hoffmann, *J. Chem. Soc., Dalton Trans.* **1997**, 3605–3613.
- [38] M. C. Aragoni, M. Arca, F. A. Devillanova, A. Garau, F. Isaia, V. Lippolis, A. Mancini, *Bioinorg. Chem. Appl.* **2007**, 17416.

- [39] X. Chen, M. A. Rickard, J. W. Hull, C. Zheng, A. Leugers, P. Simoncic, *Inorg. Chem.* **2010**, *49*, 8684–8689.
- [40] A. W. Coleman, C. M. Means, S. G. Bott, J. L. Atwood, *J. Crystallogr. Spectrosc. Res.* **1990**, *20*, 199–201.
- [41] M. A. Zolfigol, G. Chehardoli, S. Salehzadeh, H. Adams, M. D. Ward, *Tetrahedron Lett.* **2007**, *48*, 7969–7973.
- [42] H. Slebocka-Tilk, R. G. Ball, R. S. Brown, *J. Am. Chem. Soc.* **1985**, *107*, 4504–4508.
- [43] F. H. Herbstein, M. Kapon, G. M. Reisner, *Proc. R. Soc. A* **1981**, *376*, 301–318.
- [44] F. Pichierri, *Chem. Phys. Lett.* **2011**, *515*, 116–121.
- [45] A. Bondi, *J. Phys. Chem.* **1964**, *68*, 441–451.
- [46] F. B. Alhanash, N. A. Barnes, S. M. Godfrey, R. Z. Khan, R. G. Pritchard, *Polyhedron* **2013**, *65*, 102–109.
- [47] H. Haller, M. Hog, F. Scholz, H. Scherer, I. Krossing, S. Riedel, *Z. Naturforsch., B: Chem. Sci.* **2013**, *68*, 1103–1107.
- [48] M. Groessel, Z. Fei, P. J. Dyson, S. A. Katsyuba, K. L. Vikse, J. S. McIndoe, *Inorg. Chem.* **2011**, *50*, 9728–9733.
- [49] A. W. Addison, T. N. Rao, J. Reedijk, J. van Rijn, G. C. Verschoor, *J. Chem. Soc., Dalton Trans.* **1984**, 1349–1356.
- [50] R. Babu, G. Bhargavi, M. V. Rajasekharan, *Eur. J. Inorg. Chem.* **2015**, *2015*, 4689–4698.
- [51] M. Fournier, F. Fournier, J. Berthelot, *Bull. Soc. Chim. Belg.* **1984**, *93*, 157–158.
- [52] S. Kajigaeshi, M. Moriwaki, T. Tanaka, S. Fujisaki, T. Kakinami, T. Okamoto, *J. Chem. Soc., Perkin Trans. 1* **1990**, 897.
- [53] R. Bianchini, C. Chiappe, *J. Org. Chem.* **1992**, *57*, 6474–6478.
- [54] G. Bellucci, R. Bianchini, C. Chiappe, R. Ambrosetti, *J. Am. Chem. Soc.* **1989**, *111*, 199–202.
- [55] T. M. Beck, H. Haller, J. Streuff, S. Riedel, *Synthesis* **2014**, *46*, 740–747.
- [56] I. Saikia, A. J. Borah, P. Phukan, *Chemical reviews* **2016**, *116*, 6837–7042.

- [57] I. Rubinstein, M. Bixon, E. Gileadi, *J. Phys. Chem.* **1980**, *84*, 715–721.
- [58] K. Kakiage, T. Tokutome, S. Iwamoto, T. Kyomen, M. Hanaya, *Chem. Commun.* **2013**, *49*, 179–180.
- [59] V. M. Zelikman, V. S. Tyurin, V. V. Smirnov, N. V. Zyk, *Russ Chem Bull* **1998**, *47*, 1541–1546.
- [60] T. Schlama, K. Gabriel, V. Gouverneur, C. Mioskowski, *Angew. Chem. Int. Ed.* **1997**, *36*, 2342–2344.
- [61] H. Bode, E. Klesper, *Z. Anorg. Allg. Chem.* **1952**, *267*, 97–112.
- [62] L. B. Asprey, J. L. Margrave, M. E. Silverthorn, *J. Am. Chem. Soc.* **1961**, *83*, 2955–2956.
- [63] A. A. Tuinman, A. A. Gakh, R. J. Hinde, R. N. Compton, *J. Am. Chem. Soc.* **1999**, *121*, 8397–8398.
- [64] K. E. Nizzi, C. A. Pommerening, L. S. Sunderlin, *J. Phys. Chem. A* **1998**, *102*, 7674–7679.
- [65] K. Do, T. P. Klein, C. A. Pommerening, L. S. Sunderlin, *J. Am. Soc. Mass. Spectrom.* **1997**, *8*, 688–696.
- [66] K. O. Christe, *J. Fluorine Chem.* **1995**, *71*, 149–150.
- [67] F. Brosi, T. Vent-Schmidt, S. Kieninger, T. Schlöder, H. Beckers, S. Riedel, *Chem. Eur. J.* **2015**, *21*, 16455–16462.
- [68] R. J. Elema, J. L. de Boer, A. Vos, *Acta Cryst.* **1963**, *16*, 243–247.
- [69] C. Chiappe, F. Del Moro, M. Raugi, *Eur. J. Org. Chem.* **2001**, 3501–3510.
- [70] Y.-Q. Wang, Z.-M. Wang, C.-S. Liao, C.-H. Yan, *Acta Crystallogr C Cryst Struct Commun* **1999**, *55*, 1503–1506.
- [71] C. Walbaum, M. Richter, U. Sachs, I. Pantenburg, S. Riedel, A.-V. Mudring, G. Meyer, *Angew. Chem. Int. Ed.* **2013**, *52*, 12732–12735.
- [72] Y. Yagi, A. I. Popov, *J. Inorg. Nucl. Chem.* **1967**, *29*, 2223–2230.
- [73] A. Parlow, H. Hartl, *Acta Crystallogr B Struct Crystallogr Cryst Chem* **1979**, *35*, 1930–1933.
- [74] A. Parlow, H. Hartl, *Z. Naturforsch., B: Chem. Sci.* **1985**, *40*, 45–52.

- [75] R. Minkwitz, M. Berkei, R. Ludwig, *Inorg. Chem.* **2001**, *40*, 25–28.
- [76] I.-E. Parigoridi, G. J. Corban, S. K. Hadjikakou, N. Hadjiliadis, N. Kourkouvelis, G. Kostakis, V. Psycharis, C. P. Raptopoulou, M. Kubicki, *Dalton Trans.* **2008**, 5159–5165.
- [77] D. Freudenmann, S. Wolf, M. Wolff, C. Feldmann, *Angew. Chem. Int. Ed.* **2011**, *50*, 11050–11060.
- [78] C. Feldmann, M. Wolff, *Z. anorg. allg. Chem.* **2010**, *636*, 2055.
- [79] I. V. Nelson, R. T. Iwamoto, *J. Electroanal. Chem.* **1964**, *7*, 218–221.
- [80] W. J. James, R. J. Hach, D. French, R. E. Rundle, *Acta Cryst* **1955**, *8*, 814–818.
- [81] C. Lee, W. Yang, R. G. Parr, *Phys. Rev. B* **1988**, *37*, 785–789.
- [82] A. D. Becke, *J. Chem. Phys.* **1993**, *98*, 5648–5652.
- [83] S. Grimme, S. Ehrlich, L. Goerigk, *J. Comput. Chem.* **2011**, *32*, 1456–1465.
- [84] D. R. Lide, *CRC handbook of chemistry and physics. A ready reference book of chemical and physical data*, 85. Aufl., CRC, **2004**.
- [85] F. Y. Fujiwara, J. S. Martin, *J. Chem. Phys.* **1972**, *56*, 4091.
- [86] A. D. Beveridge, G. S. Harris, F. Inglis, *J. Chem. Soc., A* **1966**, 520–528.
- [87] G. A. Wiley, W. R. Stine, *Tetrahedron Lett.* **1967**, *8*, 2321–2324.
- [88] G. S. Harris, M. F. Ali, *Tetrahedron Lett.* **1968**, *9*, 37–38.
- [89] S. M. Godfrey, C. A. McAuliffe, R. G. Pritchard, J. M. Sheffield, G. M. Thompson, *J. Chem. Soc., Dalton Trans.* **1997**, 4823–4828.
- [90] Y. Zhang, J. R. G. Evans, S. Yang, *J. Chem. Eng. Data* **2011**, *56*, 328–337.
- [91] M. E. Tuttolomondo, A. Navarro, E. L. Varetti, A. Ben Altabef, *J. Raman Spectrosc.* **2005**, *36*, 427–434.
- [92] B. M. Powell, K. M. Heal, B. H. Torrie, *Mol. Phys.* **2006**, *53*, 929–939.
- [93] R. F. W. Bader, M. T. Carroll, J. R. Cheeseman, C. Chang, *J. Am. Chem. Soc.* **1987**, *109*, 7968–7979.
- [94] K.-F. Tebbe, B. Freckmann, *Z. Naturforsch., B: Chem. Sci.* **1982**, *37*, 542–549.
- [95] D. E. Woon, T. H. Dunning, *J. Chem. Phys.* **1993**, *98*, 1358–1371.

- [96] D. Schröder, *Angew. Chem. Int. Ed.* **2004**, 43, 1329–1331.
- [97] A. Klamt, G. Schüürmann, *J. Chem. Soc., Perkin Trans. 2* **1993**, 799–805.
- [98] Dovesi R., Saunders V. R., Roetti C., Orlando R., Zicovich-Wilson C.M., Pascale F., Civalleri B., Doll K., Harrison N. M., Bush I. J., D'Arco Ph., Llunel M., Causa M., Noël Y., *Crystal14. User's Manual*, University of Torino, Torino, **2014**.
- [99] G. Kresse, J. Hafner, *J. Phys.: Condens. Matter* **1994**, 6, 8245–8257.
- [100] H. S. Muddana, M. K. Gilson, *J. Chem. Theory Comput.* **2012**, 8, 2023–2033.
- [101] H. G. O. Becker, *Organikum*, 15. Aufl., VEB, Berlin, **1996**.
- [102] V. Štrukil, E. Lekšić, E. Meštrović, M. Eckert-Maksić, *Aust. J. Chem.* **2014**, 67, 1129–1133.
- [103] G. M. Sheldrick, *Acta Cryst* **2008**, 64, 112–122.
- [104] O. V. Dolomanov, L. J. Bourhis, R. J. Gildea, J. A. K. Howard, H. Puschmann, *J. Appl. Crystallogr.* **2009**, 42, 339–341.
- [105] K. Brandenburg, *Crystal Impact GbR* **2009**.
- [106] University of Karlsruhe and Forschungszentrum Karlsruhe GmbH, *TURBOMOLE V 7.0.1*, **2015**.
- [107] S. Grimme, J. Antony, S. Ehrlich, H. Krieg, *J. Chem. Phys.* **2010**, 132, 154104.

Appendix A1:

R. Brückner, H. Haller, M. Ellwanger, S. Riedel, *Chem. Eur. J.* **2012**, *18*, 5741-5747.

Passage has been removed due to copyright reasons, publication is available at:

<http://dx.doi.org/10.1002/chem.201103659>

Appendix A2:

R. Brückner, H. Haller, S. Steinhauer, C. Müller, S. Riedel,

Angew. Chem. Int. Ed. **2015**, *54*, 15579–15583.

Angew. Chem. **2015**, *127*, 15800–15804.

Passage has been removed due to copyright reasons, publication is available at:

<http://dx.doi.org/10.1002/anie.201507948>

Appendix A3:

R. Brückner, P. Pröhm, A. Wiesner, S. Steinhauer, C. Müller, S. Riedel, *Angew. Chem. Int. Ed.*, **2016**.” (accepted).

Passage has been removed due to copyright reasons, publication is available at:

<http://dx.doi.org/10.1002/anie.201604348>

Appendix B:

Calculated frequencies and bond lengths.

Table B.1 *Calculated vibrational modes of $[Cl_3]^-$ at MP2/def2-TZVPP level.*

mode	symmetry	wavenumber	IR intensity	selection rules	
#		cm^{-1}	km/mol	IR	RAMAN
1		0.00	0.00000	-	-
2		0.00	0.00000	-	-
3		0.00	0.00000	-	-
4		0.00	0.00000	-	-
5		0.00	0.00000	-	-
6	e1u	171.22	0.89011	YES	NO
7	e1u	171.22	0.89011	YES	NO
8	a1g	278.67	0.00000	NO	YES
9	a2u	310.67	540.03500	YES	NO
end					

Table B.2 *Calculated vibrational modes of $[Cl_5]^-$ at MP2/def2-TZVPP level.*

mode	symmetry	wavenumber	IR intensity	selection rules	
#		cm^{-1}	km/mol	IR	RAMAN
1		0.00	0.00000	-	-
2		0.00	0.00000	-	-
3		0.00	0.00000	-	-
4		0.00	0.00000	-	-
5		0.00	0.00000	-	-
6		0.00	0.00000	-	-
7	a1	16.47	0.02378	YES	YES
8	b1	123.64	482.30590	YES	YES
9	a1	147.58	14.32937	YES	YES
10	a2	148.15	0.00000	NO	YES
11	b1	164.97	471.49686	YES	YES
12	b2	166.08	0.66131	YES	YES
13	a1	216.33	41.27293	YES	YES
14	b1	329.72	262.36016	YES	YES
15	a1	378.00	123.20187	YES	YES
end					

Table B.3 *Calculated vibrational modes of [Cl₇]⁻ at MP2/def2-TZVPP level.*

mode	symmetry	wavenumber	IR intensity	selection rules	
#		cm ⁻¹	km/mol	IR	RAMAN
1		0.00	0.00000	-	-
2		0.00	0.00000	-	-
3		0.00	0.00000	-	-
4		0.00	0.00000	-	-
5		0.00	0.00000	-	-
6		0.00	0.00000	-	-
7	e	11.76	0.20343	YES	YES
8	e	11.76	0.20343	YES	YES
9	a1	14.53	0.13979	YES	YES
10	e	102.49	170.45350	YES	YES
11	e	102.49	170.45350	YES	YES
12	a1	122.21	7.56158	YES	YES
13	a2	129.22	0.00000	NO	NO
14	e	134.81	9.80713	YES	YES
15	e	134.81	9.80713	YES	YES
16	e	164.77	148.34648	YES	YES
17	e	164.77	148.34648	YES	YES
18	a1	183.71	18.10848	YES	YES
19	e	390.52	293.05731	YES	YES
20	e	390.52	293.05731	YES	YES
21	a1	439.30	58.30035	YES	YES

end

Table B.4 *Calculated vibrational modes of [Cl₉]⁻ at MP2/def2-TZVPP level.*

mode	symmetry	wavenumber	IR intensity	selection rules	
#		cm ⁻¹	km/mol	IR	RAMAN
1		0.00	0.00000	-	-
2		0.00	0.00000	-	-
3		0.00	0.00000	-	-
4		0.00	0.00000	-	-
5		0.00	0.00000	-	-
6		0.00	0.00000	-	-
7	t2	3.76	0.02848	YES	YES
8	t2	3.76	0.02848	YES	YES
9	t2	3.76	0.02848	YES	YES
10	e	4.28	0.00000	NO	YES
11	e	4.28	0.00000	NO	YES
12	a1	90.60	0.00000	NO	YES
13	t2	96.46	73.34586	YES	YES
14	t2	96.46	73.34586	YES	YES
15	t2	96.46	73.34586	YES	YES
16	t1	117.50	0.00000	NO	NO
17	t1	117.50	0.00000	NO	NO
18	t1	117.50	0.00000	NO	NO
19	e	127.05	0.00000	NO	YES
20	e	127.05	0.00000	NO	YES
21	t2	168.73	115.91381	YES	YES
22	t2	168.73	115.91381	YES	YES
23	t2	168.73	115.91381	YES	YES
24	t2	434.67	245.37755	YES	YES
25	t2	434.67	245.37755	YES	YES
26	t2	434.67	245.37755	YES	YES
27	a1	473.18	0.00000	NO	YES

end

Table B.5 *Calculated vibrational modes of [Cl₁₁]⁻ at B3-LYP-D3/aug-cc-pVTZ level.*

mode	symmetry	wavenumber	IR intensity	selection rules	
#		cm ⁻¹	km/mol	IR	RAMAN
1		-0.00	0.00000	-	-
2		-0.00	0.00000	-	-
3		-0.00	0.00000	-	-
4		-0.00	0.00000	-	-
5		-0.00	0.00000	-	-
6		0.00	0.00000	-	-
7		0.95	0.04840	-	-
8		0.95	0.04840	-	-
9	a2"	10.49	0.91586	YES	NO
10	e'	12.97	0.30638	YES	YES
11	e'	12.97	0.30638	YES	YES
12	e"	13.41	0.00000	NO	YES
13	e"	13.41	0.00000	NO	YES
14	a1'	56.21	0.00000	NO	YES
15	a1'	76.60	0.00000	NO	YES
16	e'	82.92	34.79273	YES	YES
17	e'	82.92	34.79273	YES	YES
18	a2"	88.28	49.32170	YES	NO
19	e"	91.50	0.00000	NO	YES
20	e"	91.50	0.00000	NO	YES
21	e'	92.83	865.929	YES	YES
22	e'	92.83	865.929	YES	YES
23	a2'	95.31	0.00000	NO	NO
24	e"	105.11	0.00000	NO	YES
25	e"	105.11	0.00000	NO	YES
26	a2"	131.31	132.36702	YES	NO
27	e'	145.77	84.00624	YES	YES
28	e'	145.77	84.00624	YES	YES
29	e'	413.84	273.17867	YES	YES
30	e'	413.84	273.17867	YES	YES
31	a1'	424.53	0.00000	NO	YES
32	a2"	436.37	301.79463	YES	NO
33	a1'	467.09	0.00000	NO	YES

end

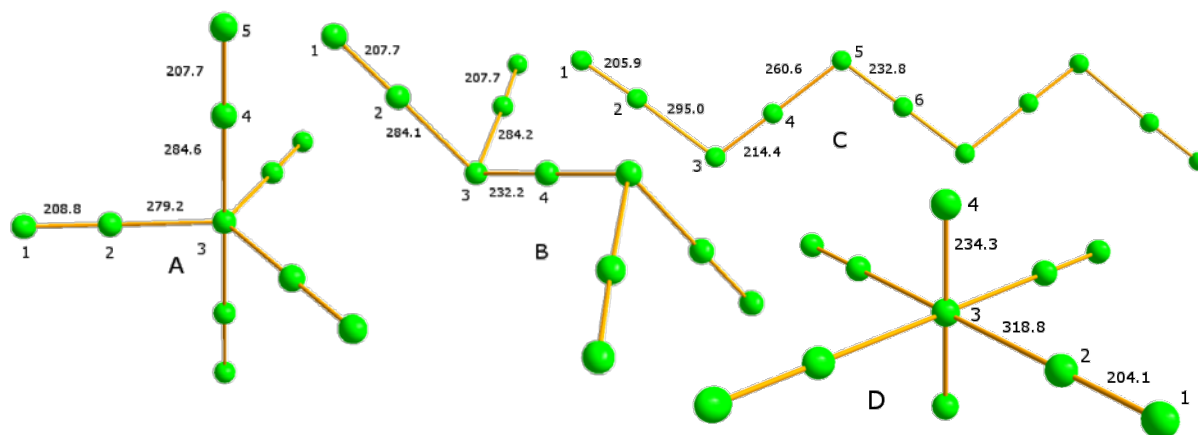
Table B.6 *Calculated vibrational modes of $[Cl_{13}]^-$ at B3-LYP/aug-cc-pVTZ level.*

mode	symmetry	wavenumber	IR intensity	selection rules	
#		cm^{-1}	km/mol	IR	RAMAN
1		-0.00	0.00000	-	-
2		-0.00	0.00000	-	-
3		-0.00	0.00000	-	-
4		0.00	0.00000	-	-
5		0.00	0.00000	-	-
6		0.00	0.00000	-	-
7	t2u	8.03	0.00000	NO	NO
8	t2u	8.03	0.00000	NO	NO
9	t2u	8.03	0.00000	NO	NO
10	t2g	14.71	0.00000	NO	YES
11	t2g	14.71	0.00000	NO	YES
12	t2g	14.71	0.00000	NO	YES
13	t1u	14.84	1.15953	YES	NO
14	t1u	14.84	1.15953	YES	NO
15	t1u	14.84	1.15953	YES	NO
16	eg	50.72	0.00000	NO	YES
17	eg	50.72	0.00000	NO	YES
18	a1g	70.23	0.00000	NO	YES
19	t1u	75.39	34.47824	YES	NO
20	t1u	75.39	34.47824	YES	NO
21	t1u	75.39	34.47824	YES	NO
22	t1g	81.66	0.00000	NO	NO
23	t1g	81.66	0.00000	NO	NO
24	t1g	81.66	0.00000	NO	NO
25	t2u	82.25	0.00000	NO	NO
26	t2u	82.25	0.00000	NO	NO
27	t2u	82.25	0.00000	NO	NO
28	t2g	93.10	0.00000	NO	YES
29	t2g	93.10	0.00000	NO	YES
30	t2g	93.10	0.00000	NO	YES
31	t1u	119.98	109.92161	YES	NO
32	t1u	119.98	109.92161	YES	NO
33	t1u	119.98	109.92161	YES	NO
34	t1u	444.65	254.72096	YES	NO
35	t1u	444.65	254.72096	YES	NO
36	t1u	444.65	254.72096	YES	NO
37	eg	446.65	0.00000	NO	YES
38	eg	446.65	0.00000	NO	YES
39	a1g	481.22	0.00000	NO	YES

end

Table B.7 Bond lengths of the calculated minimum structures of $[Cl_{11}]^-$ at B3-LYP/aug-cc-pVTZ level.

Symmetry	Bond	Length/pm
D_{3h}	r_{12}	208.8
	r_{23}	279.2
	r_{34}	286.6
	r_{45}	207.7
C_{2v}	r_{12}	207.7
	r_{23}	284.1
	r_{34}	232.2
C_i	r_{12}	205.9
	r_{23}	295.0
	r_{34}	214.4
	r_{45}	260.6
	r_{56}	232.8
D_{4h}	r_{12}	204.1
	r_{23}	318.8
	r_{34}	234.3

**Figure B.1** Different minimum structures of $[Cl_{11}]^-$ calculated at B3-LYP/aug-cc-pVTZ level.**Table B.8** Bond lengths of the calculated minimum structures of $[Cl_{13}]^-$ at B3-LYP/aug-cc-pVTZ level.

Symmetry	Bond	Length/pm
O_h	r_{12}	206.9
	r_{23}	287.2
D_{5h}	r_{12}	203.6
	r_{23}	321.9
	r_{34}	233.4

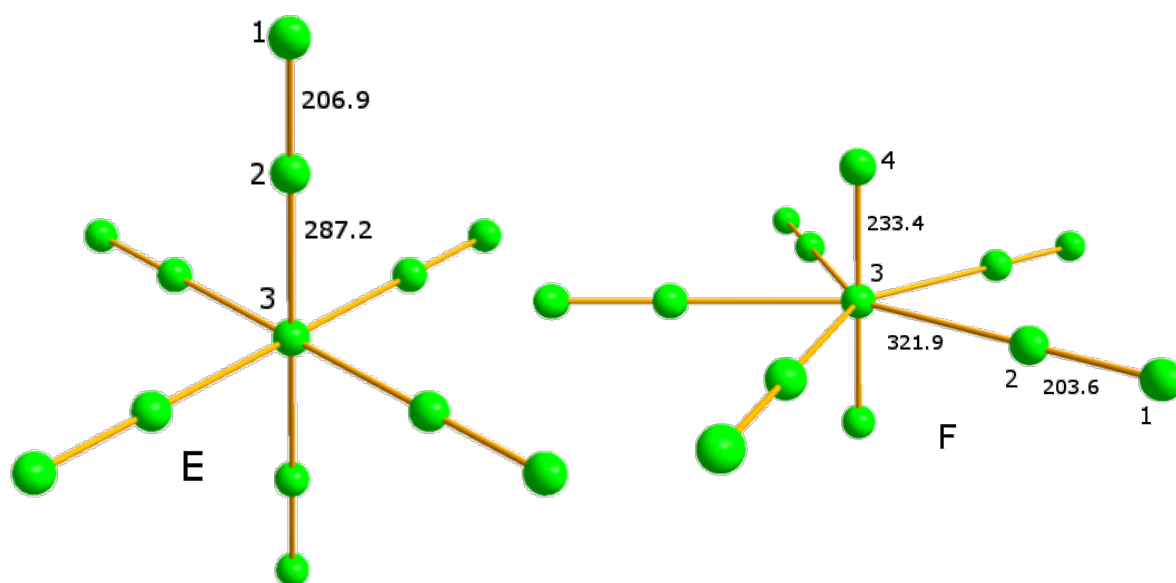


Figure B.2 Calculated minimum structures of $[Cl_{13}]^-$ at B3-LYP/aug-cc-pVTZ level.

Appendix C:

Full crystal data of tetramethylchloroamidiniumtrichloride and
N,N-dimethyl-2-chloroimidazoliniumtrichloride

Full Crystal Data for N,N-dimethyl-2-chloroimidazoliniumtrichloride

Table C.1 Crystal data and structure refinement for N,N-dimethyl-2-chloroimidazoliniumtrichloride.

Identification code	PA06
Empirical formula	C ₅ H ₁₀ Cl ₄ N ₂
Formula weight	237.96
Temperature/K	100.01
Crystal system	orthorhombic
Space group	Pbca
a/Å	11.6135(9)
b/Å	12.8276(10)
c/Å	13.1227(8)
α/°	90
β/°	90
γ/°	90
Volume/Å ³	1954.9(2)
Z	12
ρ _{calc} /g/cm ³	2.446
μ/mm ⁻¹	1.728
F(000)	1464.0
Crystal size/mm ³	0.250 x 0.490 x 0.180
Radiation	MoKα (λ = 0.71073)
2θ range for data collection/°	5.66 to 55.068
Index ranges	-15 ≤ h ≤ 15, -16 ≤ k ≤ 16, -15 ≤ l ≤ 17
Reflections collected	71343
Independent reflections	2253 [R _{int} = 0.1087, R _{sigma} = 0.0272]
Data/restraints/parameters	2253/0/140
Goodness-of-fit on F ²	1.100
Final R indexes [I ≥ 2σ (I)]	R ₁ = 0.0369, wR ₂ = 0.0789
Final R indexes [all data]	R ₁ = 0.0582, wR ₂ = 0.0884
Largest diff. peak/hole / e Å ⁻³	0.39/-0.53

Table C.2 Fractional Atomic Coordinates (×10⁴) and Equivalent Isotropic Displacement Parameters (Å²×10³) for PA06. U_{eq} is defined as 1/3 of the trace of the orthogonalised U_{ij} tensor.

Atom	x	y	z	U(eq)
Cl01	5933.3(4)	2511.4(4)	3746.9(9)	13.47(13)
Cl02	3649.9(4)	3400.5(4)	6245.2(4)	13.07(14)
Cl03	4732.7(5)	1926.8(4)	6246.3(5)	16.97(14)
Cl04	2543.1(4)	4897.0(4)	6247.7(9)	17.46(14)
N005	3848.1(14)	1699.2(13)	3760(2)	10.8(3)
N006	3890.5(15)	3413.1(13)	3732(2)	11.0(3)
C007	4477.3(17)	2543.2(15)	3744(3)	9.7(4)
C008	2648.0(18)	3179.9(17)	3697(3)	12.3(4)
C009	2621.2(18)	1985.2(17)	3788(3)	13.3(4)
C00A	4221(2)	622.8(18)	3810(3)	15.7(5)
C00B	4313(2)	4477.6(17)	3666(3)	14.5(5)

Table C.3 Anisotropic Displacement Parameters ($\text{\AA}^2 \times 10^3$) for PA06. The Anisotropic displacement factor exponent takes the form: $-2\pi^2[h^2a^{*2}U_{11}+2hka^*b^*U_{12}+\dots]$.

Atom	U_{11}	U_{22}	U_{33}	U_{23}	U_{13}	U_{12}
Cl01	8.3(2)	17.5(2)	14.6(3)	1.97(17)	-0.1(5)	0.74(18)
Cl02	12.4(2)	16.5(3)	10.3(2)	0.1(2)	0.1(2)	-3.23(19)
Cl03	19.0(3)	17.1(3)	14.8(2)	-0.2(2)	-0.5(3)	2.4(2)
Cl04	14.7(3)	15.1(3)	22.6(3)	-0.2(3)	-0.8(2)	0.21(18)
N005	10.5(8)	8.8(8)	13.0(8)	0.3(11)	-1.5(12)	0.6(6)
N006	10.2(8)	9.7(8)	13.1(8)	0.0(11)	1.7(12)	-1.1(6)
C007	9.4(9)	13.9(10)	5.8(9)	0.4(7)	-6.1(19)	-0.2(7)
C008	9.3(9)	11.9(9)	15.8(11)	-1.4(12)	0.6(13)	1.0(8)
C009	9.1(9)	14.5(11)	16.4(11)	0.5(12)	3.1(14)	-3.1(8)
C00A	18.5(10)	10.1(9)	18.5(12)	4.2(12)	-3.1(14)	2.3(9)
C00B	16.9(10)	9.4(10)	17.2(13)	-0.1(12)	0.2(12)	-3.5(8)

Table C.4 Bond Lengths for PA06.

Atom	Atom	Length/ \AA	Atom	Atom	Length/ \AA
Cl01	C007	1.691(2)	N005	C00A	1.449(3)
Cl02	Cl03	2.2705(7)	N006	C007	1.308(3)
Cl02	Cl04	2.3102(7)	N006	C008	1.474(3)
N005	C007	1.306(3)	N006	C00B	1.454(3)
N005	C009	1.472(3)	C008	C009	1.537(3)

Table C.5 Bond Angles for PA06.

Atom	Atom	Atom	Angle/ $^\circ$	Atom	Atom	Atom	Angle/ $^\circ$
Cl03	Cl02	Cl04	179.79(4)	C00B	N006	C008	121.29(17)
C007	N005	C009	109.59(17)	N005	C007	Cl01	122.62(15)
C007	N005	C00A	128.55(18)	N005	C007	N006	114.58(18)
C00A	N005	C009	121.75(17)	N006	C007	Cl01	122.80(16)
C007	N006	C008	109.71(17)	N006	C008	C009	102.69(17)
C007	N006	C00B	128.78(18)	N005	C009	C008	103.12(16)

Table C.6 Torsion Angles for PA06.

A	B	C	D	Angle/ $^\circ$	A	B	C	D	Angle/ $^\circ$
N006	C008	C009	N005	-5.3(2)	C00A	N005	C007	Cl01	1.8(7)
C007	N005	C009	C008	4.4(4)	C00A	N005	C007	N006	-177.7(3)
C007	N006	C008	C009	4.9(4)	C00A	N005	C009	C008	-179.1(3)
C008	N006	C007	Cl01	178.1(3)	C00B	N006	C007	Cl01	3.6(7)
C008	N006	C007	N005	-2.3(6)	C00B	N006	C007	N005	-176.9(3)
C009	N005	C007	Cl01	178.0(3)	C00B	N006	C008	C009	179.9(3)
C009	N005	C007	N006	-1.5(6)					

Table C.7 *Hydrogen Atom Coordinates ($\text{\AA}\times 10^4$) and Isotropic Displacement Parameters ($\text{\AA}^2\times 10^3$) for PA06.*

Atom	x	y	z	U(eq)
H00C	2310(30)	1740(20)	4440(20)	14(8)
H00A	2320(30)	3540(20)	4290(20)	9(7)
H00D	2210(30)	1690(20)	3230(20)	9(7)
H00B	2340(30)	3360(30)	3060(20)	17(8)
H00H	4010(30)	4870(20)	4270(20)	12(8)
H00I	5120(20)	4496(19)	3790(20)	9(5)
H00E	5000(20)	595(18)	3900(20)	5(6)
H00F	3850(30)	280(20)	3270(20)	20(9)
H00J	4010(40)	4770(30)	3050(30)	39(11)
H00G	3980(30)	320(20)	4420(20)	18(9)

Full Crystal Data for Tetramethylchloroamidiniumtrichloride

Table C.8 *Crystal data and structure refinement for tetramethylchloroamidiniumtrichloride.*

Identification code	PA09
Empirical formula	C ₅ H ₁₂ N ₂ Cl ₄
Formula weight	241.97
Temperature/K	100.0
Crystal system	orthorhombic
Space group	Pbca
a/Å	10.6432(5)
b/Å	13.3086(8)
c/Å	14.9014(8)
α/°	90
β/°	90
γ/°	90
Volume/Å ³	2110.7(2)
Z	8
ρ _{calc} /g/cm ³	1.523
μ/mm ⁻¹	1.067
F(000)	992.0
Crystal size/mm ³	0.280 x 0.130 x 0.070
Radiation	MoKα (λ = 0.71073)
2θ range for data collection/°	5.468 to 55.024
Index ranges	-13 ≤ h ≤ 13, -17 ≤ k ≤ 17, -19 ≤ l ≤ 19
Reflections collected	42094
Independent reflections	2424 [R _{int} = 0.2673, R _{sigma} = 0.0743]
Data/restraints/parameters	2424/0/148
Goodness-of-fit on F ²	0.923
Final R indexes [I>=2σ (I)]	R ₁ = 0.0346, wR ₂ = 0.0691
Final R indexes [all data]	R ₁ = 0.0583, wR ₂ = 0.0740
Largest diff. peak/hole / e Å ⁻³	0.36/-0.36

Table C.9 *Fractional Atomic Coordinates (×10⁴) and Equivalent Isotropic Displacement Parameters (Å²×10³) for PA09. U_{eq} is defined as 1/3 of the trace of the orthogonalised U_{ij} tensor.*

Atom	x	y	z	U(eq)
Cl01	8173.2(4)	1297.6(4)	6104.4(4)	17.34(14)
Cl02	7019.7(5)	1316.3(5)	4785.0(4)	21.63(15)
Cl03	5343.2(4)	3606.7(5)	5928.3(4)	20.49(15)
Cl04	9289.2(5)	1271.2(5)	7393.6(4)	28.01(17)
N005	7405.1(15)	3823.7(13)	5025.5(12)	13.2(4)
N006	7598.3(15)	3800.8(14)	6593.7(13)	16.0(4)
C007	6944.3(18)	3758.3(16)	5839.6(15)	13.3(5)
C008	8731.2(19)	3589(2)	4822.2(18)	18.4(5)
C009	6616(2)	3986(2)	4230.9(17)	20.3(5)
C00A	8781(2)	4356(2)	6667(2)	23.2(6)
C00B	7097(3)	3430(2)	7446.9(18)	25.7(6)

Table C.10 Anisotropic Displacement Parameters ($\text{\AA}^2 \times 10^3$) for PA09. The Anisotropic displacement factor exponent takes the form: $-2\pi^2[h^2a^{*2}U_{11}+2hka^*b^*U_{12}+\dots]$.

Atom	U_{11}	U_{22}	U_{33}	U_{23}	U_{13}	U_{12}
Cl01	18.0(2)	15.1(3)	18.9(3)	0.9(2)	4.5(2)	1.4(2)
Cl02	22.4(3)	18.8(3)	23.7(3)	0.3(3)	-3.1(2)	0.4(2)
Cl03	10.5(2)	22.5(3)	28.5(3)	-3.6(3)	3.3(2)	-2.7(2)
Cl04	27.6(3)	39.5(5)	16.9(3)	0.6(3)	1.3(2)	6.5(3)
N005	11.8(8)	13.1(11)	14.7(10)	1.0(9)	-1.9(7)	0.4(7)
N006	14.6(8)	16.9(12)	16.6(10)	-0.9(10)	-0.5(7)	2.1(7)
C007	12.5(9)	8.6(12)	18.8(12)	0.4(10)	-0.8(8)	2.3(8)
C008	13.7(10)	22.0(14)	19.4(14)	1.6(13)	5.5(9)	5(1)
C009	21.1(11)	24.2(15)	15.7(13)	2.5(12)	-6.4(9)	1.7(11)
C00A	14.6(11)	28.4(17)	26.6(17)	0.9(13)	-7.9(11)	-1.4(10)
C00B	31.1(14)	30.5(17)	15.5(14)	2.7(13)	6.0(11)	3.6(13)

Table C.11 Bond Lengths for PA09.

Atom	Atom	Length/ \AA	Atom	Atom	Length/ \AA
Cl01	Cl02	2.3181(8)	N005	C009	1.468(3)
Cl01	Cl04	2.2589(8)	N006	C007	1.323(3)
Cl03	C007	1.721(2)	N006	C00A	1.464(3)
N005	C007	1.311(3)	N006	C00B	1.464(3)
N005	C008	1.477(3)			

Table C.12 Bond Angles for PA09.

Atom	Atom	Atom	Angle/ $^\circ$	Atom	Atom	Atom	Angle/ $^\circ$
Cl04	Cl01	Cl02	179.63(4)	C007	N006	C00B	122.11(19)
C007	N005	C008	122.21(18)	C00A	N006	C00B	114.7(2)
C007	N005	C009	122.82(17)	N005	C007	Cl03	116.69(15)
C009	N005	C008	114.37(18)	N005	C007	N006	125.89(18)
C007	N006	C00A	122.5(2)	N006	C007	Cl03	117.43(16)

Table C.13 Torsion Angles for PA09.

A	B	C	D	Angle/ $^\circ$	A	B	C	D	Angle/ $^\circ$
C008	N005	C007	Cl03	-157.39(18)	C00A	N006	C007	Cl03	-151.45(19)
C008	N005	C007	N006	22.8(3)	C00A	N006	C007	N005	28.4(3)
C009	N005	C007	Cl03	13.2(3)	C00B	N006	C007	Cl03	18.8(3)
C009	N005	C007	N006	-166.6(2)	C00B	N006	C007	N005	-161.3(2)

Table C.14 *Hydrogen Atom Coordinates ($\text{\AA}\times 10^4$) and Isotropic Displacement Parameters ($\text{\AA}^2\times 10^3$) for PA09.*

Atom	<i>x</i>	<i>y</i>	<i>z</i>	U(eq)
H00A	8740(20)	3170(20)	4308(17)	23(7)
H00G	9470(20)	3881(17)	6717(15)	19(6)
H00J	6730(20)	3970(20)	7778(18)	32(8)
H00D	5890(20)	4436(17)	4363(15)	17(6)
H00B	9230(20)	4210(20)	4739(18)	40(8)
H00K	6540(20)	2890(20)	7381(17)	35(8)
H00H	8876(18)	4809(18)	6168(15)	15(7)
H00C	9100(20)	3214(19)	5305(17)	23(7)
H00E	6310(20)	3320(20)	3997(18)	39(8)
H00L	7820(30)	3200(20)	7782(18)	45(9)
H00I	8730(20)	4760(20)	7206(19)	46(9)
H00F	7150(20)	4320(20)	3769(17)	36(8)

